

University of Montana

## ScholarWorks at University of Montana

---

Graduate Student Theses, Dissertations, &  
Professional Papers

Graduate School


---

2023

# INDIVIDUAL AND POPULATION RESPONSES TO HYDROLOGIC VARIABILITY IN A HEADWATER STREAM SALAMANDER

Madaline Cochrane  
*The University Of Montana*

Follow this and additional works at: <https://scholarworks.umt.edu/etd>

 Part of the [Other Ecology and Evolutionary Biology Commons](#), [Population Biology Commons](#), and the [Terrestrial and Aquatic Ecology Commons](#)

**Let us know how access to this document benefits you.**

---

### Recommended Citation

Cochrane, Madaline, "INDIVIDUAL AND POPULATION RESPONSES TO HYDROLOGIC VARIABILITY IN A HEADWATER STREAM SALAMANDER" (2023). *Graduate Student Theses, Dissertations, & Professional Papers*. 12078.

<https://scholarworks.umt.edu/etd/12078>

This Dissertation is brought to you for free and open access by the Graduate School at ScholarWorks at University of Montana. It has been accepted for inclusion in Graduate Student Theses, Dissertations, & Professional Papers by an authorized administrator of ScholarWorks at University of Montana. For more information, please contact [scholarworks@mso.umt.edu](mailto:scholarworks@mso.umt.edu).

INDIVIDUAL AND POPULATION RESPONSES TO HYDROLOGIC VARIATION IN A  
HEADWATER STREAM SALAMANDER

By

MADALINE MARIE COCHRANE

B.A. Biology-Environmental Studies, Macalester College, St. Paul, MN, 2006  
M.S. Integrated Biosciences, University of Minnesota, Duluth, MN, 2017

Dissertation

presented in partial fulfillment of the requirements  
for the degree of

Doctor of Philosophy  
in Ecology and Evolution

The University of Montana  
Missoula, MT

May 2023

Approved by:

Scott Whittenburg,  
Graduate School Dean

Dr. Winsor H. Lowe, Chair  
Division of Biological Sciences

Dr. Lisa A. Eby  
College of Forestry and Conservation

Dr. Robert O. Hall  
Division of Biological Sciences

Dr. Bret W. Tobalske  
Division of Biological Sciences

Dr. Andrew C. Wilcox  
Department of Geosciences

© COPYRIGHT

by

Madaline Marie Cochrane

2023

All Rights Reserved

Individual and population responses to hydrologic variation in a headwater stream salamander

Chairperson: Winsor H. Lowe

### ABSTRACT

Understanding how organisms respond to environmental variability is a central goal in ecology – a goal made even more pressing by the herculean challenge global climate change presents to all organisms. Climate change is increasing the frequency and intensity of floods and droughts, which will likely have disproportionate effects on freshwater organisms. Many stream-associated species have multi-stage life histories. However, we lack an empirical understanding of life history and movement responses of these organisms to hydrologic disturbances, and how these responses may influence demographic rates. In my dissertation, I used a combination of growth, developmental, movement, and demographic data to understand individual and population responses to hydrologic disturbances in *Gyrinophilus porphyriticus*, a stream salamander.

In Chapter 1, I show that individual growth rates and mean size at metamorphosis increased with watershed area, my index of hydrologic intermittence. Population growth rates also tended to increase with watershed area. These results suggest that salamanders in hydrologically intermittent environments experience a reduction in body size and, consequently, fitness, which will be exacerbated as droughts increase due to climate change. In Chapter 2, I show that adult and larval downstream movement probability increased with discharge. The probability of terrestrial refuge use by adults also increased with discharge. Overall, my results suggest that headwater salamanders will experience more downstream movement as flood frequency and magnitude increase. These increases in downstream movement may be associated with increases in mortality due to the physical effects of flooding, and due to exposure to fish predators in downstream reaches. In Chapter 3, I show that stream drying intensity reduced larval recruitment, but increased the probability of metamorphosis (i.e., adult recruitment). Larval and adult recruitment were unaffected by flooding intensity, but larval and adult survival declined with flooding intensity. Although annual population growth rates declined with flooding and drying intensity, mean population growth rates were 1.0 between 2012 and 2021. Together, these results demonstrate population resilience to episodic hydrologic disturbances that was a consequence of compensatory effects of hydrologic extremes on the recruitment of new larvae vs. adults (i.e., reproduction vs. metamorphosis). I hope my work will help to predict and mitigate the effects of hydrologic extremes on stream salamanders and other headwater specialist taxa.

## TABLE OF CONTENTS

ABSTRACT.....	iii
TABLE OF CONTENTS.....	iv
CHAPTER 1: Individual growth rates and size at metamorphosis increase with watershed area in a stream salamander .....	1
Abstract .....	1
Introduction.....	1
Methods.....	2
Results.....	5
Discussion .....	6
Acknowledgments.....	8
Literature cited .....	8
Figures.....	11
Appendix S1.....	13
Appendix S2.....	22
Appendix S3.....	26
CHAPTER 2: Floods increase downstream movement of adult and larval life stages of a headwater stream salamander .....	30
Abstract .....	30
Introduction.....	30
Methods.....	32
Results.....	35
Discussion .....	36
Acknowledgments.....	38
Literature Cited .....	38
Figures.....	44
Supplementary Materials .....	49
CHAPTER 3: Stage-specific demographic effects of hydrologic extremes in a stream salamander .....	62
Abstract .....	62
Introduction.....	62
Methods.....	64
Results.....	67
Discussion .....	69
Acknowledgments.....	70
Literature cited .....	71
Tables.....	78
Figures.....	82
Supplementary Materials .....	87

## ACKNOWLEDGMENTS

First, I would like to thank Winsor Lowe, who has been an empowering and thoughtful mentor. Without Winsor's support and guidance this would not have been possible. I would also like to thank my Ph.D. committee: Andrew, Bob, Bret, and Lisa. Your willingness to share your expertise, brainstorm, and provide feedback has made me a better scientist. Thank you!

I was able to gain my footing and have community here at UM because of an awesome group of women. Thank you to Leah Swartz for two full but gratifying field seasons at Hubbard Brook. I appreciate your company and friendship and am lucky to have such a good friend to explore mountains with from New Hampshire to Montana. I cannot thank Brett Addis enough for her knowledge, helpfulness, and kindness. I would not have been able to thrive at Hubbard Brook if it were not for your hard work and willingness to support others. Thank you to Leah Joyce and Kara Cromwell for making our lab such a welcoming place and for your thoughtful feedback as I developed my project. Thanks to Elise Zarri for her friendship and our conversations about mentorship and quirky field stories. And a huge thanks to Laurel Genzoli whose help with coding and science talks on the skin track have strengthened my research and provided me with invaluable guidance.

This project would not have been possible without the work of many field technicians and folks at Hubbard Brook who made my four field seasons away from home worth it. Thank you to Ryan Wagner, Megan Delamont, Anna Willing, Riley Waters, and Kai Barreras for your hard work. It was fun to share my love of field biology with you all in such a beautiful place. I especially want to thank Tyler Hodges for his emphatic love of birds and incredible work ethic. Thanks to Geoff Wilson for his logistical support and tips on explorations in the White Mountains. Thanks also to Mary Martin, Nina Lany, David Zietlow, Amey Bailey, and Scott Bailey for help with data retrieval.

I would not be the person I am today without the love and support of my parents, Jean, and Tim. Thank you for role-modeling how to be considerate, hard-working, and curious people. I appreciate that you have always believed in me, often when I doubt myself. Thanks to Rainy and Bean for their unwavering love and companionship as we explored the many awesome trails across Missoula. Thank you to Talis for coming into this world at the perfect time and challenging me to grow in new ways. And last thank you to Rebekah for being my rock these last five years. I would not be where I am today without your patience, empathy, and love.

# CHAPTER 1: Individual growth rates and size at metamorphosis increase with watershed area in a stream salamander

Madaline M. Cochran<sup>1,\*</sup>, Brett R. Addis<sup>2</sup>, Leah K. Swartz<sup>3</sup>, and Winsor H. Lowe<sup>1</sup>

1. Division of Biological Sciences, University of Montana, Missoula, MT, USA

2. D.B. Warnell School of Forestry and Natural Resources, University of Georgia, Athens, GA, USA

3. Montana Freshwater Partners, Livingston, MT, USA

## Abstract

A fundamental goal of ecology is to better understand how the physical environment influences intraspecific variability in life history and consequently fitness. In streams, discharge and associated habitat conditions change along a continuum. But there are few empirical studies assessing life history and associated population responses to this continuum in aquatic organisms. We tested the prediction that individual growth, rate of development, and population growth increase with watershed area in the long-lived stream salamander *Gyrinophilus porphyriticus*, where we use watershed area as an index of hydrologic intermittence and associated habitat conditions. To address this hypothesis, we used 8 y of mark-recapture data from 58 reaches across 10 headwater streams in New Hampshire, USA. Individual growth rates and mean size at metamorphosis increased with watershed area. Population growth rates tended to increase with watershed area; however, this result was inconclusive at our sample sizes. Mean age of metamorphosis did not vary across watershed areas. Lower individual growth rates and smaller sizes at metamorphosis likely contributed to reduced lifetime fecundity and population growth in reaches with the smallest watershed areas. These responses suggest that as droughts increase due to climate change, salamanders and other headwater specialists in hydrologically intermittent environments will experience a reduction in body size and consequently reduced fitness.

## Introduction

Life history variation influences nearly all aspects of ecology, from individual fitness, to population dynamics, to community interactions (Tilley 1968, Hernández-Pacheco et al. 2021). Growth rate and time to reproductive maturity are key life history traits influencing fecundity and survival, particularly because of their effects on body size. The size of an individual at maturity influences fitness through size-mediated reproductive outputs, where larger sizes at maturity correspond to increased fecundity (Bruce 2013). Also, because successful reproduction requires surviving to reproductive age, growth and development time mediate fitness through size- and stage-specific rates of survival (Székely et al. 2020, Hernández-Pacheco et al. 2021).

Metamorphosis is a key switch point in complex life cycles, allowing individuals to maximize fitness by balancing tradeoffs between survival and growth as a larva, and survival and fecundity as an adult (Werner 1986). Generally, individuals that delay metamorphosis are larger at maturity and have greater reproductive output than those that metamorphose earlier (Bruce

2013). However, accelerated development is often favored, at the expense of fecundity, when conditions are not conducive to larval survival (Székely et al. 2017). How organisms respond to these trade-offs leads to intra and interspecific variability in the timing of growth and development (Wells and Harris 2001), and resulting population dynamics (Biek et al. 2002).

Streams and rivers exhibit predictable changes in abiotic conditions from upstream to downstream reaches, including discharge, geomorphology, and associated physical and chemical attributes (Vannote et al. 1980). Fish and invertebrates adapt their life history strategies to their position along this gradient of discharge and associated habitats (Mims and Olden 2012), but we know very little about how stream amphibians respond to this gradient. Stream amphibians – particularly plethodontid salamanders, the family with the most stream-associated species (Petranka 1998) – are top predators in many fishless headwater streams and key components of headwater ecosystems (Milanovich et al. 2015). But we lack a thorough understanding of how the physical template of streams, and particularly the gradient in discharge that occurs from upstream intermittent reaches to downstream permanent reaches, influences intraspecific variability in life history, fitness, and population dynamics of stream amphibians.

Watershed area, the total collection area that gathers runoff from a landscape (Hauer and Lamberti 2017), provides a useful metric to describe the continuum of discharge and associated habitat conditions across streams. Specifically, watershed area is an index of relative discharge magnitude because streamflow scales geometrically with watershed area within regions where precipitation, geology, and land-use are similar across space (Vogel and Kroll 1992). The smaller the watershed area, the greater likelihood of streamflow intermittence, leading to a suite of abiotic and biotic changes (Poff and Ward 1989).

To better understand how discharge and associated habitat gradients influence stream amphibian life history, we tested the prediction that individual growth rates, size at metamorphosis, age of metamorphosis, and ultimately population growth rates of *Gyrinophilus porphyriticus* (the northern spring salamander) increase with watershed area. Specifically, we hypothesized that reaches with small watershed areas would have the greatest risk of desiccation, and more stressful habitat conditions overall, causing individuals to metamorphose early and thereby reduce their reliance on permanent water availability within the stream channel. As a consequence of this phenological shift, we expected size at metamorphosis to increase with watershed area. We also expected reduced growth rates in reaches with small watershed areas because individuals are allocating more energy to development than to growth (Richter-Boix et al. 2011), and experience increased crowding and competition (Glennemeier and Denver 2002). We expected these individual responses, particularly reduced sizes at metamorphosis, to lower fecundity and population growth rates in upstream reaches with small watershed areas.

## Methods

### *Study organism*

*Gyrinophilus porphyriticus* is one of the largest plethodontid salamanders and occupies headwaters streams throughout the Appalachian Mountains (Petranka 1998). Plethodontids use cutaneous respiration to breathe through their skin, restricting them to moist environments (Feder



1983). *G. porphyriticus* has a complex life cycle where larvae are restricted to the stream channel because they respire with external gills. During metamorphosis larvae transform into their adult, semi-aquatic form, allowing individuals to leave the stream for short periods of time (Greene et al. 2008). They grow slowly, making them a difficult species to age (Bruce 1980, Bruce and Castanet 2006). Aquatic predators, particularly *Salvelinus fontinalis* (brook trout), prey on larvae, and can reduce salamander activity and growth (Resetarits 1995).

### *Study streams and sampling methods*

We conducted this research in streams at the Hubbard Brook Experimental Forest (HBEF) in New Hampshire, USA (43°56'N, 71°45' W). The HBEF is a 30 km<sup>2</sup> watershed that lies within the White Mountains and ranges in elevation from 222 to 1,015 m. This site experiences short, cool summers and long, cold winters. Streams have low conductivity (12.0–15.0 μS), slight acidity (pH of 5.0–6.0), and high dissolved oxygen content (>95% saturation).

Our sampling was designed to capture life history and population responses across a large range of watershed sizes within and among hydrologically independent headwater streams in the HBEF (see Appendix S1 for detailed description of study design). Our analyses are based on data from 58 study reaches ranging in length from 60 – 100 m and distributed across 10 first through fourth-order streams (Appendix S1: Fig. S2). We conducted mark-recapture surveys of reaches nine times each field season, June – September, of 2012 – 2015 and 2018 – 2021 (Addis and Lowe 2020). We gave each individual a unique mark, recorded the mass for all captured individuals, and measured snout-vent-length (SVL). See Appendix S1 for detailed description of survey schedule and salamander capture methodology.

### *Quantifying watershed area*

We derived watershed areas at the mid-point of each study reach with 1-m Digital Elevation Models (Fraser et al. 2022) using ArcMap Version 10.8 (Environmental Systems Research Institute, Inc., Redlands, CA). Based on observations over the eight years of sampling, the reaches with the smallest watershed areas had intermittent flow in late summer whereas larger watershed reaches were permanently flowing year-round. However, we assessed this observation statistically by testing whether watershed area predicts the annual frequency of days with no flow based on discharge data collected at nine gauged weirs across HBEF beginning in 1956 (USDA Forest Service 2020). We also assessed if watershed area predicts annual minimum discharge. See Appendix S1 for details of both models.

### *Estimating individual growth*

To test how watershed area influences *G. porphyriticus* growth and estimate age-at-length, we fit a von Bertalanffy (VB) growth function to individual body size data using a Bayesian hierarchical modeling approach that accounts for measurement error. A VB growth model is derived from basic metabolic principles (West et al. 2001), and fits plethodontid growth better than a logistic function due to its marked deceleration of growth rate over time (Staub 2016). The VB growth function estimates two parameters: the asymptotic size that individuals grow toward as they age ( $a$ ), and a growth rate coefficient ( $k$ ), which defines how rapidly individuals approach

their asymptotic size (Eaton and Link 2011). See Appendix S1 for complete model details. We estimated  $k$  separately across two seasons based on our sampling schedule: the active season (June 1 – September 30), and the inactive season (October 1 – May 31). To determine if growth parameters differed by life stage, we fit one model for individuals pooled across all life stages, then we fit separate models for larvae and adults.

### *Quantifying size and age at metamorphosis*

We used a Bayesian linear mixed model to test how watershed area influences size at metamorphosis (SVL) and age at metamorphosis in *G. porphyriticus*. We used two approaches to estimate the body size of metamorphosing individuals. First, we directly measured the size of individuals that were in the process of metamorphosis when captured – those with reduced external gills and skin color changing from gray to orange (Petranka 1998). Second, we took the average size of individuals captured as a larva and an adult in the same field season. To estimate the age of all individuals undergoing metamorphosis, we located their specific SVL position on the VB growth curve (Ogle and Isermann 2017). See Appendix S1 for detailed descriptions of both models.

### *Estimating population growth*

To estimate the population growth rate at each stream reach, we used a Bayesian formulation of the reverse-symmetry capture-recapture Pradel model (Pradel 1996). Our model was parameterized to estimate annual population growth rate ( $\lambda$ ), annual apparent survival ( $\phi$ ), and annual detection probability ( $p$ ) (Tenan et al. 2014; see Appendix S1 for model details).

### *Model fitting and analyses*

To test how watershed area affects individual growth rates, size, and age at metamorphosis, we included watershed area as an explanatory variable in each respective model (described above). We also fit a Bayesian linear mixed model to test how watershed area affects reach-specific estimates of  $\lambda$ . To account for other known environmental influences on salamander life history and population growth, we included the effect of *S. fontinalis* presence on growth, size at metamorphosis, age at metamorphosis, and population growth rate (Semasko 2013, Davenport and Lowe 2018). We also modeled the effect of stream temperature on growth. To account for lack of independence among reaches within the same stream, we estimated a separate  $k$  for each stream in the VB growth model and included stream as a random effect in our size and age at metamorphosis models, in addition to our model to describe the effect of watershed area on population growth rate.

We fit all models using Markov chain Monte Carlo (MCMC) methods (see Appendix S1 for details) in JAGS (Plummer 2003) and RStudio (R Development Core Team 2021). To assess model convergence, we inspected trace-plots to ensure mixing of chains and we ensured all parameters had  $\hat{R} < 1.05$  (Gelman et al. 2013). If a parameter estimate did not converge, or if season or stream-specific parameters overlapped in 95% credible intervals, we removed it from the model. To assess model fit for the VB growth, size, and age at metamorphosis models, we

used a posterior predictive check by simulating data under the model and calculating a Bayesian  $P$ -value (Gelman et al. 2013).

## Results

### *Watershed area-discharge relationship*

Across the nine gauged HBEF watersheds, the annual frequency of zero-discharge days declined with watershed area (mean  $\beta_{\text{Area}} = -1.71$ , 95% CI =  $-2.75 - -0.71$ ; Appendix S2: Fig. S1). Similarly, minimum discharge was strongly positively related to watershed area (mean  $\beta_{\text{Area}} = 4.51$ , 95% CI =  $2.26 - 6.49$ ; Appendix S2: Fig. S2). Both zero- and minimum-discharge models fit their data well (Bayesian  $P$ -values = 0.47 and 0.54, respectively). HBEF's nine gauged watersheds ranged in area from 0.12 to 0.77 km<sup>2</sup>, corresponding to a mean Q5 of 0.0001 m<sup>3</sup>/sec (SD = 0.0002). Our 58 study reaches ranged in watershed area from 0.14 to 3.50 km<sup>2</sup> (Appendix S2: Fig. S3; mean = 1.04, SD = 0.73).

### *Individual growth*

In the all-individuals and larvae-only growth models, growth rates increased with watershed area (Fig. 1, 2a; Appendix S3: Table S1). For the adult-only model, growth rate tended to increase with watershed area, but not as strongly ( $B_{\text{area}} = 0.14$ , 95% CI =  $-0.08 - 0.35$ ). The presence of *S. fontinalis* reduced growth in all models. All  $k$  estimates overlapped when  $k$  varied by stream, indicating that growth rates did not vary a lot among streams. All VB growth models differentiated growth rates between the active and inactive seasons (Fig. 1; Appendix S3: Table S1). Almost all growth happened in the active season, with the exception of some larval growth outside of the summer sampling season. The mean asymptotic body size and standard deviation for measurement error was 116 mm (95% CI =  $111 - 122$ ) and 3.81 mm (95% CI =  $3.69 - 3.94$ ), respectively, for the all-individuals model. Based on these parameter estimates, a salamander with a SVL in the 99<sup>th</sup> percentile (103 mm) was 20-y old (95% CI =  $10 - 34$ ). A salamander with a SVL in the 1<sup>st</sup> percentile (35 mm) was 2-y old (95% CI =  $1 - 3$ ). The growth models fit the all-individuals and adult-only data well (Bayesian  $P$ -values = 0.57, 0.58), and the larval-only data moderately well (Bayesian  $P$ -value = 0.73).

The model that included an effect of maximum stream temperature between captures on  $k$  was not significant (all: mean  $\beta_{\text{temp}} = 0.19$ , 95% CI =  $-0.46 - 1.06$ ), indicating that stream temperature did not have a large effect on *G. porphyriticus* growth rates at our site. In the eight reaches where temperature was recorded (watershed areas =  $0.3 - 1.4$  km<sup>2</sup>), water temperatures across the active season (June – September) ranged from 6 – 21°C, but there was little variability among reaches (mean SD across all hourly temperatures = 0.8°C).

Our full growth model was populated with 2,971 SVL measurements from 1,219 individuals. The larvae and adult-only models were populated with 1,788 and 773 measurements, respectively. Mean captures per individual was 2.4 (SD = 0.8), with a maximum of 8 captures for a single individual. The time intervals between captures ranged from 2 to 3,258 days (median = 33, mean = 279, SD = 456). Mean SVL ( $\pm$  SD) for larvae and adults were 53 mm ( $\pm$  9) and 79 mm ( $\pm$  10), respectively. Due to limited *G. porphyriticus* observations at watershed areas

between 1.66 and 3.50 km<sup>2</sup> (only 3% of all observations; Appendix S2: Fig. S4), we limited inference to *G. porphyriticus* from the 53 study reaches with watershed areas  $\leq 1.66$  km<sup>2</sup>.

### *Size at metamorphosis*

Size at metamorphosis increased with watershed area (Fig. 2b; Appendix S3: Table S2). Mean size at metamorphosis for *G. porphyriticus* at the smallest watershed area (0.14 km<sup>2</sup>) was 67 mm SVL (95% CI = 65–68), compared to 73 mm SVL (95% CI = 71–75) at the largest watershed area (1.65 km<sup>2</sup>). *S. fontinalis* had a slight negative effect on size at metamorphosis. Random intercepts for each stream overlapped in 95% credible intervals, indicating stream-level differences in abiotic conditions did not have a large effect on size at metamorphosis. The size at metamorphosis model fit our data well (Bayesian  $P$ -value = 0.47). Overall, we captured 193 individuals undergoing metamorphosis (3% of all captures). Mean SVL for all individuals was 69 mm (SD = 6).

### *Age at metamorphosis*

Age at metamorphosis was unrelated to watershed area (Fig. 2c; Appendix S3: Table S3) and *S. fontinalis* presence. Random intercepts for each stream overlapped in 95% credible intervals, indicating stream-level differences in abiotic conditions did not have a large effect on age at metamorphosis. The age at metamorphosis model fit our data well (Bayesian  $P$ -value = 0.48). Overall, the mean age of metamorphosis was 7.9 y (SD = 1.3).

### *Population growth*

Population growth ( $\lambda$ ) tended to increase with watershed area (mean  $\beta_{\text{area}} = 0.02$ , 95% CI = -0.02 – 0.05; Fig. 2d; Appendix S3: Table S4) and decrease with *S. fontinalis* presence (mean  $\beta_{\text{fish}} = -0.03$ , 95% CI = -0.10 – 0.04). But these relationships were inconclusive at our sample size. Random intercepts for each stream overlapped in 95% credible intervals, indicating stream-level differences in abiotic conditions did not have a large effect on  $\lambda$ . The model fit our data well (Bayesian  $P$ -value = 0.51). Overall, annual mean  $\lambda$  across all reaches was 1.01 (SD = 0.04), annual mean apparent survival ( $\phi$ ) was 0.58 (SD = 0.14), and annual mean detection probability ( $p$ ) was 0.12 (SD = 0.05).

## **Discussion**

Discharge variability constrained growth and life history of a stream salamander. *G. porphyriticus* growth rates and size at metamorphosis were lowest in stream reaches with the smallest watershed areas, where flow was intermittent (Fig. 2a-b). Smaller post-metamorphic females experience lower fecundity than larger counterparts (Bruce 2013), likely contributing to reduced population growth rates at small watershed areas (Fig 2d). These results are consistent with the majority of studies of pond-breeding amphibians, where larvae in water-limited environments have smaller sizes at metamorphosis and reduced growth rates in response to drying (Richter-Boix et al. 2011, Székely et al. 2017). However, this is the first study to document life-history and population-level responses to discharge and associate environmental

gradients in a stream-breeding amphibian. These results suggest that optimal growth occurs in the most hydrologically stable stream environments.

The proximate mechanisms limiting *G. porphyriticus* growth and metamorphic size in reaches with the smallest watershed areas, where flow is limited, are likely physiological and behavioral. Cutaneous gas exchange is reduced in dry environments because plethodontids require moisture for cutaneous respiration (Feder 1983). Therefore, reduced water availability may inhibit metabolic processes in intermittent reaches. Similarly, to avoid unnecessary water loss in dry environments, individuals may become less active, reducing foraging rates (Bendik and Gluesenkamp 2013). Reduced flows may also restrict habitat area, leading to crowding, increased competition, predation, and stress (Petranka and Sih 1986, Maher et al. 2013), or drought may reduce resource availability directly, leading to sub-optimal growth conditions. For example, when reaches become disconnected to the stream channel during periods of intermittent flow, individuals lose inputs of drifting invertebrates and organic matter, and may experience reduced availability of prey resources (Northington and Webster 2017).

In contrast to our expectations, age at metamorphosis was not affected by discharge – we found no difference in average time to metamorphosis for *G. porphyriticus* across the range of watershed areas (Fig. 2c). Mean metamorphic age was 8 y across all watershed areas, despite differences in growth rates and sizes at metamorphosis across the same range of watershed areas (Fig. 2a-b). Specifically, smaller sizes at metamorphosis and slower growth rates in low-discharge environments did not cause the timing of metamorphosis to differ from high-discharge environments, where individuals had larger sizes at metamorphosis and faster growth rates. These results contradict patterns observed in most other salamander and amphibian studies, which demonstrate variable metamorphic timing in response to extrinsic conditions (Wilbur and Collins 1973, Berven and Gill 1983). However, our results are consistent with data suggesting that metamorphic timing in plethodontids is not strongly affected by growth trajectories (Beachy et al. 2017), potentially due to evolutionary history. Ancestral plethodontids were direct developers that lacked a larval feeding stage (Bonett et al. 2014). Direct developers transform from egg to adult internally, reducing any reliance on signals that typically stimulate morphogenesis (e.g., resource or water availability) and potentially a decoupling of metamorphic timing and growth rates.

Our approach for estimating growth and metamorphic size may be useful for characterizing these life history responses in other species, and for intraspecific comparisons across environmental conditions. Using the VB growth function, we quantified the effects of watershed area on growth and development despite the challenges posed by slow and variable growth in *G. porphyriticus* – characteristics shared by many species (Arendt 1997), and which often preclude size-frequency and skeletochronology techniques (Bruce 1980, Bruce and Castanet 2006). Our estimate of a 20-y old *G. porphyriticus*, based on a SVL of 103 mm, is similar to the oldest known age of a *G. porphyriticus* individual in captivity (18 y), but younger than the age of the oldest plethodontid in captivity (36 y old *Plethodon hubrichti*; Staub 2016). Additionally, our estimate that metamorphosis occurs at approximately 8 y of age is the first for *G. porphyriticus* at the northern extent of its range, and is 3 – 4 y greater than prior estimates from further south (4 – 5 y; Bruce 1980). Even based on these prior estimates, *G. porphyriticus* have the longest recorded larval periods of all plethodontids, much greater than the second

longest – 2 y in *Pseudotriton ruber* (Bonett et al. 2014). Such a long larval period underscores the importance of hydrologic stability to *G. porphyriticus* persistence. Future studies using intensive, long-term mark-recapture data will likely continue to provide valuable information on developmental cues and constraints in this and other long-lived metamorphic species.

Our long-term data provide new, high-resolution insight on individual and population responses to longitudinal gradients in stream discharge and associated environmental conditions. In *G. porphyriticus*, individual growth rates, size at metamorphosis, and population growth rates declined in reaches with the smallest watershed areas. Generally, these are the first areas in stream networks to experience desiccation, suggesting that salamanders and other headwater specialists will fare poorly as the frequency and intensity of droughts increase with climate change (Arias et al. 2021).

### **Acknowledgments**

We thank T. Hodges, R. Wagner, M. Delamont, A. Willig, K. Barreras, R. Waters, M. Chung, M. Childs, J. Davenport, J. Hernandez, J. Jones, L. Low, J. McKenzie, T. Mitchell, L. Nagel, J. Newman, J. Razor, M. Smith, and N. Steijn for assistance in the field. The research was funded by the U.S. NSF (DEB-1114804, DEB-1050459, DEB-1655653). This work was conducted under Montana State IACUC #003-14WLDBS-012714. This work is a contribution of the Hubbard Brook Ecosystem Study. Hubbard Brook is part of the LTER network, which is supported by the U.S. NSF. The Hubbard Brook Experimental Forest is operated and maintained by the US Department of Agriculture, Forest Service, Northern Research Station.

### **Literature cited**

- Addis, B. R., and W. H. Lowe. 2020. Long-term survival probability, not current habitat quality, predicts dispersal distance in a stream salamander. *Ecol.* 101:1–14.
- Arias, P., N. Bellouin, E. Coppola, R. Jones, G. Krinner, J. Marotzke, V. Naik et al. 2021. Climate Change 2021: The Physical Science Basis. Contribution of Working Group I to the Sixth Assessment Report of the Intergovernmental Panel on Climate Change; Technical Summary.
- Beachy, C. K., T. J. Ryan, and R. M. Bonett. 2017. How metamorphosis is different in Plethodontids: larval life history perspective on life-cycle evolution. *Herpetologica* 176:139–148.
- Bendik, N. F., and A. G. Gluesenkamp. 2013. Body length shrinkage in an endangered amphibian is associated with drought. *J. Zool.* 290:35–41.
- Berven, K. A., and D. E. Gill. 1983. Interpreting geographic variation in life-history traits. *Integrative and Comparative Biology* 23:85–97.
- Biek, R., W. C. Funk, B. A. Maxell, and L. S. Mills. 2002. What is missing in amphibian decline research: insights from ecological sensitivity analysis. *Conserv. Bio.* 16:728–734.
- Bonett, R. M., M. A. Steffen, and G. A. Robison. 2014. Heterochrony repolarized: a phylogenetic analysis of developmental timing in plethodontid salamanders. *EvoDevo* 5:27.
- Bruce, R. C. 1980. A model of the larval period of the spring salamander, *Gyrinophilus porphyriticus*, based on size-frequency distributions. *Herpetologica* 36:78–86.

- Bruce, R. C. 2013. Size-mediated tradeoffs in life-history traits in dusky salamanders. *Copeia* 2013:262–267.
- Bruce, R. C., and J. Castanet. 2006. Application of skeletochronology in aging larvae of the salamanders *Gyrinophilus porphyriticus* and *Pseudotriton ruber*. *J. Herpetol.* 40:85–90.
- Eaton, M. J., and W. A. Link. 2011. Estimating age from recapture data: Integrating incremental growth measures with ancillary data to infer age-at-length. *Ecol. Appl.* 21:2487–2497.
- Feder, M. E. 1983. Integrating the ecology and physiology of plethodontid salamanders. *Herpetologica* 39:291–310.
- Fraser, O.L., K.J. McGuire, and S.W. Bailey. 2022. Hubbard Brook Experimental Forest: 1 meter LiDAR-derived Digital Elevation Models, 2012 ver 2. Environmental Data Initiative. <https://doi.org/10.6073/pasta/dcab665da20b8e75a57506b19f90262a>
- Gelman, A., J. B. Carlin, H. S. Stern, D. B. Dunson, A. Vehtari, and D. B. Rubin. 2013. *Bayesian Data Analysis*. 3rd Editio. Chapman & Hall, Boca Raton, FL.
- Glennemeier, K. A., and R. J. Denver. 2002. Developmental changes in interrenal responsiveness in anuran amphibians. *Integr. Comp. Biol.* 42:565–573.
- Greene, B. T., W. H. Lowe, and G. E. Likens. 2008. Forest succession and prey availability influence the strength and scale of terrestrial-aquatic linkages in a headwater salamander system. *Freshw. Biol.* 53:2234–2243.
- Hauer, F. R., and G. a. Lamberti. 2017. *Methods in Stream Ecology*. 3rd edition. Elsevier Inc., Cambridge, MA.
- Hernández-Pacheco, R., F. Plard, K. L. Grayson, and U. K. Steiner. 2021. Demographic consequences of changing body size in a terrestrial salamander. *Ecol. and Evol.* 11:174–185.
- Maher, J. M., E. E. Werner, and R. J. Denver. 2013. Stress hormones mediate predator-induced phenotypic plasticity in amphibian tadpoles. *Procs R Soc B*: 280:20123075.
- Milanovich, J. R., J. C. Maerz, and A. D. Rosemond. 2015. Stoichiometry and estimates of nutrient standing stocks of larval salamanders in Appalachian headwater streams. *Freshw. Biol.* 60:1340–1353.
- Mims, M. C., and J. D. Olden. 2012. Life history theory predicts fish assemblage response to hydrologic regimes. *Ecol.* 93:35–45.
- Northington, R. M., and J. R. Webster. 2017. Experimental reductions in stream flow alter litter processing and consumer subsidies in headwater streams. *Freshw. Biol.* 62:737–750.
- Ogle, D. H., and D. A. Isermann. 2017. Estimating age at a specified length from the von Bertalanffy growth function. *N. Am. J. Fish. Manag.* 37:1176–1180.
- Petranka, J. W. 1998. *Salamanders of the United States and Canada*. Smithsonian Institution, Washington.
- Petranka, J. W., and A. Sih. 1986. Environmental instability, competition, and density-dependent growth and survivorship of a stream-dwelling salamander. *Ecol.* 67:729–736.
- Plummer, M. 2003. JAGS: A program for analysis of Bayesian graphical models using Gibbs sampling. *Proceedings of the 3rd international workshop on distributed statistical computing* 125:1–10.
- Poff, N. L., and J. V. Ward. 1989. Implications of streamflow variability and predictability for lotic community structure: a regional analysis of streamflow patterns. *Can. J. of Fish. Aquat. Sci.* 46:1805–1818.
- Pradel, R. 1996. Utilization of capture-mark-recapture for the study of recruitment and population growth rate. *Biometrics* 52:703–709.

- R Development Core Team. 2021. R: A language and environment for statistical computing. R Foundation for Statistical Computing. Vienna, Austria.
- Resetarits, W. J. 1995. Competitive asymmetry and coexistence in size-structured populations of Brook Trout and Spring Salamanders. *Oikos* 73:188–198.
- Richter-Boix, A., M. Tejedo, and E. L. Rezende. 2011. Evolution and plasticity of anuran larval development in response to desiccation. A comparative analysis. *Ecol. Evol.* 1:15–25.
- Staub, N. L. 2016. The age of Plethodontid salamanders: a short review on longevity. *Copeia* 2016:118–123.
- Székely, D., D. Cogălniceanu, P. Székely, D. Armijos-Ojeda, V. Espinosa-Mogrovejo, and M. Denoël. 2020. How to recover from a bad start: size at metamorphosis affects growth and survival in a tropical amphibian. *BMC Ecol.* 20:1–8.
- Székely, D., M. Denoël, P. Székely, and D. Cogălniceanu. 2017. Pond drying cues and their effects on growth and metamorphosis in a fast developing amphibian. *J. Zool.* 303:129–135.
- Tenan, S., R. Pradel, G. Tavecchia, J. M. Igual, A. Sanz-Aguilar, M. Genovart, and D. Oro. 2014. Hierarchical modelling of population growth rate from individual capture-recapture data. *Methods Ecol. and Evol.* 5:606–614.
- Tilley, S. G. 1968. Size-fecundity relationships and their evolutionary implications in five Desmognathine salamanders. *Evol.* 22:806.
- USDA Forest Service, Northern Research Station. 2020. Hubbard Brook Experimental Forest: Instantaneous Streamflow by Watershed, 1956 – present ver 14. Environmental Data Initiative. <https://doi.org/10.6073/pasta/87584eda806dd5a480423b6bfefec577>
- Vannote, R. L., G. W. Minshall, K. W. Cummings, J. R. Sedell, and C. E. Cushing. 1980. The river continuum concept. *Can. J. of Fish. Aquat. Sci.* 37:130–137.
- Vogel, R. M., and C. N. Kroll. 1992. Regional geohydrologic-geomorphic relationships for the estimation of low-flow statistics. *Water Resour. Res.* 28:2451–2458.
- Wells, C. S., and R. N. Harris. 2001. Activity level and the tradeoff between growth and survival in the salamanders *Ambystoma jeffersonianum* and *Hemidactylium scutatum*. *Herpetologica* 57:116–127.
- Werner, E. E. 1986. Amphibian metamorphosis: growth rate, predation risk, and the optimal size at transformation. *Am. Nat.* 128:319–341.
- West, G. B., J. H. Brown, and B. J. Enquist. 2001. A general model for ontogenetic growth. *Nature* 413:628–631.
- Wilbur, H. M., and J. P. Collins. 1973. Ecological aspects of amphibian metamorphosis. *Science* 182:1305–1314.



## Figures

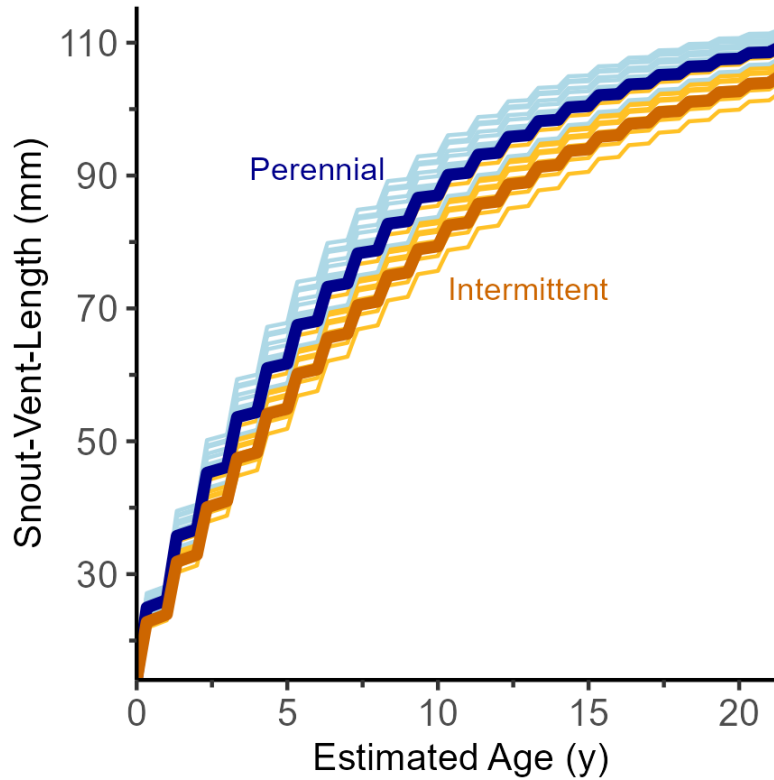


Figure 1. Difference between mean (bold lines) posterior parameter estimates for individual growth trajectories for *Gyrinophilus porphyriticus* from intermittent (0.32 km<sup>2</sup>; orange) and perennial watershed areas (1.39 km<sup>2</sup>; blue) at the Hubbard Brook Experimental Forest, New Hampshire, USA. Growth was estimated with a von Bertalanffy growth function. The stepped profile of the lines represents the lack of growth during the inactive season (October – May). Unbolded (small) colored lines represent 10 randomly selected posterior predictive outputs for each watershed area.

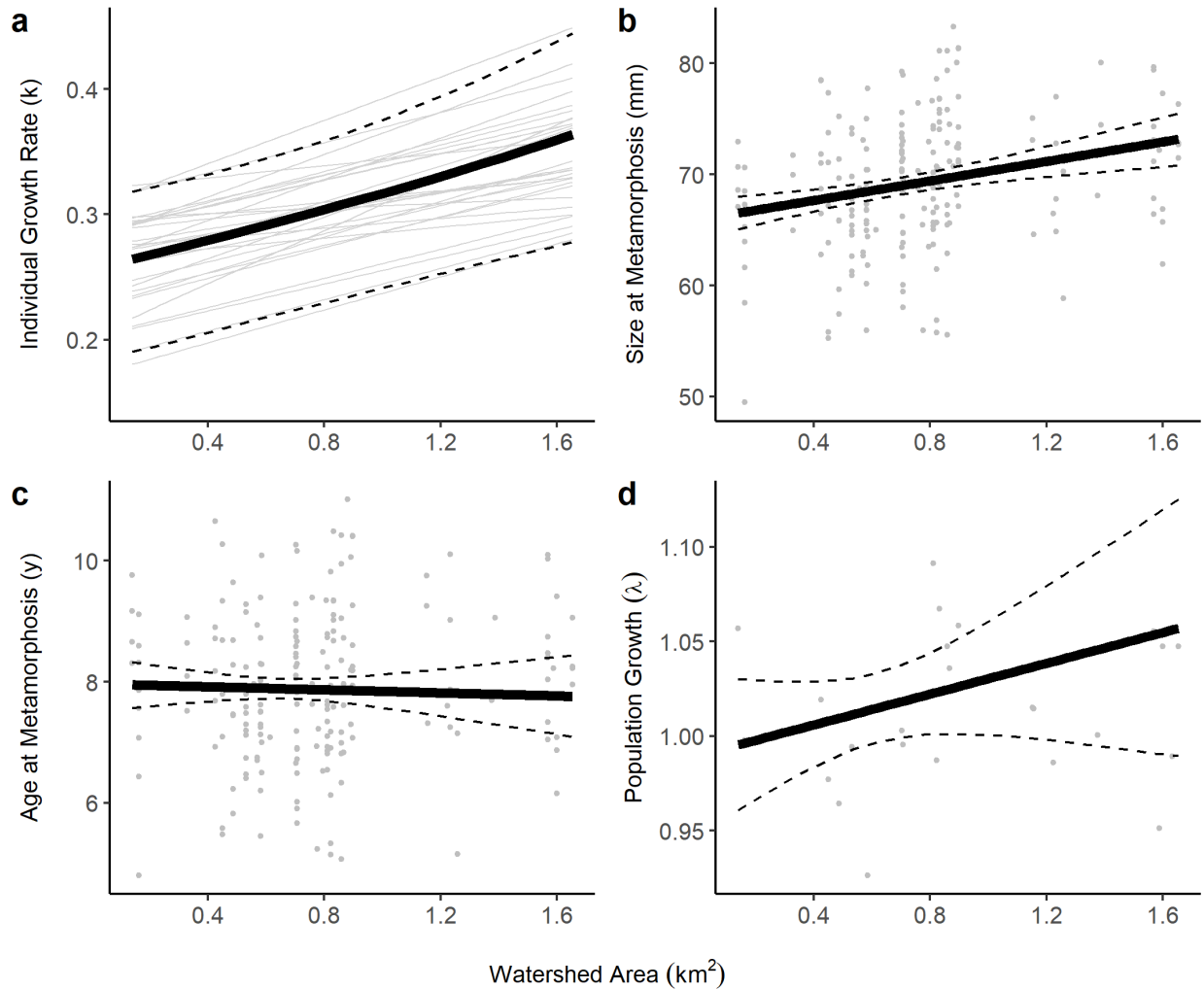


Figure 2. Effect of watershed area, on the individual growth rate ( $k$ ) (a); size (SVL) at metamorphosis (b), age at metamorphosis (c), and the population growth rate ( $\lambda$ ) of *Gyrinophilus porphyriticus* at the Hubbard Brook Experimental Forest, New Hampshire, USA. Solid, black lines represent estimated mean and dotted, black lines represent 95% credible intervals for all posterior parameter estimates. Gray points represent SVL data (b), estimated age of metamorphic individuals (c), and mean  $\lambda$  estimates for each stream reach (d). Also included are 30 randomly selected posterior predictive  $k$  outputs (grey lines; a).

## Appendix S1

### *Study design*

The HBEF is well-suited for characterizing headwater streamflow variability because there are gauged weirs on nine headwater streams that began recording daily discharge readings in 1956 (Bailey et al. 2003). Streams at the HBEF typically have the lowest streamflow in August, when transpiration is high (Likens and Bormann 1995, Bailey et al. 2003). However, intense rainstorms may occur throughout the year (Fig. S1). Stream hydrographs in the HBEF are flashy, where streams respond to precipitation events with a sharp peak and a quick return to baseflow (Campbell et al. 2011).

Our analyses are based on data from 58 (60 – 100 m) study reaches across 10 first through fourth-order streams. This included 50 100-m contiguous reaches across five headwater streams and an additional eight 60-m isolated reaches across another five streams. At contiguous reaches we used long-term mark-recapture survey data designed to compare salamander survival and performance along environmental gradients in streams (Lowe et al. 2018, Addis and Lowe 2020). These surveys occurred in five headwater streams, where each stream was divided into upstream and downstream survey sections, each 500 m in length. Because discharge increases quickly as you move downstream, we split each 500-m survey section into five contiguous 100-m reaches to quantify the streamflow conditions experienced by individual salamanders that have small 3-5 m<sup>2</sup> home ranges (Lowe 2003) more precisely. Additionally, to increase independence among study reaches, we completed surveys at eight 60-m isolated reaches across five other streams. These isolated reaches were chosen to expand the range of watershed sizes included in our analyses. *Salvelinus fontinalis* (brook trout) occurred in 16 study reaches (Warren et al. 2008, Lowe et al. 2018).

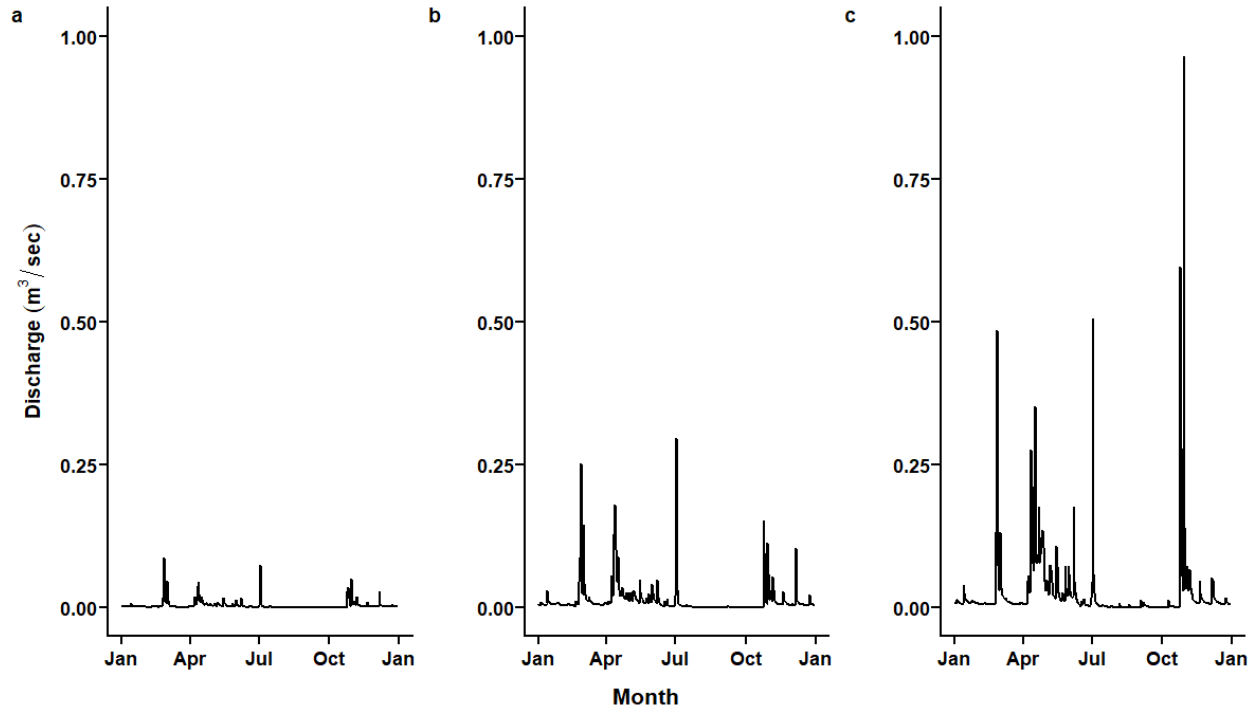
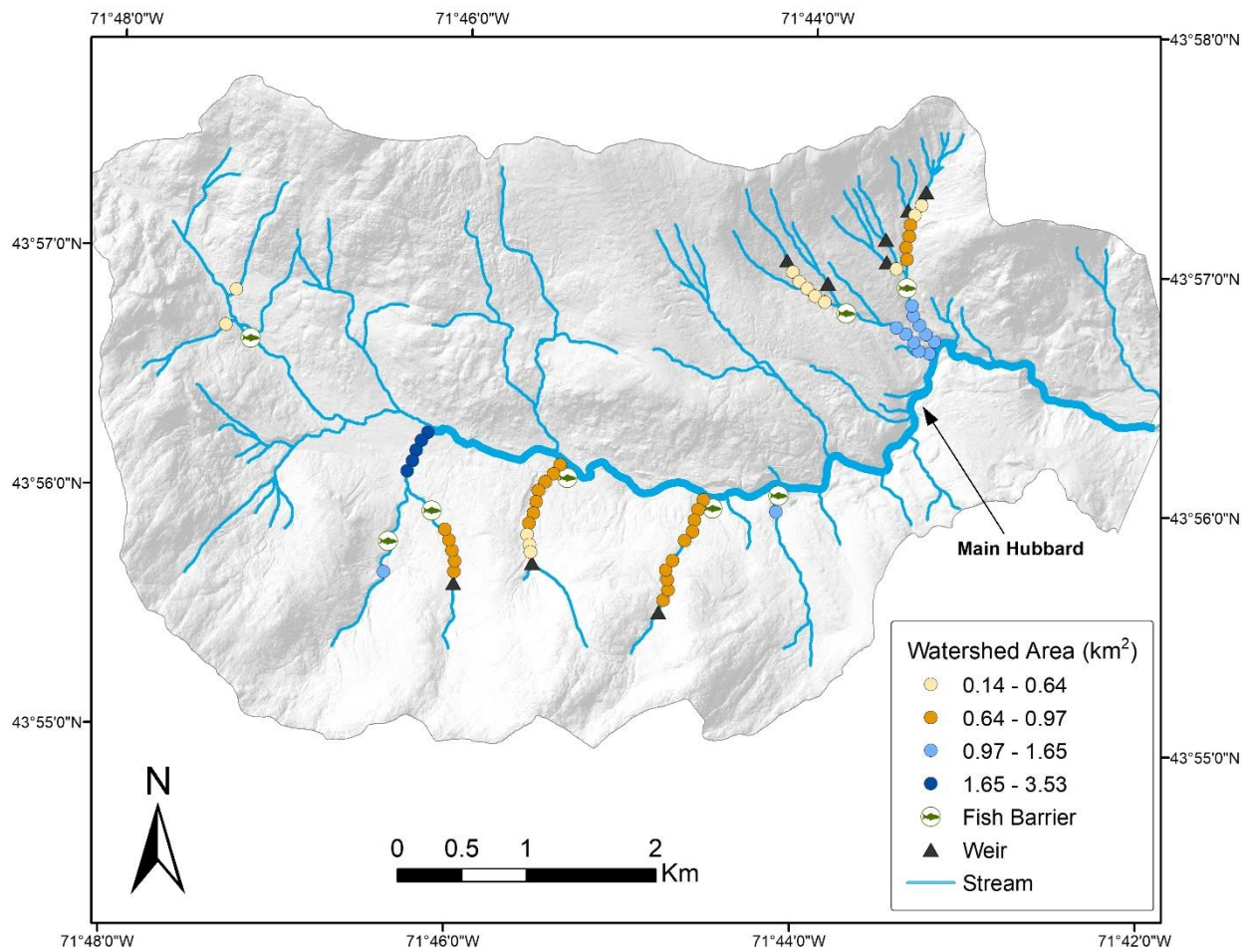


Figure S1. Comparison of stream hydrographs for the year 2017 for three gauged weirs of different watershed areas at the Hubbard Brook Experimental Forest, New Hampshire, USA. Includes Weir 1 (0.12 km<sup>2</sup>), Weir 4 (0.36 km<sup>2</sup>), and Weir 7 (0.78 km<sup>2</sup>).



### *Survey schedule*

We conducted mark-recapture surveys of contiguous reaches nine times each field season, from June – September. This included 27 repeat surveys across two streams (20 reaches) from 2012 – 2014, and 72 repeat surveys across three streams (30 reaches) from 2012 – 2015 and 2018 – 2021 (Lowe et al. 2018, Addis and Lowe 2020). In each survey, a constant search effort was maintained by turning one cover object per meter of stream length (Heyer et al. 1994). We conducted surveys of isolated reaches weekly throughout the June – September field season. Four of these reaches were surveyed 46 times from 2019 – 2021, and four additional sites were added in 2020 and surveyed 30 times from 2020 – 2021.

### *Salamander capture*

At contiguous reaches from 2012 – 2015, salamanders > 30 mm snout-vent-length (SVL) were marked with visual implant elastomer (Northwest Marine Technology, Inc., Anacortes, Washington, USA). From 2018 – 2021, salamanders > 35 mm SVL were marked with 8 mm passive integrated transponders (PIT-tags; Hecere Electronic Col, Ltd., Quanzhou, China; Connette and Semlitsch 2012). At the eight isolated reaches, salamanders > 50 mm SVL were marked with 12 mm PIT-tags (HPR Plus reader, BP Lite portable antenna, Biomark Inc., Boise, ID, USA), which allowed us to relocate them using portable antennas (i.e., PIT-tag telemetry), as opposed to direct capture (Ousterhout and Semlitsch 2014). Therefore, surveys included initial active search sampling, followed by repeat PIT-tag telemetry surveys. Telemetry surveys increased detection rates compared to traditional capture methods (Cucherousset et al. 2008, Connette and Semlitsch 2012), so we only recaptured and processed each individual once per month to avoid over-handling. We measured SVL from photographs with ImageJ 1.50i software (Schneider et al. 2012).

### *Quantifying watershed area*

To test whether watershed area ( $\beta_{Area}$ ) at the nine gauged weirs across the HBEF predicts the annual frequency of days with no flow ( $Q_{no\ flow}$ ), we fit a Bayesian linear model with a gamma distribution (Equation 1). We used a gamma distribution because its lower bound is zero and the distribution can vary in shape.

$$Q_{no\ flow} \sim \text{Gamma}(\mu, \text{shape}) \quad (1)$$

$$\log(\mu) \sim \beta_0 + \beta_{Area}$$

We specified weakly informative priors for all parameters, including a normal prior (mean = 0, SD = 5) for  $\beta_{Area}$ , a normal prior (mean = -3, SD = 5) for the intercept ( $\beta_0$ ), and a gamma prior (shape = 1, scale = 2) for  $\text{shape}$ . To test whether watershed area predicts minimum discharge ( $Q_5$ ), or the discharge that was exceeded over 95% of the historical record, we fit a Bayesian linear model with a Gaussian distribution (Equation 2).

$$\log(Q_5) \sim N(\beta_0 + \beta_{Area}, \sigma^2) \quad (2)$$

We specified weakly informative priors for all parameters, including a normal prior (mean = 0, SD = 5) for  $\beta_{Area}$ , a normal prior (mean = -3, SD = 5) for  $\beta_0$ , and half-normal prior (mean = 2.3, SD = 5) for  $\sigma^2$ . Both models were implemented in the brms package and consisted of two chains and 2000 iterations (Bürkner 2021).

### Estimating Growth

To model growth and estimate age-at-length of *G. porphyriticus*, we fit a von Bertalanffy (VB) growth function to individual body size data using a Bayesian hierarchical modeling approach that accounts for measurement error ( $\epsilon$ ). The VB growth function estimates two primary parameters: the asymptotic size that individuals grow toward as they age ( $a$ ; mm), and a growth rate coefficient ( $k$ ), which defines how rapidly individuals approach  $a$ . We separated  $k$  into active season growth ( $k_{active}$ ) and inactive season growth ( $k_{inactive}$ ). Using this parameterization, Equation 3 represents the body size ( $S$ ; mm) of an individual at age ( $t$ ; yrs), given a parameter ( $b$ ) that relates hatchling size to asymptotic size, such that hatchling size =  $a(1-b)$ .

$$S_t = a \left( 1 - b e^{\left( -k_{active} \frac{days}{365} - k_{inactive} \frac{days}{365} \right)} \right) + \epsilon \quad (3)$$

We set the initial hatchling size of *G. porphyriticus* at 14 mm SVL based on historic observations (Bruce 1980, 2005). These season-specific growth rates were calculated given the interval between captures (number of days) but scaled for 365-day (1-y) increments. Because we were characterizing growth over time, we only included individuals recaptured at least once in our analysis. We incorporated a log-link function (Equation 4) to estimate the fixed effects of environmental conditions, including watershed area ( $\beta_{area}$ ), fish presence ( $\beta_{fish}$ ) and stream ( $\beta_{stream}$ ), on  $k_{active}$ .

$$\log(k_{active}) = \beta_0 + \beta_{area} + \beta_{fish} + \beta_{stream} \quad (4)$$

All continuous covariates were scaled and centered prior to model fitting. We assigned weakly informed priors to all parameters, including uniform priors (min = -12, max = 0) to  $\beta_0$  (to describe both  $k_{active}$  and  $k_{inactive}$ ), normal priors (mean = 0; variance = 1) to all fixed effects on  $k$  (e.g.,  $\beta_{area}$ ,  $\beta_{fish}$ , and  $\beta_{stream}$ ), uniform priors for asymptotic sizes ( $a$ ; adult: min = 80 mm, max = 130 mm; larval: min = 50 mm, max = 100 mm), and a Gamma prior (shape and rate = 0.001) for measurement error precision ( $\epsilon$ ; such that SD for measurement error =  $1/\sqrt{\epsilon}$ ). Because our capture-recapture data had limited repeat samples per individual (proportion of individuals with only a single measurement = 70%), a parameter to describe individual variation on  $k$  could not converge.

As temperature affects growth in plethodontids (Keen et al. 1984, Beachy 2018), we also fit a second VB growth model to estimate the effect of maximum stream temperature on *G. porphyriticus* growth rate. We placed HOBO temperature loggers (Onset Computer Corporation, Bourne, MA, USA) in each of the eight isolated reaches and recorded hourly stream temperatures from June 2020 – September 2021. We fit a separate growth model for temperature because our temperature dataset only overlapped with a small portion of the growth dataset.

### Quantifying size at metamorphosis

Equation 5 represents the Bayesian linear mixed model we fit to describe the fixed effect of watershed area ( $B_{area}$ ) on size at metamorphosis ( $SVL_m$ ). For each of the nine streams ( $j$ ), we estimated  $\beta_j$  or a stream-specific mean SVL.

$$SVL_m \sim N(\beta_0 + \beta_j + B_{area} + B_{fish}, \sigma^2) \quad (5)$$

$$\beta_j \sim N(\mu, \sigma_{site}^2)$$

We assumed all  $SVL_m$  measurements were normal random variables ( $N$ ), with a mean of expected size ( $B_0$ ), variation in that mean due to watershed area and the presence of fish ( $B_{fish}$ ), and an estimated variance ( $\sigma^2$ ). The mean SVL for each stream was also drawn from a normal distribution with its own mean ( $\mu$ ) and estimated variance ( $\sigma_{site}^2$ ). All continuous covariates were scaled and centered prior to model fitting. We assigned weakly informed priors to all parameters, including a normal prior (mean = 0; variance = 1) to  $B_{area}$ , a normal prior (mean = 0, variance = 5) for  $B_{fish}$ , and based on previous analyses (Bruce 1980) a normal prior (mean = 65, variance = 25) to  $B_0$ . We also assigned a uniform prior (min = 0, max = 100) for  $\sigma^2$  and a uniform prior (min = 0, max = 100) for  $\sigma_{site}^2$ .

#### *Age at metamorphosis model*

To estimate age at metamorphosis, we rearranged Equation 3 to solve for  $t$  (age in years) given an observed size at metamorphosis ( $S_m$ ) for each individual and their specific location (Equation 4). Thus, age at metamorphosis ( $t_m$ ) for each *G. porphyriticus* was estimated by determining the specific position of  $S_m$  on the mean fitted larval VB growth curve (Ogle and Isermann 2017). To then model the effect of watershed area ( $B_{area}$ ) on age at metamorphosis we used Equation 6. For any stream,  $j$ , we estimated  $\beta_j$  or a stream-specific mean age at metamorphosis.

$$t_m \sim N(\beta_0 + \beta_j + B_{area} + B_{fish}, \sigma^2) \quad (6)$$

$$\beta_j \sim N(\mu, \sigma_{site}^2)$$

We assumed all  $t_m$  estimates were normal random variables ( $N$ ), with a mean of expected age ( $B_0$ ), variation in that mean due to watershed area and the presence of fish ( $B_{fish}$ ), and an estimated variance ( $\sigma^2$ ). The mean age at metamorphosis for each stream was also drawn from a normal distribution with its own mean ( $\mu$ ) and estimated variance ( $\sigma_{site}^2$ ). All continuous covariates were scaled and centered prior to model fitting. We assigned weakly informed priors to all parameters, including a normal prior (mean = 0; variance = 1) to  $B_{area}$ , a normal prior (mean = 0, variance = 5) for  $B_{fish}$ , and based on previous analyses (Bruce 1980) a normal prior (mean = 4, variance = 4) to  $B_0$ . We also assigned a uniform prior (min = 0, max = 25) for  $\sigma^2$  and a uniform prior (min = 0, max = 25) for  $\sigma_{site}^2$ .

#### *Estimating population growth*



We used a Bayesian formulation of the Pradel model (Tenan et al. 2014, Saracco et al. 2020) to estimate annual population growth rate ( $\lambda$ ), annual apparent survival probability ( $\phi$ ), and annual detection probability ( $p$ ) for each stream reach. The Pradel model combines standard-time and reverse-time approaches to individual recapture data within the same likelihood, allowing the estimation of both survival and recruitment parameters, and thus allowing inference on population growth rate (Pradel 1996). To meet the assumptions of the model, we only used the last 6 mark-capture periods for each summer from contiguous reaches to ensure closure and consistent sampling technique. To ensure estimable parameter estimates, only reaches with  $> 3$  years of mark-recapture data and  $> 5$  individuals were included in this analysis. This included a total of 29 reaches across three streams. We set  $p = 0$  in 2016 and 2017 when no surveys occurred. We assigned a uniform prior between 0 and 3 for  $\lambda$ , a uniform prior between 0.02 and 0.95 for  $\phi$ , and a uniform prior between 0.01 and 0.40 for  $p$ .

To then model the effect of watershed area ( $B_{area}$ ) on population growth rate ( $\lambda$ ), we used Equation 7. For each of the three streams,  $j$ , we estimated  $\beta_j$  or a stream-specific  $\lambda$ .

$$\lambda \sim N(\beta_0 + \beta_j + B_{area} + B_{fish}, \sigma^2) \quad (7)$$

$$\beta_j \sim N(\mu, \sigma_{site}^2)$$

We assumed all stream-specific  $\lambda$  estimates were normal random variables ( $N$ ), with a mean of expected  $\lambda$  ( $B_0$ ), variation in that mean due to watershed area and the presence of fish ( $B_{fish}$ ), and an estimated variance ( $\sigma^2$ ). The mean  $\lambda$  for each stream was also drawn from a normal distribution with its own mean ( $\mu$ ) and estimated variance ( $\sigma_{site}^2$ ). All continuous covariates were scaled and centered prior to model fitting. We assigned weakly informed priors to all parameters, including normal priors (mean = 0; variance = 1) to  $B_{area}$  and  $B_{fish}$ , and a normal prior (mean = 1, variance = 0.5) to  $B_0$ . We also assigned a uniform prior (min = 0, max = 1) for  $\sigma^2$  and a uniform prior (min = 0, max = 1) for  $\sigma_{site}^2$ .

### *Model fitting and analyses*

We generated three chains for each model. This included 250,000, 40,000, and 40,000 iterations for the growth, size at metamorphosis, and age at metamorphosis models, respectively. We included 70,000 iterations for each model to describe reach-specific population growth parameters, and 40,000 iterations to then model the effect of watershed area on population all growth rate estimates. We thinned all iterations by a rate of 5. We included burn-ins for each model such that we only retained 2,000 iterations from each chain to estimate all posterior distributions. All models we fit using the package *R2jags* (Su and Yajima 2020).

### *Literature Cited*

- Addis, B. R., and W. H. Lowe. 2020. Long-term survival probability, not current habitat quality, predicts dispersal distance in a stream salamander. *Ecology* 101:1–14.
- Bailey, A. S., J. W. Hornbeck, J. L. Campbell, and C. Eagar. 2003. Hydrometeorological database for Hubbard Brook Experimental Forest: 1955-2000. Newtown Square, PA, USA.

- Barr, G. E., and K. J. Babbitt. 2007. Trout affect the density, activity and feeding of a larval plethodontid salamander. *Freshwater Biology* 52:1239–1248.
- Beachy, C. K. 2018. Effects of growth rate and temperature on metamorphosis in *Eurycea wilderae* (Caudata, Plethodontidae, Hemidactyliinae, Spelerpini; Blue Ridge Two-lined Salamander). *Southeastern Naturalist* 17:423–432.
- Bruce, R. C. 1980. A model of the larval period of the spring salamander, *Gyrinophilus porphyriticus*, based on size-frequency distributions. *Herpetologica* 36:78–86.
- Bruce, R. C. 2005. Theory of complex life cycles: application in Plethodontid salamanders. *Herpetological Monographs* 19:180.
- Bürkner, P. C. 2021. Bayesian item response modeling in R with brms and Stan. *Journal of Statistical Software* 100.
- Campbell, J. L., C. T. Driscoll, A. Pourmokhtarian, and K. Hayhoe. 2011. Streamflow responses to past and projected future changes in climate at the Hubbard Brook Experimental Forest, New Hampshire, United States. *Water Resources Research* 47:1–15.
- Connette, G. M., and R. D. Semlitsch. 2012. Successful use of a passive integrated transponder (PIT) system for below-ground detection of plethodontid salamanders. *Wildlife Research* 39:1–6.
- Cucherousset, J., P. Marty, L. Pelozuelo, and J. M. Roussel. 2008. Portable PIT detector as a new tool for non-disruptively locating individually tagged amphibians in the field: A case study with Pyrenean brook salamanders (*Calotriton asper*). *Wildlife Research* 35:780–787.
- Davenport, J. M., and W. H. Lowe. 2018. Testing for microgeographic effects on the strength of interspecific competition. *Copeia* 106:501–506.
- Heyer, W. R., M. A. Donnelly, R. W. McDiarmid, L. C. Hayek, and M. S. Foster. 1994. *Measuring and monitoring biodiversity: standard methods for amphibians*. Smithsonian Institution Press, Washington, DC.
- Keen, W. H., J. Travis, and J. Juilianna. 1984. Larval growth in three sympatric Ambystoma salamander species: species differences and the effects of temperature. *Canadian Journal of Zoology* 62:1043–1047.
- Likens, G. E., and F. H. Bormann. 1995. *Biogeochemistry of a Forested Ecosystem*. 2nd edition. Springer-Verlag, New York.
- Lowe, W. H. 2003. Linking dispersal to local population dynamics: a case study using a headwater salamander system. *Ecology* 84:2145–2154.
- Lowe, W. H., B. R. Addis, M. R. Smith, and J. M. Davenport. 2018. The spatial structure of variation in salamander survival, body condition and morphology in a headwater stream network. *Freshwater Biology* 63:1287–1299.
- Ogle, D. H., and D. A. Isermann. 2017. Estimating age at a specified length from the von Bertalanffy growth function. *North American Journal of Fisheries Management* 37:1176–1180.
- Ousterhout, B. H., and R. D. Semlitsch. 2014. Measuring terrestrial movement behavior using passive integrated transponder (PIT) tags: Effects of tag size on detection, movement, survival, and growth. *Behavioral Ecology and Sociobiology* 68:343–350.
- Pradel, R. 1996. Utilization of capture-mark-recapture for the study of recruitment and population growth rate. *Biometrics* 52:703–709.
- Saracco, J. F., L. Helton, J. Liske-Clark, and P. Radley. 2020. Recent dynamics and trends of landbird populations on Saipan, Northern Mariana Islands. *Pacific Science* 74:319–329.

- Schneider, C. A., W. S. Rasband, and K. W. Eliceiri. 2012. NIH Image to ImageJ: 25 years of image analysis. *Nature Methods* 9:671–675.
- Semasko, A. J. 2013. Size and age variation of larval *Gyrinophilus porphyriticus porphyriticus* in sympatry with *Salvelinus fontinalis*. Ph.D. dissertation. Marshall University.
- Su, Y.-S., and M. Yajima. 2020. R2jags: a package for running jags from R.
- Tenan, S., R. Pradel, G. Tavecchia, J. M. Igual, A. Sanz-Aguilar, M. Genovart, and D. Oro. 2014. Hierarchical modelling of population growth rate from individual capture-recapture data. *Methods in Ecology and Evolution* 5:606–614.
- Warren, D. R., G. E. Likens, D. C. Buso, and C. E. Kraft. 2008. Status and distribution of fish in an acid-impacted watershed of the Northeastern United States (Hubbard Brook, NH). *Northeastern Naturalist* 15:375–390.

## Appendix S2

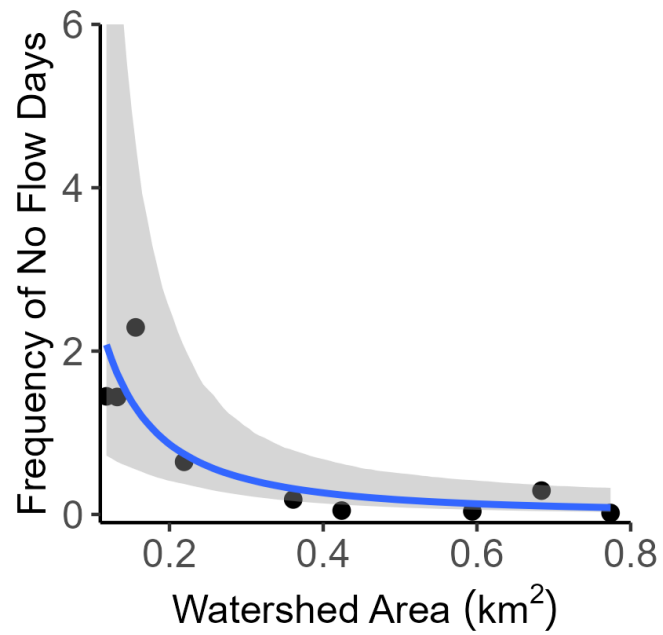


Figure S1. Negative relationship (blue line) between watershed area and the annual frequency of zero discharge days at nine gauged weirs on headwater streams at the Hubbard Brook Experimental Forest, New Hampshire, USA. Black dots represent data and grey ribbon represents the 95% credible interval.

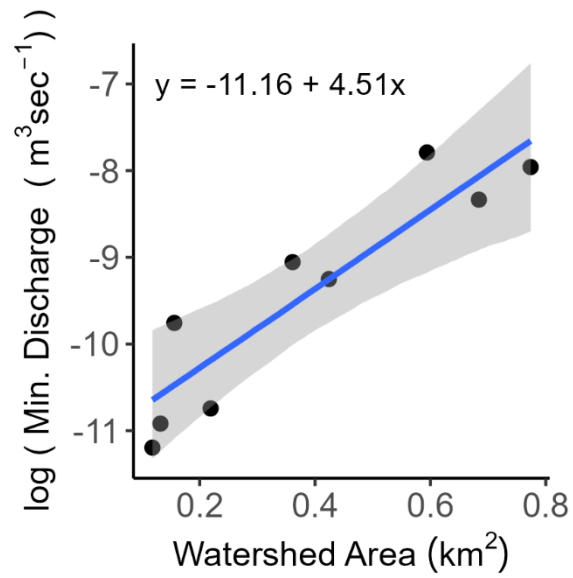


Figure S2. Positive relationship (blue line) between watershed area and minimum discharge at nine gauged weirs on headwater streams at the Hubbard Brook Experimental Forest, New Hampshire, USA. Minimum discharge was calculated as the minimum annual discharge (Q5), or discharge which was exceeded for 95% of the historical record. Black dots represent data and grey ribbon represents the 95% credible interval.

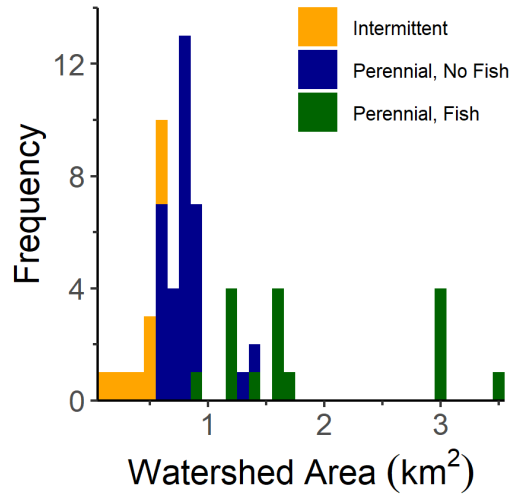


Fig. S3. Frequency distribution of watershed areas of study reaches at the Hubbard Brook Experimental Forest, New Hampshire, USA. Each of the 58 reaches is colored to represent dominant hydrology (intermittent [orange] v. perennial [blue and green]) and occurrence of predatory brook trout (*Salvelinus fontinalis*) within perennial reaches (fish absent [blue] v. fish present [green]). Dominant hydrology and trout occurrence were based on field observations and fish sampling before and during the eight years of sampling (2012 – 2015, 2018 – 2021). Intermittent-reaches typically stopped flowing in late summer. Perennial-reaches maintained flow year-round.

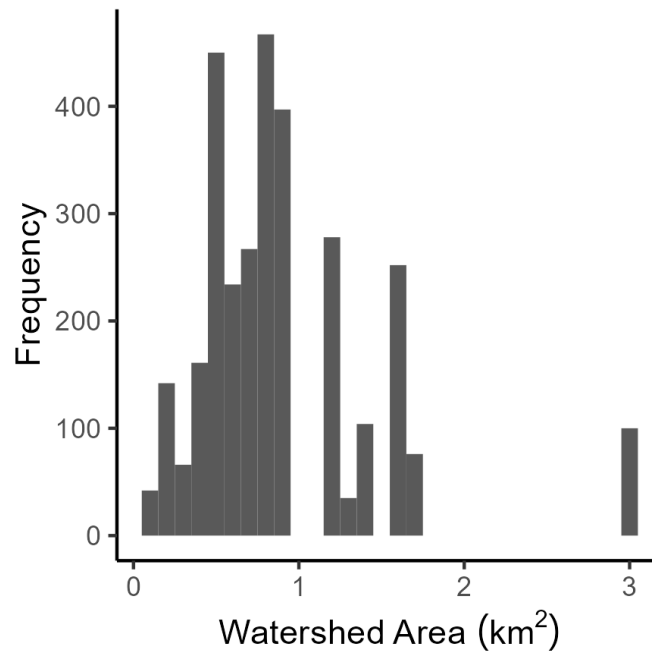


Figure S4. Frequency distribution for the watershed areas of *Gyrinophilus porphyriticus* observations ( $n = 3071$ ) from the Hubbard Brook Experimental Forest, New Hampshire, USA. Due to limited observations at the largest watersheds, we restricted inference on growth rates to individuals from reaches with watershed areas  $\leq 1.66$  km<sup>2</sup>.

## Appendix S3

Table S1. Mean and 95% credible interval (LCI, HCI) posterior parameter estimates for a von Bertalanffy growth model for *Gyrinophilus porphyriticus* captures in 53 study reaches at the Hubbard Brook Experimental Forest, New Hampshire, USA. Growth models are based on all individuals (a), only larval individuals (b), and only adult individuals (c). Parameters include asymptotic body size (SVL) ( $a$ ), mean growth rates specific to the active ( $k_{\text{active}}$ ) or inactive season ( $k_{\text{inactive}}$ ), the effect of watershed area on growth rate ( $\beta_{\text{area}}$ ), the effect of fish on growth rate ( $\beta_{\text{fish}}$ ), and the standard deviation for measurement error ( $\sigma$ ). Watershed areas varied from 0.14 to 1.66 km<sup>2</sup>.

### A. All captures

Parameter	Mean	LCI	HCI
a	115.68	110.53	122.06
$k_{\text{active}}$	0.30	0.22	0.37
$\beta_{\text{area}}$	0.09	0.03	0.16
$\beta_{\text{fish}}$	-0.17	-0.33	-0.02
$k_{\text{inactive}}$	0.00	0.00	0.06
$\sigma$	3.81	3.69	3.94

### B. Larvae only

Parameter	Mean	LCI	HCI
a	80.40	76.24	85.71
$k_{\text{active}}$	0.52	0.33	0.78
$\beta_{\text{area}}$	0.20	0.08	0.36
$\beta_{\text{fish}}$	-0.56	-0.99	-0.25
$k_{\text{inactive}}$	0.08	0.00	0.19
$\sigma$	3.25	3.41	3.12

### C. Adult only

Parameter	Mean	LCI	HCI
a	113.89	105.38	125.43
$k_{\text{active}}$	0.43	0.28	0.63
$\beta_{\text{area}}$	0.14	-0.08	0.35
$\beta_{\text{fish}}$	-0.86	-1.40	-0.37
$k_{\text{inactive}}$	0.00	0.00	0.03
$\sigma$	3.79	4.07	3.56



Table S2. Mean and 95% credible interval (LCI, HCI) posterior parameter estimates to describe the effect of watershed area ( $\beta_{\text{area}}$ ) on size at metamorphosis (SVL) for *Gyrinophilus porphyriticus* in 53 study reaches at the Hubbard Brook Experimental Forest, New Hampshire, USA. Parameters estimates include mean size ( $\beta_0$ ; mm) and standard deviation for size ( $\sigma$ ). Watershed areas varied from 0.14 to 1.66 km<sup>2</sup>.

<b>Parameter</b>	<b>Mean</b>	<b>LCI</b>	<b>HCI</b>
$\beta_0$	69.30	68.38	70.21
$\beta_{\text{area}}$	1.55	0.55	2.52
$\beta_{\text{fish}}$	-0.87	-3.66	1.82
$\sigma$	5.91	5.34	6.56

Table S3. Mean and 95% credible interval (LCI, HCI) posterior parameter estimates to describe the effect of watershed area ( $\beta_{\text{area}}$ ) on age at metamorphosis (SVL) for *Gyrinophilus porphyriticus* in 53 study reaches at the Hubbard Brook Experimental Forest, New Hampshire, USA.

Parameters estimates include mean age ( $\beta_0$ ; yrs), standard deviation for age ( $\sigma$ ), the effect of fish ( $\beta_{\text{fish}}$ ) on age at metamorphosis. Watershed areas varied from 0.14 to 1.66 km<sup>2</sup>.

<b>Parameter</b>	<b>Mean</b>	<b>LCI</b>	<b>HCI</b>
$\beta_0$	7.87	7.65	8.09
$\beta_{\text{area}}$	-0.04	-0.32	0.23
$\beta_{\text{fish}}$	0.49	-0.33	1.29
$\sigma$	1.27	1.15	1.41

Table S4. Mean and 95% credible interval (LCI, HCI) posterior parameter estimates to describe the effect of watershed area on population growth rate ( $\lambda$ ) for *Gyrinophilus porphyriticus* across 29 study reaches at the Hubbard Brook Experimental Forest, New Hampshire, USA. Parameters estimates include mean population growth rate ( $\beta_0$ ), standard deviation for population growth rate ( $\sigma$ ), and the linear effect of watershed area ( $\beta_{\text{area}}$ ) and fish ( $\beta_{\text{fish}}$ ). Watershed areas varied from 0.14 to 1.66 km<sup>2</sup>.

<b>Parameter</b>	<b>Mean</b>	<b>LCI</b>	<b>HCI</b>
$\beta_0$	1.03	1.00	1.06
$\beta_{\text{area}}$	0.02	-0.02	0.05
$\beta_{\text{fish}}$	-0.03	-0.10	0.04
$\sigma$	0.04	0.03	0.06

## CHAPTER 2: Floods increase downstream movement of adult and larval life stages of a headwater stream salamander

Madaline M. Cochrane<sup>1,\*</sup> and Winsor H. Lowe<sup>1</sup>

1. Division of Biological Sciences, University of Montana, Missoula, MT, USA

### Abstract

Climate change is increasing the frequency and intensity of flood events, which will likely have disproportionate effects on freshwater organisms. Salamanders are often top predators in the small, fishless headwater streams that are highly responsive to hydrologic changes. Although these salamanders persist in dynamic stream environments, we lack the empirical understanding of how they respond to flooding intensity that would allow us to predict future responses to climate-related changes in hydrology. We used three years of passive-integrated-transponder (PIT-tag) surveys to better understand how flooding affects movement in *Gyrinophilus porphyriticus*, the northern spring salamander, in eight headwater stream reaches. We found that downstream movement probability increased with discharge, and adult *G. porphyriticus* moved downstream more frequently than larvae during floods. We also found that the probability of terrestrial refuge use by adults increased with discharge and in stream reaches with steep channel slopes. In contrast, upstream movement probability decreased with channel slope. Adults also moved upstream more frequently than larvae. Both downstream and upstream movement distances were unrelated to discharge conditions. Overall, we suggest that headwater salamanders will move downstream as flood frequency and magnitude increase. We believe these increases in downstream movement may be associated with increased mortality due to the physical effects of flooding, and due to exposure to fish predators in downstream reaches. The ability to exploit in-stream and terrestrial refugia during flooding will likely be crucial to the persistence of stream salamanders and other headwater specialists.

### Introduction

Extreme climatic events are becoming more common with climate change (IPCC 2021, Rodell and Reager 2023), including increases in the frequency, intensity, and volume of precipitation events (Hoerling et al. 2016). For example, heavy precipitation events increased in intensity by 6 to 7% for each °C of temperature increase (Easterling et al. 2017). These changes in precipitation coincide with similar changes in the frequency and intensity of flood events (Chegwidden et al. 2020, Tabari 2020), which will undoubtedly shape the demography, ecology, and evolution of stream organisms in the coming decades (Pujolar et al. 2011, McMullen and Lytle 2012, Letcher et al. 2015).

Flooding is a key factor underlying variation in freshwater biodiversity (Resh et al. 1988, Woodward et al. 2010). Organisms that inhabit streams and rivers evolved to withstand flood events (Lytle and Poff 2004), and the diverse behavioral, morphological, and life history adaptations that provide this resilience are well documented (Resh et al. 1988, Poff and Allan

1995, Lake 2003). Some organisms even require floods for dispersal into previously unavailable habitats (Schofield et al. 2018), and benefit from flood-related increases in productivity, hydrologic connectivity, and removal of competitors (Leigh et al. 2015). However, we also know that many species persist at the limits of flood tolerance (Fritz and Dodds 2004, Thurman et al. 2020), and that pushing species beyond these limits can cause population and community-level consequences (Walls et al. 2013, Michel et al. 2017). As flooding intensity continues to increase, it is critical that we gain a more precise understanding of these limits, and of the specific behavioral and demographic effects of flooding on freshwater species.

Headwater streams are particularly hydrologically dynamic (Wohl 2017, Richardson 2019), and may be the first place we see the ecological consequences of increasing flood intensities (Cover et al. 2010, Chegwiddden et al. 2020). Because headwater streams have small watersheds, often steep elevation gradients, and lack floodplains, they are highly responsive to water inputs (Richardson and Danehy 2007, Campbell et al. 2011). Consequently, streamflow may range from ephemeral conditions during drought, to floods – both seasonal and following precipitation events – that increase volume by as much as 400 percent, often in short periods of time (Bailey et al. 2003, Datry et al. 2014, Johnson et al. 2022). Headwater streams also account for the majority of stream channel length worldwide (Downing et al. 2012), and are home to diverse communities of fish, amphibians, and invertebrates (Meyer et al. 2007).

Salamanders in the family Plethodontidae, the lungless salamanders, are often the top predators in fishless headwater streams of eastern North America, where they contribute to a global hotspot of salamander diversity (Petranka 1998). These salamanders require moisture to survive (Feder 1983), but thrive in headwater stream environments that are too hydrologically dynamic to support fish (Davic and Welsh 2004). Broadly, this tolerance of variable streamflow is likely a consequence of a complex life history, where larvae are exclusively aquatic and adults are semi-aquatic, but able to leave the stream for short periods of time (Petranka 1998). Both stages also have morphological and behavioral traits that allow them to access refuges in the streambed during high and low flows (Feral et al. 2005, Martin et al. 2012). Despite these traits, several studies suggest that stream salamanders may be vulnerable to intensifying floods and droughts (Price et al. 2012, Lowe et al. 2019), although the proximate mechanisms underlying these negative demographic effects remain unresolved (Walls et al. 2013).

Our goal was to address this gap in our understanding of the proximate effects of floods by testing how flooding affects movement along stream channels and into the riparian zone by the headwater stream salamander *Gyrinophilus porphyriticus*, the northern spring salamander. A better understanding of where, when, and why species move is crucial for effective conservation management. For instance, this information will help to identify critical habitat attributes for resilient stream populations, including the dimensions of riparian buffers (Crawford and Semlitsch 2007) and the optimal spatial configuration of occupied reaches on the landscape (Campbell Grant et al. 2010, Sinsch 2014). Understanding the relationship between flooding and movement will also help in isolating environmental triggers for dispersal that lead to changes in gene flow (Baguette et al. 2013) and range shifts (Travis et al. 2013). Finally, this information will help in assessing the threat posed by catastrophic drift, where strong flood events restructure the streambed, leading to high mortality and downstream displacement in stream organisms (Reinhardt et al. 2018).

In this study, we quantified how flooding affects the movement by larval and adult life stages of a headwater stream salamander. We conducted weekly passive integrated transponder (PIT-tag) surveys of eight fishless stream reaches to compare *G. porphyriticus* movement across a range of discharge conditions. With data from those surveys, we tested three interrelated predictions. First, we predicted that *G. porphyriticus* move downstream during flood events, with the largest floods leading to the highest probability and distance of downstream movements, particularly for larval individuals. Second, we predicted that *G. porphyriticus* compensates for downstream movements during floods by increasing the probability and distance of upstream movements during periods of reduced flow. And last, we predicted that the probability of terrestrial habitat use by *G. porphyriticus* adults increases during floods as they seek refuge from high shear forces within the stream channel. Overall, this research will help identify behavioral adaptations and vulnerabilities of stream salamanders to flood-related disturbances.

## Methods

### *Study organism*

*Gyrinophilus porphyriticus* is a lungless salamander (family Plethodontidae) that lives in small, cool, well-oxygenated streams along the Appalachian uplift in the eastern United States (Petranka 1998). This species has a biphasic life cycle. Larvae are restricted to aquatic environments because they respire with external gills. During metamorphosis, larvae transform into an adult body form and lose their external gills (Petranka 1998). Adults respire cutaneously, so require moist conditions to survive (Feder 1983). Adults are most often found in stream channels, springs, and seeps, but can also be found foraging terrestrially at night (Deban and Marks 2002, Greene et al. 2008). We do not know how extensively adults use terrestrial habitats during the day, including as a refuge to avoid flooding.

Lowe (2003) estimated *G. porphyriticus* home ranges to be approximately 3 m in channel length, but home range size has not been quantified directly. We know that *G. porphyriticus* larvae and adults move both downstream and upstream along the channel (Lowe et al. 2006a, Addis et al. 2019, Addis and Lowe 2020), and genetic data suggest that movement rates decline as stream slope increases (Lowe et al. 2006b). In addition, Lowe et al. (2006a) found that individuals with high body condition were more likely to move upstream and low-condition individuals were more likely to move downstream, suggesting that downstream movements may represent a cost rather than an optimal behavior. The effects of extrinsic factors on variation in movement directionality have not been assessed. However, *G. porphyriticus* adults return to their original position along streams after experimental displacement, suggesting that individuals benefit from the ability to home after movement (Deitchler et al. 2015).

### *Study site*

We conducted this research at the Hubbard Brook Experimental Forest (HBEF) in New Hampshire, USA (43°56'N, 71°45' W). We sampled eight 60-m reaches (i.e., sites) distributed across seven headwater streams within the 32-km<sup>2</sup> HBEF (Fig. 1). Sites were chosen based on their location above barriers to *Salvelinus fontinalis* (brook trout; Warren et al. 2008), known

presence of *G. porphyriticus* populations, and ease of access for repeat sampling. Watershed areas of the sites ranged from 0.33 to 1.38 km<sup>2</sup>, resulting in an expected range of absolute discharge (Bailey et al. 2003, Leopold 1994). Dominant stream channel morphology was step-pool, consisting of a regular series of steep steps spaced between deeper, slower-moving pools which maintain lower hydraulic stress (Montgomery and Buffington 1997). The HBEF streams have low conductivity (12.0 – 15.0 μS), slight acidity (pH of 5.0 – 6.0), and high dissolved oxygen content (> 95% saturation; Likens and Bormann 1995). Stream discharge has been recorded at the HBEF since 1957 (Bailey et al. 2003). Discharge in the HBEF streams typically peaks in the spring due to melting snow, but floods can occur throughout the year after isolated rainstorms. Base flows usually occur in late summer and early fall (Likens and Bormann 1995).

### *Survey methods*

*G. porphyriticus* were initially captured at all sites by haphazardly turning cover objects while walking up the stream and along the stream bank. We began tagging individuals at four sites in 2019 (Lower Canyon, Paradise, Upper Canyon, and Weir 4) and added an additional four sites in 2020 (Bagley, Cushman, Steep, and West Branch of Zigzag; Fig. 1). All captured *G. porphyriticus* were anesthetized in a water bath of tricaine methane sulfonate (MS-222; Peterman and Semlitsch 2006) before making a small incision in the skin anterior to the left hind limb to implant the passive integrated transponder (PIT-tag; APT12 PIT tag, Biomark, Boise, ID, U.S.A.; Connette and Semlitsch 2012). We used 12 mm PIT-tags, which increase recapture rates compared to smaller tags (Ousterhout and Semlitsch 2014). Only *G. porphyriticus* > 50 mm snout-vent length (SVL) were tagged. After recovery, all salamanders were released at their original capture location.

We conducted telemetry surveys for tagged *G. porphyriticus* individuals approximately every week from June through September of 2019 – 2021 with a PIT-tag antenna and wand (HPR Plus reader and BP Lite portable antenna, Biomark). Telemetry surveys included walking all habitat within the bankfull width of the channel, as indicated by evidence of scour (Radeck-Pawlik 2015), and 10 m-wide corridors of terrestrial habitat on both sides of the bankfull channel. All surveys occurred during the day. When the PIT-tag antenna detected an individual, we flipped the nearest cover objects to confirm the presence of the individual and determine its stage (larva or adult). We also recorded the individual's position along the stream channel as meters from the downstream end of the 60-m reach. Last, we recorded the lateral microhabitat of each individual: thalweg vs. wetted edge. We considered an individual to be in the thalweg if it was in the deepest part of the channel, whereas an individual in the wetted edge was along the stream margins, between the thalweg and bankfull edge. If an individual was located beyond the bankfull channel edges, we considered it to be in terrestrial habitat.

### *Quantifying movement events*

We quantified movements as the distance along the stream channel between subsequent detections. We only included movements  $\geq 2$  m, to target movements beyond an individual's home range. To test for effects of flooding on downstream and upstream movements, we also eliminated movements of individuals in terrestrial habitat. We limited all recapture intervals to  $\leq 30$  days to increase the temporal resolution of movement and associated hydrologic data, and

thereby increase the likelihood that movements reflected hydrology during the recapture interval. This limited inferences to the June – September sampling season. Because PIT-tags can be detected within the streambed after a mortality event that occurred outside of the sampling season, we only included movements if an individual was seen alive at least once during the sampling season. We also calculated the proportion of homing events after downstream movement. We defined homing as movement back to an individual's original location within 30 days. We also calculated 95% annual channel length home ranges for each individual.

### *Quantifying environmental controls on movement*

To quantify maximum discharge between *G. porphyriticus* detection events, we used instantaneous discharge readings collected every 5 minutes from the HBEF hydrologic reference stream (Paradise; USDA Forest Service 2022). We then scaled discharge by the watershed area of each site because we did not have discharge data specific to each site (Bailey et al. 2003). We also calculated the return interval and exceedance probability for annual peak floods based on maximum daily discharge data from the hydrologic reference stream from 1957 – 2021. We derived watershed areas at the mid-point of a site with 1-m Digital Elevation Models (DEM; Fraser et al. 2022) using ArcMap Version 10.8 (Environmental Systems Research Institute, Inc., Redland, CA). To assess other potential controls on movement, we measured average bed substrate sizes (D50) with a Wolman pebble count that included  $\geq 100$  particles for every 10 m channel section within each site (Wolman 1954). We also estimated maximum channel slope for every 10 m channel section within each site by measuring the slope using 1-m DEM data in ArcMap.

### *Statistical analyses*

To test our first prediction that *G. porphyriticus* downstream movement probability and distance increase with flooding, we fit two models: one model to estimate the probability of downstream movement and another to characterize the magnitude (i.e., distance) of downstream movement. We used a generalized linear mixed model with a Bernoulli distribution and logit link function to quantify the effect of maximum discharge on the probability of downstream movement. To quantify the effect of maximum discharge on the distance of downstream movement, we fit a generalized linear mixed model with a hurdle gamma distribution and log link function for the mean. We subtracted two meters from all downstream movement distances. For both models, we quantified maximum discharge during each salamanders' recapture interval.

To test our second prediction that upstream movement probability and distance decrease with flooding, we used the same two model structures as the analyses of downstream movement, but with upstream movement data as the dependent variable. For all of these models, we *a priori* included length of the recapture interval (days) as a random effect to account for any relationship between interval length and maximum discharge. To test our third prediction that the probability of terrestrial habitat use increases during floods, we fit a generalized linear mixed model with a Bernoulli distribution and logit link function. For this independent variable, we used discharge at the time of capture. To account for non-independence of movements by the same salamander, we included individual as a random effect in models of downstream movement, upstream movement, and terrestrial habitat use.



All Bayesian mixed-effects models were implemented in the brms package (Bürkner 2021) in RStudio (Version 1.4.1716; R Development Core Team 2021). All models were fit in RStan (Stan Development Team 2023) and included four chains made up of 6000 iterations each, after an initial burn in of 1000 iterations. To assess model convergence, we inspected trace-plots to ensure mixing of chains and we ensured all parameters had  $\hat{R} < 1.05$  (Gelman et al. 2013). We performed posterior predictive checks between modeled responses and data for all models (in Supporting Information). All continuous covariates were scaled prior to model fitting. We specified weakly informative Gaussian priors (mean = 0, SD = 2) for all fixed and random effects. We specified Gaussian (mean = -2.2, SD = 2) priors for the family-specific intercept parameter in Bernoulli models. We also specified Gamma (shape = 0.2, scale = 1) priors for the shape parameter and Beta (alpha = 1, beta = 5) priors for the binomial parameter in all hurdle gamma models.

## Results

We tagged 204 *G. porphyriticus*, including 71 adults, 115 larvae, and 18 individuals that metamorphosed from larvae to adults between 2019 – 2021 (see Table S1 for summary data on individuals per site). Movements were recorded on 2285 occasions (adult = 707, larval = 1578; Fig. 2). The mean number of detections per individual was 14 (SD = 9), with a maximum of 41. The mean number of detections per individual per year was 8 (SD = 5), with a maximum of 20. The mean number of days between detections was 6 (SD = 5; median = 5). The mean channel length of individual home ranges was 4 m (SD = 5; median = 3). Maximum site-specific discharge between detections ranged from 0 to 1028 L/S (mean = 38, SD = 83). The largest flood occurred in 2021 and had a return interval of 1.8 y and an exceedance probability of 0.29% (Fig. S1). Site-specific discharge during surveys ranged from 0 to 346 L/S (mean = 8, SD = 28). Across all sites, mean substrate particle size (D50) was 317 mm (SD = 463; min = 45, max = 4096) and all sites included pebble, cobble, boulder, and bedrock substrates. The average maximum channel slope was 31° (SD = 15, min = 9, max = 78).

The probability of downstream movement by *G. porphyriticus* individuals increased as maximum discharge increased (Fig. 3; Fig. S2). Adults experienced a higher probability of downstream movement than larvae. For example, as maximum discharge increased, downstream movement by adults increased from 10% (95% CI = 7 – 14) to 45% (95% CI = 14 – 77), and downstream movement by larvae increased from 6% (95% CI = 5 – 8) to 32% (95% CI = 9 – 65) as maximum discharge increased from 0 to 1028 L/S. The distance of *G. porphyriticus* downstream movements was not strongly influenced by maximum discharge or life stage (Fig. S4). Downstream movements  $\geq 2$  m occurred on 197 occasions (72 adult, 125 larval), with a mean movement distance of 3 m (SD = 4, median = 2; max = 41). We recorded 110 incidences of homing after downstream movement. The percentage of larvae that homed after downstream movement was slightly greater than the percentage of adults that homed (39% vs 32%). The average time to home was 9 days (SD = 7). Of individuals that moved downstream, 86% were presumed alive because they were either seen alive during surveys occurring after the movement event or they homed after the movement event.

Maximum discharge did not influence the probability of upstream movement by *G. porphyriticus* (Fig. S6). The probability of upstream movement did, however, decrease with maximum stream slope (Fig. 4), and adults were more likely to move upstream than larvae. For example, the probability of upstream movement by adults decreased from 14% (95% CI = 10 – 18) to 5% (95% CI = 3 – 10) as stream slope increased from 9° to 78°. Over the same range of slopes, the probability of upstream movement by larvae decreased from 11% (95% CI = 7 – 14) to 4% (95% CI = 2 – 8). The distance of *G. porphyriticus* upstream movements was not influenced by stream slope or life stage (Fig. S8). Upstream movements  $\geq 2$  m occurred on 275 occasions (104 adult, 171 larval), with a mean movement distance of 4 m (SD = 5, median = 2; max = 43).

The probability of terrestrial habitat use by *G. porphyriticus* adults increased with maximum discharge and stream slope (Fig. 5a, Fig. S10). For example, the probability of terrestrial habitat use increased from 4% (95% CI = 2 - 6) to 33% (95% CI = 3 – 85) as maximum discharge increased from 0 to 346 L/S. As stream slopes increased from 9° to 60°, the probability of terrestrial habitat use increased from 2% (95% CI = 1 – 3) to 7% (95% CI = 5 – 16; Fig. 5b). We located adults using terrestrial habitat on 62 occasions.

## Discussion

Larger floods increased the probability of downstream movement in the headwater stream salamander *G. porphyriticus*. Contrary to our prediction, the probability of downstream movement was greater in adults than larvae (Fig. 3). Previous research suggests that floods increase downstream drift rates of small, larval salamanders (Barrett et al. 2010, Segev and Blaustein 2014, Veith et al. 2019), but this is the first study to document effects on larger larvae ( $\geq 50$  mm) and adults, which we assumed have greater capacity to withstand increased flow velocities (Reinhardt et al. 2018, Schafft et al. 2022). Downstream movement may increase gene flow and colonization of downstream habitats (Lowe et al. 2006b, Baguette et al. 2013). However, the potential for downstream colonization by *G. porphyriticus* is limited because the species is subject to fish predation (Resetarits 1995, Lowe and Bolger 2002, Lowe et al. 2018), which become more abundant in larger streams (Schlosser 1999, Meyer et al. 2007). Overall, we interpret these results as evidence that increasing flood intensity represents a threat to stream salamanders due to increasing fish predation pressure in downstream reaches and likely increases in mortality due to the physical effects of flooding.

Downstream movement by *G. porphyriticus* during floods may be passive, or the result of active behavior (Oberrisser and Waringer 2011, Reinhardt et al. 2018). In this dynamic headwater system where storm pulses are common, passive drift where individuals are flushed downstream because of increasing flow velocity, seem feasible (Segev and Blaustein 2014). The larger body size of adult salamanders can increase drag (Addis et al. 2019), which increases the energetic cost of resisting streamflow and may result in greater displacement downstream. Future research on the relationship between *G. porphyriticus* limb length and downstream movement during flooding could help clarify if longer-limbed stream organisms are more likely to be displaced downstream compared to their shorter-limb counterparts (Blake 2006, Addis et al. 2019). Similarly, flume experiments that simulate natural streambed environments would help to

identify the mechanisms by which salamanders resist stream currents, and the discharge threshold at which drift occurs, especially in larger body individuals.

Catastrophic drift, where large floods disturb bed substrates and set them into incipient motion, often result in large-scale loss of organisms that reside in the streambed (Brittain and Eikeland 1988, Gibbins et al. 2007). In this study, 86% of individuals moving downstream were presumed alive afterwards, either by direct observation or indirectly if we recorded upstream homing behavior. This high rate suggests that most recorded downstream movements were not catastrophic. Streambeds are infrequently mobilized in small, steep headwater streams with cobble and boulder substrates (Church 2002, 2006), and we did not see increased rates of downstream movement at sites with the smallest and most easily entrained sediments. However, 14% of downstream movers had unknown fates, which – combined with undetectable downstream movements out of surveyed reaches during flooding – could help explain why survival analyses at HBEF show flooding-related reductions in survival (Cochrane *unpublished data*).

It is likely that some downstream *G. porphyriticus* movements were intentional, where individuals used stream currents to seek refuge or avoid competition (Hart and Finelli 1999, Sinsch 2014). Individuals may cue into the rising limb of a flood (Lytle and Poff 2004) and take advantage of increased water volumes to move into aquatic refuge habitats that was not previously accessible. Exploiting increased streamflows to move downstream may also act as density regulation, where limited food or shelter availability cause individuals to initiate movement to reduce intraspecific competition (Veith et al. 2019). However, because reduced flows did not increase the probability of upstream movements into reaches with higher rates of survival away from fish predation (Lowe et al. 2018), we believe that flooding is primarily displacing individuals downstream, rather than providing a means for active relocation. Increased stream channel slopes did limit upstream movement probability (Fig. 4), supporting previous research suggesting that steep slopes act as a barrier to dispersal and gene flow along streams (Lowe et al. 2006b).

The probability of terrestrial refuge use by adult *G. porphyriticus* increased with discharge (Fig. 5a). In fact, *G. porphyriticus* stayed in terrestrial refuges for extended periods of time, including during the day, when relative humidity typically constrains use of terrestrial habitats by plethodontids (Riddell et al. 2018; Table S2). We located adults in moist terrestrial refuges for up to 11 consecutive days, including in decomposing logs, leaf litter, and rock cavities. The use of PIT-tag telemetry allowed us to identify refuges that would have been very difficult to locate with traditional sampling methods, such as active searches. Other stream salamander species are known to use terrestrial cavities for protection (Peterman and Semlitsch 2014), but *G. porphyriticus* adults were believed to be primarily aquatic, using terrestrial habitats only in very humid conditions, and particularly at night (Petranka and Smith 2005, Greene et al. 2008). Terrestrial refuge use also increased at the steepest sites (Fig. 5b), which coincide with greater shear stresses (Scheingross et al. 2013). This suggests that in-stream refugia may be limited in steeper reaches, requiring the use of terrestrial habitats during flooding. Together, these findings suggest that riparian habitat corridors along headwater streams should be prioritized as refuges for semi-aquatic salamanders.

Empirical understanding of how environmental conditions influence animal movement will be critical to sustaining biodiversity in landscapes influenced by climate change (Schloss et al. 2012, Hays et al. 2016). For species that inhabit streams and rivers in the eastern United States, flooding intensity is likely to be the most significant environmental control on movement under future climate scenarios (IPCC 2021). This study shows that flooding increases downstream movement of both adult and larval stream salamander. The loss of adult life stages to downstream drift may be particularly challenging for amphibians because population growth is most sensitive to changes to adult survival (Schmidt et al. 2005, Kissel et al. 2020). Stream salamander populations experience a reduction in adult abundance and survival associated with increased precipitation (Lowe 2012, Cochrane et al. *unpublished data*). Even floods that do not cause mortality directly can reduce population growth indirectly by relocating individuals to downstream reaches where they must contend with fish predation (Resetarits 1995, Lowe and Bolger 2002, Lowe et al. 2018). Our results indicate that protection of intact headwater stream habitat with ample interstitial and hyporheic refuges, and riparian habitat corridors that provide terrestrial refuges will help reduce downstream movements of stream salamanders with intensifying flooding.

## Acknowledgments

We thank T. Hodges, L. Swartz, R. Wagner, M. Delamont, A. Willig, K. Barreras, and R. Waters, for assistance in the field. The research was funded by the U.S. NSF (DEB-1114804, DEB-1050459, DEB-1655653). This work was conducted under Montana State IACUC #003-14WLDBS-012714. This work is a contribution of the Hubbard Brook Ecosystem Study. Hubbard Brook is part of the LTER network, which is supported by the U.S. NSF. The Hubbard Brook Experimental Forest is operated and maintained by the US Department of Agriculture, Forest Service, Northern Research Station.

## Literature Cited

- Addis, B. R., and W. H. Lowe. 2020. Long-term survival probability, not current habitat quality, predicts dispersal distance in a stream salamander. *Ecology* 101:1–14.
- Addis, B. R., B. W. Tobalske, J. M. Davenport, and W. H. Lowe. 2019. A distance-performance trade-off in the phenotypic basis of dispersal. *Ecology and Evolution*:1–10.
- Anholt, B. R. 1995. Density dependence resolves the stream drift paradox. *Ecology* 76:2235–2239.
- Baguette, M., S. Blanchet, D. Legrand, V. M. Stevens, and C. Turlure. 2013. Individual dispersal, landscape connectivity and ecological networks. *Biological Reviews* 88:310–326.
- Bailey, A. S., J. W. Hornbeck, J. L. Campbell, and C. Eagar. 2003. Hydrometeorological database for Hubbard Brook Experimental Forest: 1955-2000. Newtown Square, PA, USA.
- Barrett, K., B. S. Helms, C. Guyer, and J. E. Schoonover. 2010. Linking process to pattern: Causes of stream-breeding amphibian decline in urbanized watersheds. *Biological Conservation* 143:1998–2005.
- Blake, R. W. 2006. Biomechanics of rheotaxis in six teleost genera. *Canadian Journal of Zoology* 84:1173–1186.

- Brittain, J. E., and T. J. Eikeland. 1988. Invertebrate drift - a review. *Hydrobiologia* 166:77–93.
- Bruce, R. C. 1986. Upstream and downstream movements of *Eurycea bislineata* and other salamanders in a southern Appalachian stream. *Herpetologica* 42:149–155.
- Bürkner, P. C. 2021. Bayesian item response modeling in R with brms and Stan. *Journal of Statistical Software* 100.
- Campbell Grant, E. H., J. D. Nichols, W. H. Lowe, and W. F. Fagan. 2010. Use of multiple dispersal pathways facilitates amphibian persistence in stream networks. *Proceedings of the National Academy of Sciences* 107:6936–6940.
- Campbell, J. L., C. T. Driscoll, A. Pourmokhtarian, and K. Hayhoe. 2011. Streamflow responses to past and projected future changes in climate at the Hubbard Brook Experimental Forest, New Hampshire, United States. *Water Resources Research* 47:1–15.
- Chegwidden, O. S., D. E. Rupp, and B. Nijssen. 2020. Climate change alters flood magnitudes and mechanisms in climatically-diverse headwaters across the northwestern United States. *Environmental Research Letters* 15.
- Church, M. 2002. Geomorphic thresholds in riverine landscapes. *Freshwater Biology* 47:541–557.
- Church, M. 2006. Bed material transport and the morphology of alluvial river channels. *Annual Review of Earth and Planetary Sciences* 34:325–354.
- Connette, G. M., and R. D. Semlitsch. 2012. Successful use of a passive integrated transponder (PIT) system for below-ground detection of plethodontid salamanders. *Wildlife Research* 39:1–6.
- Cover, M. R., J. A. de la Fuente, and V. H. Resh. 2010. Catastrophic disturbances in headwater streams: The long-term ecological effects of debris flows and debris floods in the Klamath Mountains, northern California. *Canadian Journal of Fisheries and Aquatic Sciences* 67:1596–1610.
- Crawford, J. A., and R. D. Semlitsch. 2007. Estimation of core terrestrial habitat for stream-breeding salamanders and delineation of riparian buffers for protection of biodiversity. *Conservation Biology* 21:152–158.
- Datry, T., S. T. Larned, and K. Tockner. 2014. Intermittent rivers: A challenge for freshwater ecology. *BioScience* 64:229–235.
- Davic, R. D., and H. H. Welsh. 2004. On the ecological role of salamanders. *Annual Review of Ecology, Evolution, and Systematics* 35:405–434.
- Deitchler, E. A., J. M. Davenport, and W. H. Lowe. 2015. Homing behavior of the northern spring salamander, *Gyrinophilus porphyriticus*, in a northeastern United States headwater stream. *Herpetological Conservation and Biology* 10:235–241.
- Downing, J. A., J. J. Cole, C. M. Duarte, J. J. Middelburg, J. M. Melack, Y. T. Prairie, P. Kortelainen, R. G. Striegl, W. H. McDowell, and L. J. Tranvik. 2012. Global abundance and size distribution of streams and rivers. *Inland Waters* 2:229–236.
- Easterling, D.R., K.E. Kunkel, J.R. Arnold, T. Knutson, A.N. LeGrande, L.R. Leung, R.S. Vose, D.E. Waliser, and M.F. Wehner, 2017: Precipitation change in the United States. *Climate Science Special Report: Fourth National Climate Assessment, Volume I*. Wuebbles, D.J., D.W. Fahey, K.A. Hibbard, D.J. Dokken, B.C. Stewart, and T.K. Maycock, Eds. U.S. Global Change Research Program, Washington, DC, USA, 207-230. <http://dx.doi.org/10.7930/J0H993CC>
- Feder, M. E. 1983. Integrating the ecology and physiology of plethodontid salamanders. *Herpetologica* 39:291–310.

- Feral, D., M. A. Camann, and H. H. Welsh. 2005. *Dicamptodon tenebrosus* larvae within hyporheic zones of intermittent streams in California. *Herpetological Review* 36:26–27.
- Fritz, K. M., and W. K. Dodds. 2004. Resistance and resilience of macroinvertebrate assemblages to drying and flood in a tallgrass prairie stream system. *Hydrobiologia* 527:99–112.
- Gelman, A., J. B. Carlin, H. S. Stern, D. B. Dunson, A. Vehtari, and D. B. Rubin. 2013. *Bayesian Data Analysis*. 3rd Editio. Chapman & Hall, Boca Raton, FL.
- Gibbins, C., D. Vericat, and R. J. Batalla. 2007. When is stream invertebrate drift catastrophic? The role of hydraulics and sediment transport in initiating drift during flood events. *Freshwater Biology* 52:2369–2384.
- Greene, B. T., W. H. Lowe, and G. E. Likens. 2008. Forest succession and prey availability influence the strength and scale of terrestrial-aquatic linkages in a headwater salamander system. *Freshwater Biology* 53:2234–2243.
- Hart, D. D., and C. M. Finelli. 1999. Physical-biological coupling in streams: the pervasive effects of flow on benthic organisms. *Annual Review of Ecology and Systematics* 30:363–395.
- Hays, G. C., L. C. Ferreira, A. M. M. Sequeira, M. G. Meekan, C. M. Duarte, H. Bailey, F. Bailleul, W. D. Bowen, M. J. Caley, D. P. Costa, V. M. Eguíluz, S. Fossette, A. S. Friedlaender, N. Gales, A. C. Gleiss, J. Gunn, R. Harcourt, E. L. Hazen, M. R. Heithaus, M. Heupel, K. Holland, M. Horning, I. Jonsen, G. L. Kooyman, C. G. Lowe, P. T. Madsen, H. Marsh, R. A. Phillips, D. Righton, Y. Ropert-Coudert, K. Sato, S. A. Shaffer, C. A. Simpfendorfer, D. W. Sims, G. Skomal, A. Takahashi, P. N. Trathan, M. Wikelski, J. N. Womble, and M. Thums. 2016. Key questions in marine megafauna movement ecology. *Trends in Ecology and Evolution* 31:463–475.
- Hoerling, M., J. Eischeid, J. Perlwitz, X.-W. Quan, K. Wolter, and L. Cheng, 2016: Characterizing recent trends in U.S. heavy precipitation. *Journal of Climate*, 29 (7), 2313-2332. <http://dx.doi.org/10.1175/jcli-d-15-0441.1>
- IPCC. 2021. *Climate Change 2021: The Physical Science Basis*. Contribution of Working Group I to the Sixth Assessment Report of the Intergovernmental Panel on Climate Change.
- Johnson, B. G., C. S. Morris, H. L. Mase, P. S. Whitehouse, and C. J. Paradise. 2022. Seasonal flashiness and high frequency discharge events in headwater streams in the North Carolina Piedmont (United States). *Hydrological Processes* 36:1–19.
- Kissel, A. M., S. Tenan, and E. Muths. 2020. Density dependence and adult survival drive dynamics in two high elevation amphibian populations. *Diversity* 12:1–15.
- Lake, P. S. 2003. Ecological effects of perturbation by drought in flowing waters. *Freshwater Biology* 48:1161–1172.
- Leigh, C., A. Bush, E. T. Harrison, S. S. Ho, L. Luke, R. J. Rolls, and M. E. Ledger. 2015. Ecological effects of extreme climatic events on riverine ecosystems: Insights from Australia. *Freshwater Biology* 60:2620–2638.
- Leopold L.B. 1994. *A View of the River*. Harvard University Press, Cambridge, MA, 298 pp.
- Letcher, B. H., P. Schueller, R. D. Bassar, K. H. Nislow, J. A. Coombs, K. Sakrejda, M. Morrissey, D. B. Sigourney, A. R. Whiteley, M. J. O’Donnell, and T. L. Dubreuil. 2015. Robust estimates of environmental effects on population vital rates: An integrated capture-recapture model of seasonal brook trout growth, survival and movement in a stream network. *Journal of Animal Ecology* 84:337–352.

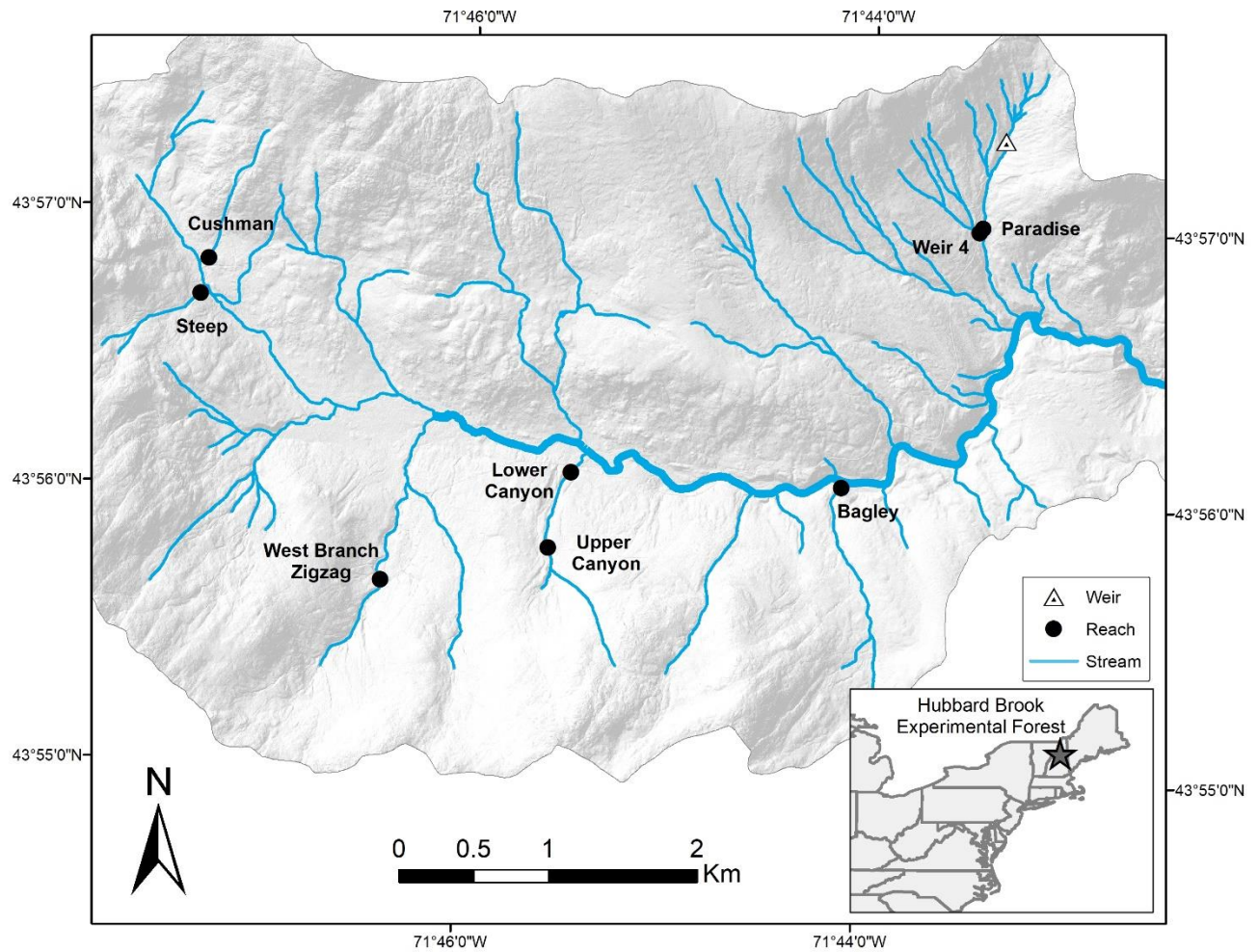
- Likens, G. E., and F. H. Bormann. 1995. *Biogeochemistry of a Forested Ecosystem*. 2nd edition. Springer-Verlag, New York.
- Lowe, W. H. 2003. Linking dispersal to local population dynamics: a case study using a headwater salamander system. *Ecology* 84:2145–2154.
- Lowe, W. H. 2012. Climate change is linked to long-term decline in a stream salamander. *Biological Conservation* 145:48–53.
- Lowe, W. H., and D. T. Bolger. 2002. Local and landscape-scale predictors of salamander abundance in New Hampshire. *Conservation Biology* 16:183–193.
- Lowe, W. H., B. R. Addis, M. R. Smith, and J. M. Davenport. 2018. The spatial structure of variation in salamander survival, body condition and morphology in a headwater stream network. *Freshwater Biology* 63:1287–1299.
- Lowe, W. H., G. E. Likens, and B. J. Cosentino. 2006a. Self-organisation in streams: the relationship between movement behaviour and body condition in a headwater salamander. *Freshwater Biology* 51:2052–2062.
- Lowe, W. H., G. E. Likens, M. A. McPeck, and D. C. Buso. 2006b. Linking direct and indirect data on dispersal: isolation by slope in a headwater stream salamander. *Ecology* 87:334–339.
- Lowe, W. H., L. K. Swartz, B. R. Addis, and G. E. Likens. 2019. Hydrologic variability contributes to reduced survival through metamorphosis in a stream salamander. *Proceedings of the National Academy of Sciences* 116:19563–19570.
- Lytle, D. A., and N. L. R. Poff. 2004. Adaptation to natural flow regimes. *Trends in Ecology and Evolution* 19:94–100.
- Martin, S. D., B. A. Harris, J. R. Collums, and R. M. Bonett. 2012. Life between predators and a small space: substrate selection of an interstitial space-dwelling stream salamander. *Journal of Zoology* 287:205–214.
- Mcmullen, L. E., and D. A. Lytle. 2012. Quantifying invertebrate resistance to floods: A global-scale meta-analysis. *Ecological Applications* 22:2164–2175.
- Meyer, J. L., D. L. Strayer, J. B. Wallace, S. L. Eggert, G. S. Helfman, and N. E. Leonard. 2007. The contribution of headwater streams to biodiversity in river networks. *Journal of the American Water Resources Association* 43:86–103.
- Michel, M. J., H. Chien, C. E. Beachum, M. G. Bennett, and J. H. Knouft. 2017. Climate change, hydrology, and fish morphology: predictions using phenotype-environment associations. *Climatic Change* 140:563–576.
- Montgomery, D. R., and J. M. Buffington. 1997. Channel-reach morphology in mountain drainage basins. *Bulletin of the Geological Society of America* 109:596–611.
- Oberriesser, P., and J. Waringer. 2011. Larval salamanders and diel drift patterns of aquatic invertebrates in an Austrian stream. *Freshwater Biology* 56:1147–1159.
- Ousterhout, B. H., and R. D. Semlitsch. 2014. Measuring terrestrial movement behavior using passive integrated transponder (PIT) tags: Effects of tag size on detection, movement, survival, and growth. *Behavioral Ecology and Sociobiology* 68:343–350.
- Peterman, W. E., and R. D. Semlitsch. 2006. Effects of tricaine methanesulfonate (MS-222) concentration on anesthetization and recovery in four plethodontid salamanders. *Herpetological Review* 37:303–304.
- Peterman, W. E., and R. D. Semlitsch. 2014. Spatial variation in water loss predicts terrestrial salamander distribution and population dynamics. *Oecologia* 176:357–369.

- Petranka, J. W. 1998. Salamanders of the United States and Canada. Smithsonian Institution, Washington.
- Petranka, J. W., and C. K. Smith. 2005. A functional analysis of streamside habitat use by southern Appalachian salamanders: Implications for riparian forest management. *Forest Ecology and Management* 210:443–454.
- Poff, N. L., and J. D. Allan. 1995. Functional organization of stream fish assemblages in relation to hydrological variability. *Ecology* 76:606–627.
- Price, S. J., R. A. Browne, and M. E. Dorcas. 2012. Resistance and resilience of a stream salamander to suprasedasonal drought. *Herpetologica* 68:312–323.
- Pujolar, J. M., S. Vincenzi, L. Zane, D. Jesensek, G. A. de Leo, and A. J. Crivelli. 2011. The effect of recurrent floods on genetic composition of marble trout populations. *PLoS ONE* 6.
- R Development Core Team. 2021. R: A language and environment for statistical computing. R Foundation for Statistical Computing, Vienna, Austria.
- Radecki-Pawlik, A. 2015. Why Do We Need Bankfull and Dominant Discharges? In P. Rowiński & A. Radecki-Pawlik (Eds.), *Rivers – Physical, Fluvial and Environmental Processes*. pp. 49.
- Reinhardt, T., L. Baldauf, M. Ilić, and P. Fink. 2018. Cast away: drift as the main determinant for larval survival in western fire salamanders (*Salamandra salamandra*) in headwater streams. *Journal of Zoology* 306:171–179.
- Resetarits, W. J. 1995. Competitive asymmetry and coexistence in size-structured populations of Brook Trout and Spring Salamanders. *Oikos* 73:188–198.
- Resh, V. H., A. V Brown, A. P. Covich, M. E. Gurtz, W. Hiram, G. W. Minshall, S. R. Reice, A. L. Sheldon, J. B. Wallace, C. Robert, M. E. Gurtz, H. W. Li, and G. W. Minshall. 1988. The role of disturbance in stream ecology. *Journal of the North American Benthological Society* 7:433–455.
- Richardson, J. S. 2019. Biological diversity in headwater streams. *Water* 11:1–19.
- Richardson, J. S., and R. J. Danehy. 2007. A synthesis of the ecology of headwater streams and their riparian zones in temperate forests. *Forest Science* 53:131–147.
- Riddell, E. A., J. McPhail, J. D. Damm, and M. W. Sears. 2018. Trade-offs between water loss and gas exchange influence habitat suitability of a woodland salamander. *Functional Ecology* 32:916–925.
- Rodell, M., and J. T. Reager. 2023. Water cycle science enabled by the GRACE and GRACE-FO satellite missions. *Nature Water* 1:47–59.
- Schafft, M., N. Wagner, T. Schuetz, and M. Veith. 2022. A near-natural experiment on factors influencing larval drift in *Salamandra salamandra*. *Scientific Reports* 12:1–10.
- Scheingross, J. S., E. W. Winchell, M. P. Lamb, and W. E. Dietrich. 2013. Influence of bed patchiness, slope, grain hiding, and form drag on gravel mobilization in very steep streams. *Journal of Geophysical Research: Earth Surface* 118:982–1001.
- Schloss, C. A., T. A. Nuñez, and J. J. Lawler. 2012. Dispersal will limit ability of mammals to track climate change in the Western Hemisphere. *Proceedings of the National Academy of Sciences of the United States of America* 109:8606–8611.
- Schlosser, I. J. 1999. Stream fish ecology: a landscape perspective. *NCASI Technical Bulletin* 2:471–472.



- Schmidt, B. R., R. Feldmann, and M. Schaub. 2005. Demographic processes underlying population growth and decline in *Salamandra salamandra*. *Conservation Biology* 19:1149–1156.
- Schofield, K. A., L. C. Alexander, C. E. Ridley, M. K. Vanderhoof, K. M. Fritz, B. C. Autrey, J. E. DeMeester, W. G. Kepner, C. R. Lane, S. G. Leibowitz, and A. I. Pollard. 2018. Biota connect aquatic habitats throughout freshwater ecosystem mosaics. *Journal of the American Water Resources Association* 54:372–399.
- Segev, O., and L. Blaustein. 2014. Influence of water velocity and predation risk on fire salamander (*Salamandra infraimmaculata*) larval drift among temporary pools in ephemeral streams. *Freshwater Science* 33:950–957.
- Sinsch, U. 2014. Movement ecology of amphibians: From individual migratory behaviour to spatially structured populations in heterogeneous landscapes. *Canadian Journal of Zoology* 92:491–502.
- Stan Development Team. 2023. RStan: the R interface to Stan. R package version 2.21.8, <https://mc-stan.org/>.
- Tabari, H. 2020. Climate change impact on flood and extreme precipitation increases with water availability. *Scientific Reports* 10:1–10.
- Thurman, L. L., B. A. Stein, E. A. Beever, W. Foden, S. R. Geange, N. Green, J. E. Gross, D. J. Lawrence, O. LeDee, J. D. Olden, L. M. Thompson, and B. E. Young. 2020. Persist in place or shift in space? Evaluating the adaptive capacity of species to climate change. *Frontiers in Ecology and the Environment* 18:520–528.
- Travis, J. M. J., M. Delgado, G. Bocedi, M. Baguette, K. Bartoń, D. Bonte, I. Boulangeat, J. A. Hodgson, A. Kubisch, V. Penteriani, M. Saastamoinen, V. M. Stevens, and J. M. Bullock. 2013. Dispersal and species' responses to climate change. *Oikos* 122:1532–1540.
- USDA Forest Service, Northern Research Station. 2022. Hubbard Brook Experimental Forest: Instantaneous Streamflow by Watershed, 1956 – present ver 15. Environmental Data Initiative. <https://doi.org/10.6073/pasta/3fb23a2cced495d48a939b5c9076d53c>.
- Veith, M., M. Baubkus, S. Kugel, C. Kulpa, T. Reifenrath, M. Schafft, and N. Wagner. 2019. Drift compensation in larval European fire salamanders, *Salamandra salamandra* (Amphibia: Urodela)? *Hydrobiologia* 828:315–325.
- Walls, S., W. Barichivich, and M. Brown. 2013. Drought, deluge and declines: the impact of precipitation extremes on amphibians in a changing climate. *Biology* 2:399–418.
- Warren, D. R., G. E. Likens, D. C. Buso, and C. E. Kraft. 2008. Status and distribution of fish in an acid-impacted watershed of the Northeastern United States (Hubbard Brook, NH). *Northeastern Naturalist* 15:375–390.
- Wohl, E. 2017. The significance of small streams. *Frontiers of Earth Science* 11:447–456.
- Wolman, M. G. 1954. A method for sampling coarse river-bed material. *Transactions, American Geophysical Union* 35:951–956.
- Woodward, G., D. M. Perkins, and L. E. Brown. 2010. Climate change and freshwater ecosystems: Impacts across multiple levels of organization. *Philosophical Transactions of the Royal Society B: Biological Sciences* 365:2093–2106.

## Figures



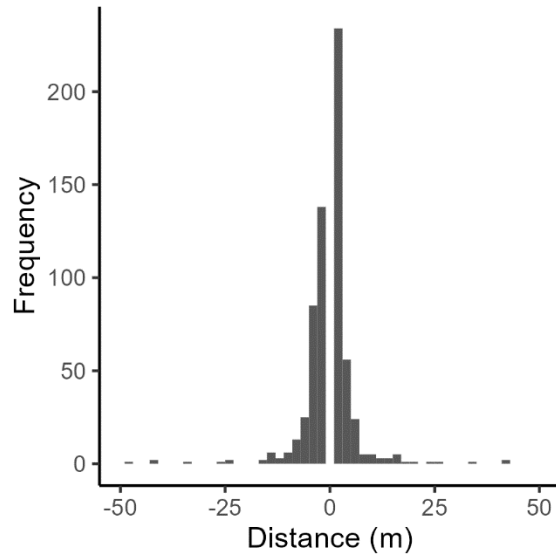


Figure 2. Movement distances (in longitudinal stream meters) of *Gyrinophilus porphyriticus* from eight sites in the Hubbard Brook Experimental Forest, New Hampshire, USA. Distances are from individuals relocated  $\geq 2$  m from their previous location, between 2019 and 2021 ( $n = 2285$ ). Negative distances indicate downstream movements; positive distances indicate upstream movements. Data are binned in 2 m increments.

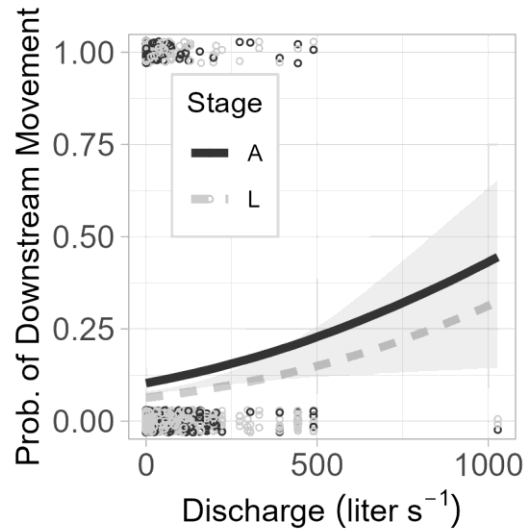


Figure 3. Estimated relationship between maximum discharge and the probability of downstream movement for adult (black solid line) and larval (grey dashed line) *Gyrinophilus porphyriticus* across eight stream reaches in the Hubbard Brook Experimental Forest, New Hampshire, USA. Movement was characterized as any downstream movement within the stream channel  $\geq 2$  m. Movements occurred between 2019 and 2021 ( $n = 2285$ ). A total of 197 observations of downstream movement were recorded. The grey ribbon represents the 95% credible interval of response. Black and grey circles represent adult and larval data, respectively.

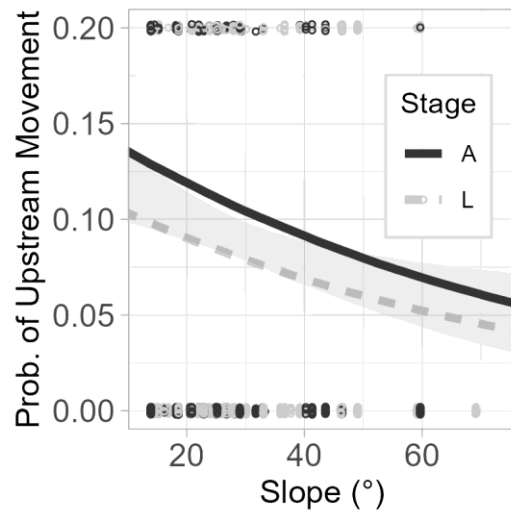


Figure 4. Estimated relationship between the slope of the stream channel and the probability of upstream movement for adult (black solid line) and larval (grey dotted line) *Gyrinophilus porphyriticus* across eight stream reaches in the Hubbard Brook Experimental Forest, New Hampshire, USA. Upstream movement was characterized as any movement  $\geq 2$  m. Movements occurred between 2019 and 2021 ( $n = 2285$ ). A total of 275 observations of upstream movement were recorded. The grey ribbon represents the 95% credible interval of response. Black and grey circles represent adult and larval data, respectively (y-data points moved from 1.0 to 0.20 for figure only).

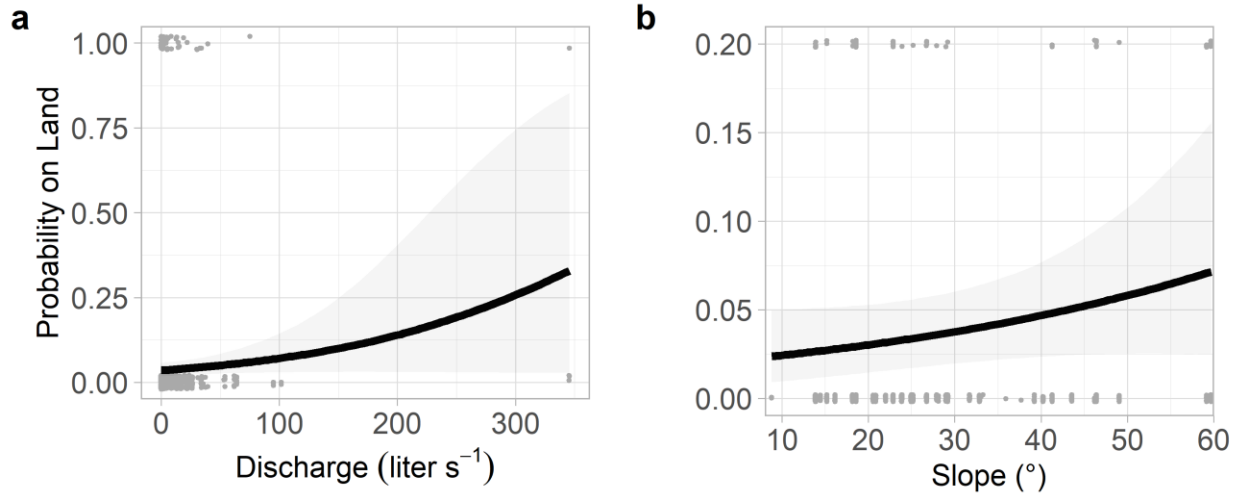


Figure 5. Estimated relationship between current discharge (a) and the slope of the stream channel (b), and adult *Gyrinophilus porphyriticus* terrestrial habitat use, across eight stream reaches in the Hubbard Brook Experimental Forest, New Hampshire, USA. A total of 62 terrestrial habitat observations were recorded (out of 2792), between 2019 to 2021. The grey ribbon represents the 95% credible interval of response. Grey circles represent data (in panel b, y-data points moved from 1.0 to 0.20 for figure only).

## Supplementary Materials

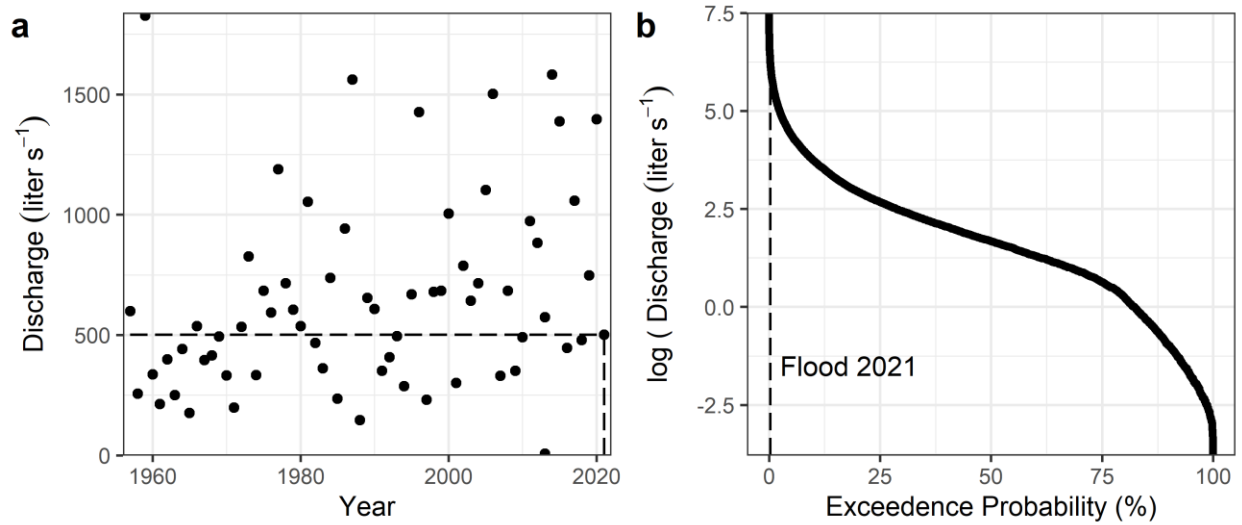


Figure S1. Annual maximum discharge (a) and exceedance probabilities (b) for the hydrologic reference stream in the Hubbard Brook Experimental Forest, New Hampshire, USA from 1957 – 2021. Black dashed lines represents the peak flood discharge across this study period (2019 – 2021), which occurred in 2021 and had a return interval of 1.8 y and an exceedance value of 0.29%.

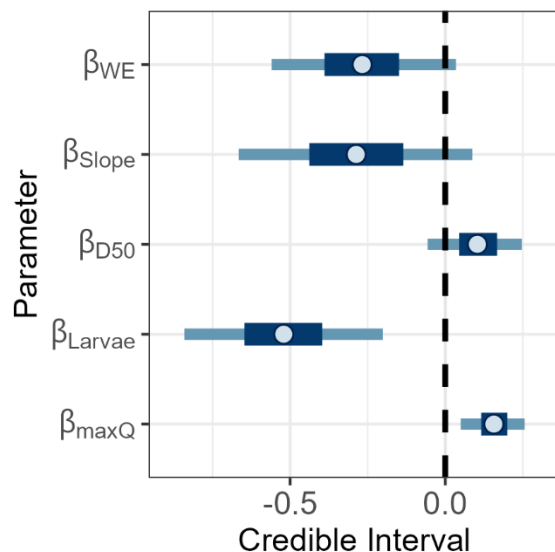


Figure S2. Fixed effect posterior probability parameter estimates from a Bayesian generalized linear mixed model to describe the effect of maximum discharge (maxQ) on the probability of downstream movement for *Gyrinophilus porphyriticus* in the Hubbard Brook Experimental Forest, New Hampshire, USA. Downstream movement was defined as any downstream movement  $\geq 2$  m within the stream channel. Other parameters included lateral stream location (wetterted edge or WE vs thalweg); slope of the stream channel; average substrate particle size (D50); and the difference between adult and larval stages (larvae). Circles represent mean posterior probability estimates; dark, wide blue lines represent 50<sup>th</sup> percentile posterior estimates; and narrow, blue lines represent 90<sup>th</sup> percentile posterior estimates.



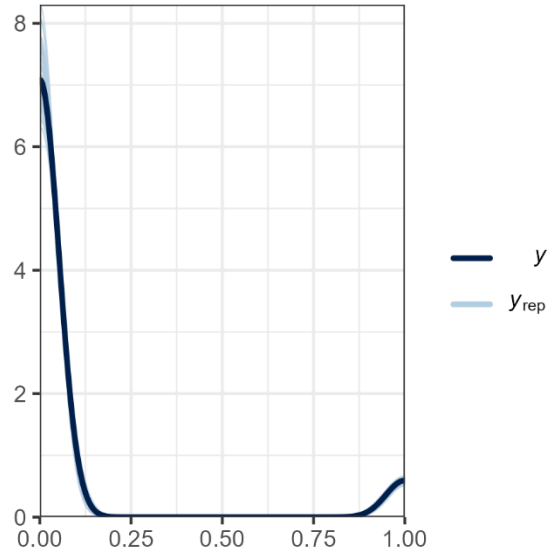


Figure S3. Posterior predictive check for a Bayesian generalized linear mixed model to describe the effect of maximum discharge (maxQ) on the probability of downstream movement for *Gyrinophilus porphyriticus* in the Hubbard Brook Experimental Forest, New Hampshire, USA. The dark blue line is the distribution of the observed outcomes  $y$ , and each of the 50 lighter lines is the kernel density estimate of one of the replications of  $y$  from the posterior predictive distribution.

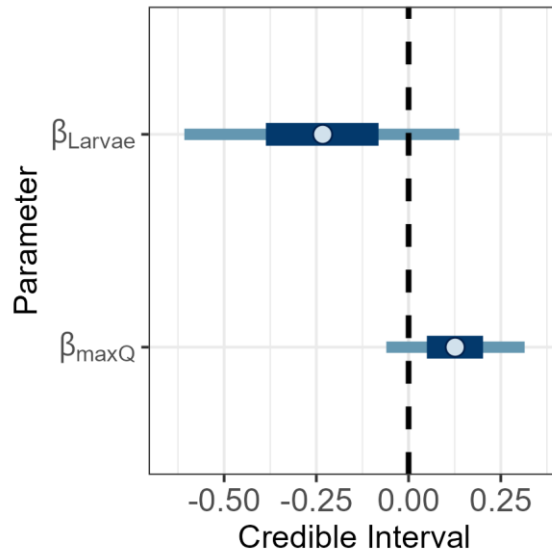


Figure S4. Fixed effect posterior probability parameter estimates from a Bayesian generalized linear mixed model to describe the effect of maximum discharge (maxQ) and the difference between adult and larval stages (larvae) on the magnitude of downstream movement for *Gyrinophilus porphyriticus* in the Hubbard Brook Experimental Forest, New Hampshire, USA. Downstream movement was defined as any downstream movement  $\geq 2$  m within the stream channel. Circles represent mean posterior probability estimates; dark, wide blue lines represent the 50<sup>th</sup> percentile posterior estimates; and narrow, blue lines represent the 90<sup>th</sup> percentile posterior estimates.

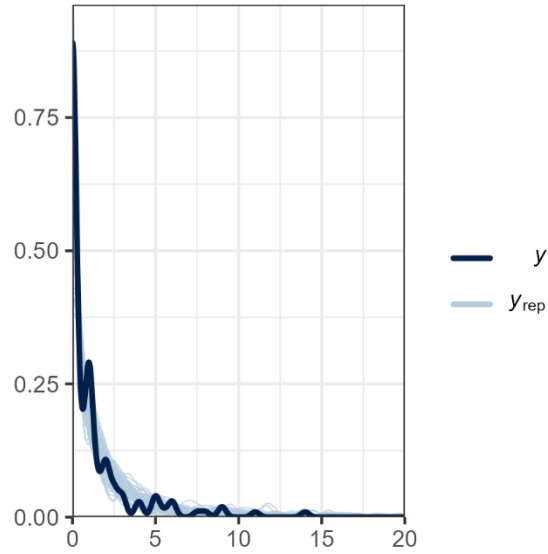


Figure S5. Posterior predictive check for a Bayesian generalized linear mixed model to describe the effect of maximum discharge (maxQ) and stage (larvae) on the magnitude of downstream movement for *Gyrinophilus porphyriticus* in the Hubbard Brook Experimental Forest, New Hampshire, USA. The dark blue line is the distribution of the observed outcomes  $y$ , and each of the 50 lighter lines is the kernel density estimate of one of the replications of  $y$  from the posterior predictive distribution.

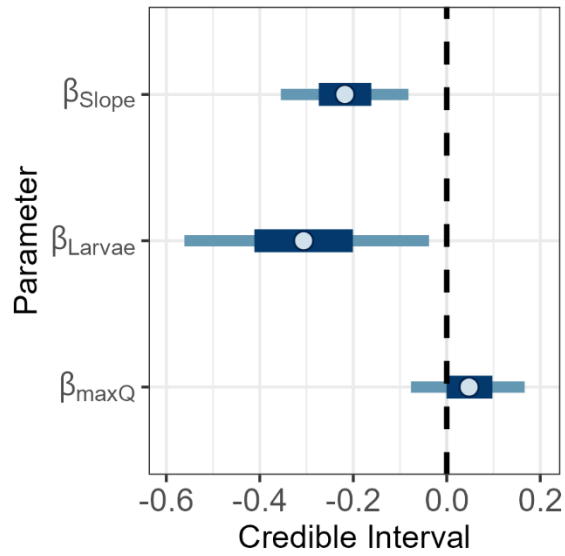


Figure S6. Fixed effect posterior probability parameter estimates from a Bayesian generalized linear mixed model to describe the effect of maximum discharge (maxQ) and the difference between adult and larval stages (larvae) on the probability of upstream movement for *Gyrinophilus porphyriticus* in the Hubbard Brook Experimental Forest, New Hampshire, USA. Upstream movement was defined as any upstream movements  $\geq 2$  m. The other parameter included was the slope of the stream channel. Circles represent mean posterior probability estimates; dark, wide blue lines represent the 50<sup>th</sup> percentile posterior estimates; and narrow, blue lines represent the 90<sup>th</sup> percentile posterior estimates.

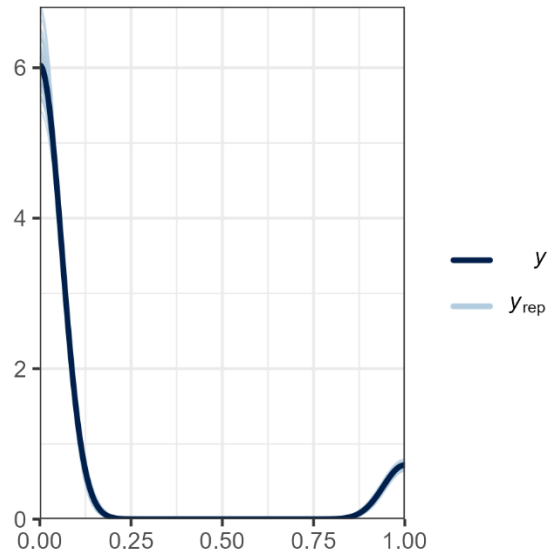


Figure S7. Posterior predictive check for a Bayesian generalized linear mixed model to describe effect of maximum discharge (maxQ) and the difference between adult and larval stages (larvae) on the probability of upstream movement for *Gyrinophilus porphyriticus* in the Hubbard Brook Experimental Forest, New Hampshire, USA. The dark blue line is the distribution of the observed outcomes  $y$ , and each of the 50 lighter lines is the kernel density estimate of one of the replications of  $y$  from the posterior predictive distribution.

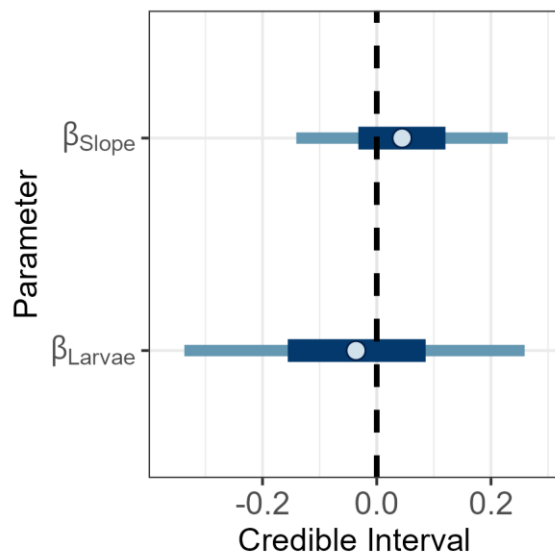


Figure S8. Fixed effect posterior probability parameter estimates from a Bayesian generalized linear mixed model to describe the effect of the slope of the stream channel and the difference between adult and larval stages (larvae) on the magnitude of upstream movement for *Gyrinophilus porphyriticus* in the Hubbard Brook Experimental Forest, New Hampshire, USA. Upstream movement was defined as any upstream movements  $\geq 2$  m. Circles represent mean posterior probability estimates; dark, wide blue lines represent the 50<sup>th</sup> percentile posterior estimates; and narrow, blue lines represent the 90<sup>th</sup> percentile posterior estimates.

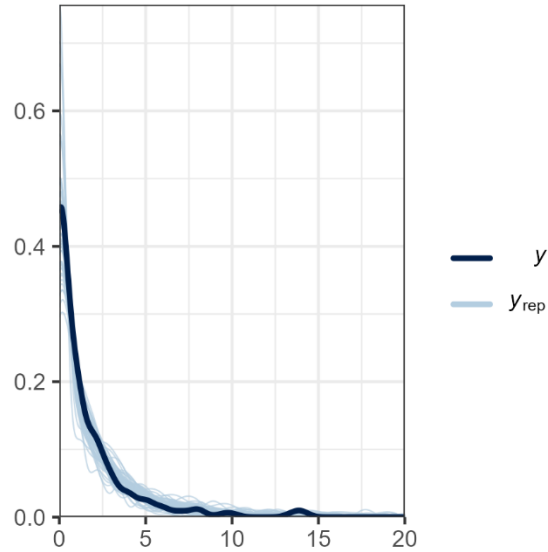


Figure S9. Posterior predictive check for a Bayesian generalized linear mixed model to describe the effect of the slope of the stream channel and the difference between adult and larval stages on the magnitude of upstream movement for *Gyrinophilus porphyriticus* in the Hubbard Brook Experimental Forest, New Hampshire, USA. The dark blue line is the distribution of the observed outcomes  $y$ , and each of the 50 lighter lines is the kernel density estimate of one of the replications of  $y$  from the posterior predictive distribution.

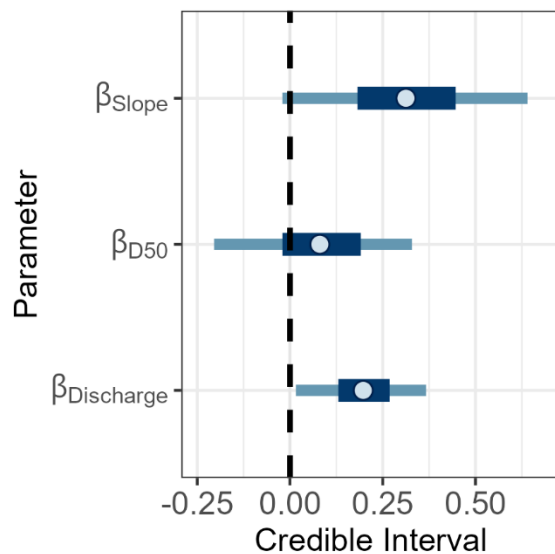


Figure S10. Fixed effect posterior probability parameter estimates from a Bayesian generalized linear mixed model to describe the effect of current discharge on the probability of an adult *Gyrinophilus porphyriticus* terrestrial habitat use in the Hubbard Brook Experimental Forest, New Hampshire, USA. Other parameters included the slope of the stream channel and average substrate particle size (D50). Circles represent mean posterior probability estimates; dark, wide blue lines represent the 50<sup>th</sup> percentile posterior estimates; and narrow, blue lines represent the 90<sup>th</sup> percentile posterior estimates.



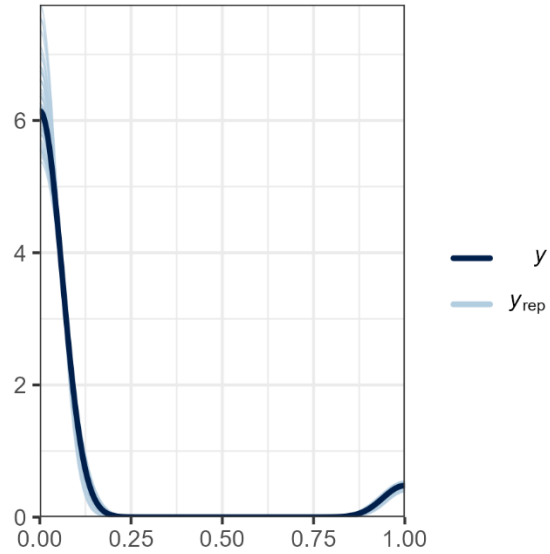


Figure S11. Posterior predictive check for a Bayesian generalized linear mixed model to describe the effect of current discharge on the probability of an adult *Gyrinophilus porphyriticus* terrestrial habitat use in the Hubbard Brook Experimental Forest, New Hampshire, USA. The dark blue line is the distribution of the observed outcomes  $y$ , and each of the 50 lighter lines is the kernel density estimate of one of the replications of  $y$  from the posterior predictive distribution.

Table S1. List of the number of *Gyrinophilus porphyriticus* individuals tracked across eight stream reaches (sites) in the Hubbard Brook Experimental Forest, New Hampshire, USA.

<b>Site</b>	<b>Individuals (n)</b>
Bagley	33
Cushman	23
Lower Canyon	17
Paradise	23
Steep	28
Upper Canyon	20
Weir 4	39
West Branch Zigzag	21

Table S2. Summary of consecutive terrestrial habitat locations for adult *Gyrinophilus porphyriticus* in the Hubbard Brook Experimental Forest, New Hampshire, USA. Data include the stream reach (site), salamander identification number (ID), start and end dates, number of consecutive days on terrestrial habitat, number of consecutive observations, and general habitat description.

Site	ID	Start Date	End Date	Days	Obs. (n)	Habitat
Steep	644	7/4/2020 10:00	7/15/2020 9:00	11	2	Rotting log
Steep	644	7/29/2020 12:00	8/12/2020 11:00	14	2	Moist rock cave on hillslope
Upper Canyon	707	8/14/2021 9:00	8/18/2021 9:00	4	2	Rotting log
Upper Canyon	710	7/1/2019 10:00	7/6/2019 13:00	5	3	Hole in ground, below leaf litter
Upper Canyon	710	7/13/2020 10:00	7/15/2020 12:00	2	2	Rotting log

## CHAPTER 3: Stage-specific demographic effects of hydrologic extremes in a stream salamander

Madaline M. Cochrane<sup>1,\*</sup>, Brett R. Addis<sup>2</sup>, and Winsor H. Lowe<sup>1</sup>

1. Division of Biological Sciences, University of Montana, Missoula, MT, USA

2. D.B. Warnell School of Forestry and Natural Resources, University of Georgia, Athens, GA, USA

### Abstract

We lack a strong understanding of how organisms with complex life histories respond to extreme climatic events. Many stream-associated species have multi-stage life histories that are likely to influence the demographic consequences of floods and droughts. However, tracking stage-specific demographic responses to hydrologic extremes requires high-resolution, long-term data that are rare. We used eight years of capture-recapture data for the headwater stream salamander *Gyrinophilus porphyriticus* to quantify the effects of flooding and drying intensity on stage-specific vital rates and overall population growth. We found that drying intensity reduced larval recruitment but increased the probability of metamorphosis (i.e., adult recruitment). Larval and adult recruitment were unaffected by flooding intensity. Larval and adult survival declined with flooding intensity, but were unaffected by drying intensity. Annual population growth rates ( $\lambda$ ) declined with flooding and drying intensity, but mean  $\lambda$  was 1.0 between 2012 and 2021. Our results demonstrated that *G. porphyriticus* populations are resilient to episodic hydrologic disturbances, and that this resilience is a consequence of compensatory effects of hydrologic extremes on the recruitment of new larvae vs. adults (i.e., reproduction vs. metamorphosis). Complex life cycles may increase resilience to climate extremes by creating opportunities for compensatory demographic responses across stages, like those we observed in *G. porphyriticus*.

### Introduction

Earth's climate, a key force governing the distribution and demography of animal populations, is becoming more variable (Halsch et al. 2021, Paniw et al. 2021). This intensifying climate variability leads to more severe and frequent extreme events, including floods and droughts (IPCC 2021). Understanding the effects of these extreme events on natural populations is a crucial challenge facing ecologists and conservation biologists in the Anthropocene (Vázquez et al. 2017). More specifically, effective management and conservation will rely on identifying how demographic rates respond to climatic extremes, and the species traits that lead to population resilience in the face of these extremes (Munoz et al. 2016, Amburgey et al. 2018).

Isolating the demographic effects of climatic extremes is particularly challenging in species with complex life cycles, which include the majority of animals on Earth (Wilbur 1980, Laudet 2011). These organisms undergo metamorphosis or other discrete life stage transitions that entail major changes in physical and physiological traits, in addition to changes to vital rates

(Kingsolver et al. 2011, Rose et al. 2021). Because of these abrupt ontogenetic changes, animals may be particularly vulnerable to climate extremes during metamorphosis (Geffen et al. 2007, Lowe et al. 2021). However, organisms with complex life cycles also have greater life history flexibility than those with simple life cycles, creating more opportunities for demographic compensation across life stages (Doak and Morris 2010, Denoël and Ficetola 2014, Vilellas et al. 2015). Teasing out these stage-specific responses to environmental extremes is necessary for a complete understanding of the demographic effects of climate change in organisms with complex life cycles.

Most species that inhabit streams and rivers have complex life histories, and these species are likely to be affected directly by floods and droughts associated with changing precipitation regimes. However, the magnitude and directionality of these responses is not easy to predict. For example, floods may kill or displace organisms (Gibbins et al. 2007, Veith et al. 2019), or reduce population growth rates by limiting food resources or habitat availability (Lake et al. 2006). But floods also alter the geomorphological template of streams and rivers, which can increase habitat complexity, benefitting flood-tolerant species and increasing biodiversity (Death et al. 2015, Hauer et al. 2016, Larson et al. 2018). Droughts have largely negative effects on stream organisms (Boulton 2003), including reducing survivorship due to dehydration (Spotila 1972) and increasing crowding and the intensity of negative interactions among species (Lake 2003, Kupferberg et al. 2021). Yet, the strengths of these responses vary depending on historic flow regimes and associated phenotypic and life history adaptations (Lytle and Poff 2004, Walls et al. 2013, Weinbach et al. 2018). As floods and droughts continue to increase in severity, isolating the demographic mechanisms underlying population-level responses will become more crucial.

We have a rare opportunity to assess the effects of hydrologic extremes throughout the complex life cycle of a headwater stream salamander. Most stream salamanders have a biphasic life cycle (Petranka 1998). Larvae respire with external gills and are thus exclusively aquatic. Individuals then go through metamorphosis, where larvae transform into their adult form, lose their external gills, and begin breathing cutaneously, allowing them to use terrestrial habitats (Greene et al. 2008, Campbell Grant et al. 2010). Stream salamander diversity is also highest in headwater systems (Hairston and Hairston 1987, Petranka 1998), where they experience dynamic hydrologic environments that range from ephemeral conditions during droughts, to floods that may occur seasonally or following precipitation events (Datry et al. 2014). Our goal was to advance basic understanding of the demographic and life history mechanisms by which species with complex life cycles, like stream salamanders, respond to hydrologic extremes.

We used eight years of intensive capture-recapture data on *Gyrinophilus porphyriticus*, the northern spring salamander, to determine how stage-specific vital rates respond to variation in the intensity of stream flooding and drying over time, and how these vital rate responses influence population growth rates. We tested the overarching prediction that intense flooding and drying reduce recruitment and survival of *G. porphyriticus* larvae and adults, reducing population growth. Specifically, we predicted that larger floods would cause the most vulnerable individuals, including hatchling larvae and individuals undergoing metamorphosis, to experience increased mortality due to physical disturbance, thereby reducing larval and adult recruitment. We also predicted that drying intensity would increase mortality of all larvae due to the risk of desiccation in dry stream channels. Because adult stages can survive terrestrially and larval

stages cannot, we expected intensity of these hydrologic conditions to have larger negative effects on larval survival than adult survival. Finally, we expected this combination of responses to cause population growth rates to decline in years with intense flooding or drying.

## Methods

### *Study organism*

*Gyrinophilus porphyriticus* is a lungless salamander (family Plethodontidae) that lives in small, cool, well-oxygenated streams along the Appalachian uplift in the eastern United States (Petranka 1998). This species has a biphasic life cycle: larvae are exclusively aquatic (Bruce 1972), and adults are predominantly aquatic but can leave the stream in humid conditions (Greene et al. 2008). Larvae feed on aquatic invertebrates and smaller larval salamanders (Burton 1976), whereas adults also feed on terrestrial invertebrates (Lowe et al. 2005). *G. porphyriticus* exhibit slow and variable growth rates (Bonett et al. 2014, Beachy et al. 2017), metamorphosing at 2 – 10 years in age, and living up to 20 years (M. M. Cochrane, *unpublished data*). Aquatic predators include *Salvelinus fontinalis* (brook trout; Resetarits 1995) and terrestrial predators include *Thamnophis sirtalis* (common garter snakes; Petranka 1998). Previous research has shown that changing precipitation and discharge regimes in the northeastern USA are associated with changes in *G. porphyriticus* survival through metamorphosis and adult abundance (Lowe 2012, Lowe et al. 2019), but previous studies have not assessed the specific hydrologic conditions affecting survival (e.g., droughts v. floods) or the population-level consequences of these effects.

### *Study site*

We conducted this research at the Hubbard Brook Experimental Forest (HBEF) in New Hampshire, USA (43°56'N, 71°45' W). We sampled three hydrologically independent headwater streams within the 32-km<sup>2</sup> HBEF: Bear Brook, Paradise Brook, and Zigzag Brook (Fig. S1). We surveyed two 500-m long reaches in each stream. Downstream reaches started at the confluence with Hubbard Brook, a fifth-order stream flowing into the Pemigewasset River. Upstream reaches ended at weirs where long-term water quality and discharge data are collected and beyond which sampling is prohibited (Bormann and Likens 1979). Distances between downstream and upstream reaches, measured along stream channels, were 400 m in Bear Brook, 250 m in Paradise Brook, and 500 m in Zigzag Brook (Addis and Lowe 2020). *S. fontinalis* occur in all downstream reaches.

Discharge in the HBEF streams typically peaks in the spring due to melting snow, but flood events can occur throughout the year after isolated rainstorms. Base flows usually occur in late summer and early fall (Likens and Bormann 1995). The study streams drain small, high-gradient watersheds with watershed areas ranging from 0.14 to 3.53 km<sup>2</sup> and gradients ranging from 4° to 25°, based on measurements every 100 m along the stream channels. The majority of stream habitats are characterized as step-pools (Montgomery and Buffington 1997). Streams have low conductivity (12.0 – 15.0 µS), slight acidity (pH of 5.0 – 6.0), and high dissolved oxygen content (> 95% saturation; Likens and Bormann 1995). Stream water temperatures range from 0 – 20°C throughout the year (M. M. Cochrane, *unpublished data*). Other stream

salamanders include *Eurycea bislineata* and *Desmognathus fuscus* (both Plethodontidae). The HBEF landscape is dominated by northern hardwood forest (Bormann and Likens 1979).

### *Survey Methods*

Our analyses are based on six mark-recapture surveys of all reaches conducted during July and August of 2012 – 2015 and 2018 – 2021, for a total of 48 surveys per reach. In each survey, we used cover-controlled, active search sampling (Heyer et al. 1994b), where one haphazardly-selected cover object was turned per meter of stream length. From 2012 – 2015, salamanders were marked with visual implant elastomer (Northwest Marine Technology, Inc., Anacortes, Washington, USA). From 2018 – 2021, salamanders were marked with 8-mm passive integrated transponders (PIT-tags; Hecere Electronic Col, Ltd., Quanzhou, China). We recorded the stage and mass of all individuals, and snout-vent-lengths (SVL) were measured from photographs with ImageJ 1.50i software (Schneider et al. 2012).

### *Quantifying hydrologic extremes*

To characterize flooding and drying intensity, we quantified annual peak discharge (i.e., floods) and lowest discharge (i.e., stream drying) in each stream for each year of this study (Fig. 1). These calculations were based on daily discharge data collected at weirs immediately upstream of our upstream survey reaches on each stream (USDA Forest Service 2022). Discharge data were reported in units of depth per unit time (mm/day) because the streamflow rate was divided by the watershed area at the weir where the data was collected (Bailey et al. 2003). This standardized discharge by unit area. To then account for variable increases in watershed area (and thus stream volume) between upstream and downstream reaches in each stream we included watershed area in all models. Watershed areas were calculated every 100 m along each reach from 1-m Digital Elevation Models (University of New Hampshire, Durham, NH) using ArcMap Version 10.8 (Environmental Systems Research Institute, Inc., Redlands, CA). Years were defined as the 12-month period preceding salamander surveys (July 1 – June 30). To characterize annual flood intensity for each stream, we calculated Q99, which is the discharge exceeded only 1% of the year. To quantify annual stream drying intensity for each stream, we calculated the minimum 7-day lowest discharge for each year (Olden and Poff 2003, Ries et al. 2016).

### *Analyses overview*

We used two different capture-recapture models to calculate all stage-specific vital rates and test for effects of flooding and drying intensity on those vital rates. First, we used a reverse-time Pradel model to test our predictions that larval recruitment and population growth decline with flooding and drying intensity. Pradel models invert capture histories to estimate the probability of entry into a population (i.e., larval recruitment; Pradel 1996). We also used this model to estimate annual population growth rates ( $\lambda$ ), because it quantifies both gains and losses in a population. Next, we used a multi-state Cormack-Jolly-Seber (CJS) model to test our predictions that larval survival and adult recruitment are reduced by flooding and drying intensity. The CJS model allowed us to estimate annual survival probabilities of larvae and adults separately, as well as the probability of transitioning between those life stages (i.e.,

metamorphosis or adult recruitment; Lebreton et al. 2009). Both models accommodate variable time intervals between surveys, including the interval between surveys in 2015 and 2018.

### *Pradel model*

The Pradel model estimates annual recruitment probability ( $f$ ), annual apparent survival probability ( $\phi$ ), and capture probability ( $p$ ), but can also be used to derive population change ( $\lambda$ ) across years. We included both larval and adult individuals in these analyses, so  $f$  estimates include any new individuals entering the population, both young-of-the year (larval recruitment) and immigrating individuals from outside the study reach. However, we assumed that the majority of recruitment was in the form of new larvae because previous analyses suggest that immigration from outside of study reaches is very low (Lowe et al. 2006b, Addis and Lowe 2020). Apparent survival is defined as the probability of any individual (larvae or adult) surviving and staying within the study reach between sampling occasions. Population growth is the sum of  $f$  and  $\phi$ . Capture probability is the probability that a marked individual is available for detection (i.e., present) and is captured during the sampling period.

We implemented a robust design version of the Pradel model that used our six surveys in late summer of each year to estimate  $p$ , and the period between years to estimate  $f$  and  $\phi$  (Pradel 1996). This parameterization assumes a population is closed to demographic changes between July and August (i.e., secondary intervals) but open between years (i.e., primary intervals). This design is more robust to heterogeneity in capture and demographic rates than closed or open-population methods alone (Kendall 2006). Within the closed population model structure, we used the Otis (1978) full likelihood formulation to estimate population size (White and Burnham 1999).

### *Multi-state Cormack-Jolly-Seber Model*

Multi-state CJS models estimate apparent survival and recapture probabilities for larval and adult stages separately, in addition to the probability of initiating and surviving the transition from larva to adult ( $\Psi_{LA}$ ; adult recruitment). In our model, this transition probability is the conditional probability that a larval individual stays alive and is available for capture, but transitions into an adult life stage by the next year. To get an unbiased estimate of  $\Psi_{LA}$  we needed to remove the assumption that survival is dependent on stage of an individual at time  $t$  (Williams et al. 2002). Thus, we ultimately fit two sets of multi-state CJS models. In the first set, we estimated  $\Psi_{LA}$  by fixing larval survival ( $\phi_L$ ) at 1.0. In the second set, we did not fix larval survival to get accurate estimates of stage-specific survival ( $\phi_L$  and  $\phi_A$ ). Because individuals cannot transition from adults back to larva, we set  $\Psi_{AL} = 0$  in all models.

We used a robust design version of the multi-state CJS model to increase the precision of parameter estimates (Bailey et al. 2010). Because this model assumes that individuals cannot change states within secondary capture sessions, we only included the stage at initial capture for the seven individuals (< 0.01% of all recaptures) that began to transition from larvae to adults during the two-month closed sampling window (July – August).

### *Model selection*



We implemented all models in Program MARK (White and Burnham 1999), accessed through RStudio (Version 1.4.1716; R Development Core Team 2021) using the RMark interface (Laake 2013). To assess goodness of model fit and potential overdispersion, we calculated the variance inflation factor ( $\hat{c}$ ) for this dataset (program RELEASE global test: TEST 2 + TEST 3; Anderson and Burnham 2002, Perret et al. 2003, Muths et al. 2017).

To first account for variability in capture rates in both Pradel and CJS models, we selected the best covariate structure for  $p$  by allowing capture rates to vary based on capture occasion (i.e., time), stream, reach (i.e., upstream vs. downstream), or none of the above, while keeping a full time-varying structure for survival and recruitment parameters (Doherty et al. 2012, Muths et al. 2017). We assumed capture and recapture rates were equivalent as we do not expect any type of trap response. In multi-state CJS models, we also allowed  $p$  to vary by stage (larva, adult). Next, we forced all survival and recruitment covariate structures to include stream and watershed area to account for unknown sources of variability among streams (Addis and Lowe 2020), consistent differences in flow magnitude as watershed area increases from upstream to downstream reaches within streams (M. M. *unpublished data*), and increased occurrence of *S. fontinalis* at larger watershed areas (Warren et al. 2008).

For both Pradel and CJS models, we used a logit transformation to test if and how flooding and drying intensity influenced recruitment and survival parameters. Discharge covariates were scaled and centered prior to model fitting, and we used a Pearson's correlation test to ensure they were not significantly correlated with one another. Candidate models – which included effects of flooding intensity, drying intensity, both, and neither on recruitment and survival parameters (see Table S1 for complete list of models) – were ranked by second-order AIC differences, corrected for small sample sizes ( $\Delta AIC_c$ ; Burnham and Anderson 2002). When  $\Delta AIC_c < 2$ , we used pairwise likelihood ratio tests (LRTs) to compare model fit. We assumed a significant LRT result ( $P < 0.05$ ) indicated support for the model with more parameters, whereas a nonsignificant LRT result indicated equal support for both models, so we selected the model with fewer parameters (White and Burnham 1999). We also estimated the relative likelihood of each model with  $AIC_c$  weights ( $AIC_c$  wt; Anderson and Burnham 2002).

To summarize how the *G. porphyriticus* population at Hubbard Brook changed over time, we calculated geometric mean  $\lambda$  from stream specific  $\lambda$  estimates across all eight years. We used geometric mean  $\lambda$  because it is the appropriate average for stochastic population growth (White and Burnham 1999). To approximate standard errors for  $\lambda$  (a derived demographic parameter), we used the delta method (Powell 2007). We considered flooding and drying intensity to affect  $\lambda$  significantly if 95% confidence intervals for  $\lambda$  did not overlap when comparing  $\lambda$  at minimum and maximum flooding intensity, and at minimum and maximum drying intensity. Similarly, to quantify effect sizes of flooding and drying intensity on all stream-specific demographic rates, we compared rate estimates (and 95% confidence intervals) following the minimum and maximum measures of flooding and drying intensity observed between 2012 – 2021.

## Results

### *Salamander surveys*

We marked 3307 individual salamanders across all streams and years. The total number of captures was 4094, including new individuals and recaptures. This included 2767 larvae and 1327 adults. Total number of captures by stream were 1515 in Bear, 1511 in Paradise, and 1068 in Zigzag.

### *Discharge extremes*

The mean Q99, representing peak annual discharge (i.e., largest flood) across all years and streams was 62 mm/day (SD = 20; range = 32 – 97) and typically occurred on March 20<sup>th</sup> (SD = 75 days; Fig. 1). The minimum 7-day lowest discharge, our index of drying intensity, across all years and streams was 0.05 mm/day (SD = 0.05; range = 0.00 – 0.18) and typically occurred between August 10<sup>th</sup> – 16<sup>th</sup> (SD = 25 days). Annual drying and flooding intensities were not correlated ( $r = -0.05$ ,  $P = 0.83$ ,  $df = 19$ ).

### *Pradel model*

Our data were not overdispersed ( $\hat{c} = 0.39$ ), and the final covariate structure for capture probability ( $p$ ) included stream and reach (Table S2). The top two Pradel models included an effect of flooding intensity on annual apparent survival ( $\phi$ ) and an effect of drying intensity on annual larval recruitment ( $f$ ), but differed in the inclusion of an effect of flooding intensity on  $f$  (Table 1). Support for these two models was somewhat ambiguous ( $\Delta AIC_c = 1.69$ ); however, the LRT was not significant ( $\chi^2 = 0.33$ ,  $P = 0.57$ ), indicating that the model with fewer parameters was more parsimonious. In that model, drying intensity reduced  $f$  by 20% (95% CI: 12 – 24) when comparing the highest 7-day lowest discharge (0.16 mm/day) to the lowest 7-day lowest discharge (0.00 mm/day; Fig. 2a; Table S3). Flooding intensity decreased  $\phi$  by 52% (95% CI: 43 – 57) when comparing the smallest flood (40 mm/day) to the largest flood (97 mm/day). Based on these rate estimates, drying intensity reduced  $\lambda$  by 15% (95% CI: 14 – 16) and flooding intensity reduced  $\lambda$  by 32% (95% CI: 31 – 33) when comparing minimum to maximum measures across the 8-yr study period (Fig. 3). Geometric mean population growth ( $\lambda$ ) across all streams and years was 1.00 (SD = 0.09; Fig. 4). Mean annual  $f$  for all streams and years was 0.57 (SD = 0.03). Mean annual  $\phi$  across all streams and years was 0.44 (SD = 0.09).

### *Multi-state Cormack-Jolly-Seber Model*

The final capture probability ( $p$ ) covariate structure for unbiased estimation of transition probability ( $\Psi_{LA}$ , with larval apparent survival [ $\phi_L$ ] fixed at 1.0) included stream, reach, and life stage. The top two  $\Psi_{LA}$  models included the effect of drying intensity on  $\Psi_{LA}$ , but differed in the inclusion of the effect of flooding intensity on  $\Psi_{LA}$  (Table 2). Support for these two was somewhat ambiguous ( $\Delta AIC_c = 1.83$ ), but the LRT was not significant ( $\chi^2 = 0.19$ ,  $P = 0.66$ ), indicating that the model with fewer parameters was more parsimonious. In that model, drying intensity increased  $\Psi_{LA}$  by 173% (95% CI: 80 – 359) when comparing the lowest and highest 7-day lowest discharges across this 8-yr period (Fig. 2b; Table S4). Mean annual  $\Psi_{LA}$  across all streams and years was 0.68 (SD = 0.09).

For stage-specific survival models, the final  $p$  covariate structure included stream, reach, and life stage. The top models estimating stage-specific survival rates included the effect of

flooding intensity on annual larval survival ( $\phi_L$ ) and adult survival ( $\phi_A$ ), but differed in the inclusion of an effect of drying intensity on  $\phi_L$  and  $\phi_A$  (Table 3). Support for the top two was ambiguous ( $\Delta AICc = 0.78$ ), but the LRT was not significant ( $\chi^2 = 3.27$ ,  $P = 0.20$ ), indicating that the model with fewer parameters was more parsimonious. In that model, flooding intensity reduced  $\phi_L$  by 65% (95 CI: 58 – 71) and reduced  $\phi_A$  by 40% (95% CI: 27 – 52) when comparing the smallest to the largest floods across the 8-yr study period (Fig. 5; Table S5). Mean  $\phi_L$  and mean  $\phi_A$  across all streams and years was 0.43 (SD = 0.12) and 0.50 (SD = 0.08), respectively.

## Discussion

We found that stream flooding and drying intensity reduce *G. porphyriticus* population growth rates in the short term (Fig. 3), but differential demographic responses to these disturbances across this species' complex life cycle provide resiliency over longer timespans. Stage-specific survival and recruitment rates responded differently to flooding and drying intensity (Table 4), dampening the net effect of these hydrologic extremes on population growth. In fact, the mean population growth rate ( $\lambda$ ) was 1.0 between 2012 – 2021 across all streams, despite considerable year-to-year variation (min = 0.84, max = 1.17; Fig. 4). This long-term population stability appears to be a consequence of demographic compensation, where the positive effects of drying intensity on adult recruitment (i.e., the probability of larvae initiating and surviving metamorphosis) helped to offset the negative effects of drying intensity on larval recruitment. A negligible change in larval and adult survival in response to drying intensity, in contrast to the strong negative effect of flooding intensity, also aided in this resilience. These varied responses appear to allow *G. porphyriticus* population growth rates to rebound after intense stream drying or flooding.

Drying intensity reduced recruitment of *G. porphyriticus* larvae (Fig. 2a) – the first documentation of this response in a stream salamander. The mechanisms driving this result may include breeding failure due to limited water availability (Taylor et al. 2006), increased competition for breeding sites (Berven 1990), or reduced survival rates for the smallest and most vulnerable life stages (Price et al. 2012, Cayuela et al. 2015). It is not possible to distinguish among these mechanisms with our current data because we find few visibly gravid females or egg masses during our surveys, and the smallest larvae (< 35 mm) cannot be tagged with current methods. It is also possible that females skip breeding in drought years, reducing larval recruitment (Kinkead and Otis 2007). *G. porphyriticus* is known to oviposit every year in the southern part of its range (Bruce 1972); however, breeding intervals may be more plastic in the northern portion of the range where the active season is shorter (Church et al. 2007). Predation on larvae by *S. fontinalis* and conspecifics may also increase during droughts, as stream reaches dry and both prey and predators become concentrated in isolated pools (Lake 2003).

Adult recruitment, the probability of larvae initiating and surviving metamorphosis to become adults, increased with drying intensity (Fig. 2b). This is likely due to an increase in the proportion of larvae initiating metamorphosis during droughts to avoid desiccation in drying streambeds. Pond breeding amphibians are known to exhibit plasticity in the duration of the larval period, and to accelerate metamorphosis to avoid pond drying (Denver 1997, Székely et al. 2017), often initiated by stress hormones (Bonett et al. 2010, Denver 2021). However, ours is the first study of stream amphibians to document this response directly. Importantly, this response

will increase the size of the breeding population, providing demographic compensation for reduced larval recruitment after droughts (Fig. 2a). Because our estimate of adult recruitment ( $\Psi_{LA}$ ) incorporates both the probability of initiating metamorphosis and the probability of surviving the transition from larva to adult, it is also possible that drying increases rates of survival through the transition. This would be surprising considering that metamorphosis is an inherently vulnerable life stage (Székely et al. 2020, Lowe et al. 2021), and drought is unlikely to mitigate that vulnerability (Zylstra et al. 2015).

Flooding intensity reduced survival of larvae and adults, though this effect was stronger in larvae (Fig. 5). This result matched our predictions, and it is consistent with studies showing that flooding – including higher discharge and debris transport – causes declines in other stream amphibians (Barrett et al. 2010, Cover et al. 2010) and in aquatic invertebrates (Gibbins et al. 2007). *G. porphyriticus* adults can leave the stream to avoid high flows, which likely accounts for the stronger effect of flooding on larval mortality. In addition to direct physical effects on individuals, flooding and shear stress can destroy debris dams and remove allochthonous material from the stream channel, reducing secondary production (i.e., in-stream prey resources; Bilby and Likens 1980, Wallace et al. 1997, Wohl 2010). This reduction in prey resources may exacerbate intraspecific competition and predation in the nutrient-limited headwater streams of Hubbard Brook (Hall et al. 2001, McGuire et al. 2014), ultimately reducing survival rates, particularly in *G. porphyriticus* larvae (Resetarits 1995). We did not find a strong effect of drying intensity on larval or adult survival, suggesting that both stages have access to refuges in the streambed and riparian zone with sufficient water availability during droughts (Feral et al. 2005, Bonett and Chippindale 2006).

Our results illustrate how complex life cycles enable compensatory demographic responses that stabilize populations in the face of intensifying climate extremes. In *G. porphyriticus*, recruitment of breeding adults increased with the intensity of stream drying, and appears to compensate for larval mortality due to drying. Additionally, flooding intensity reduced survival of *G. porphyriticus* larvae and adults, but drying intensity did not affect these stage-specific survival probabilities. Ultimately, this combination of responses to hydrologic extremes led to long-term population stability in our three study streams over the last decade, despite significant annual variation in population growth rates. Isolating these stage-specific demographic rates is critical to assessing demographic compensation, which may be more common in amphibians and other species with complex life cycles than previously acknowledged (Radchuk et al. 2013, Cayuela et al. 2022). However, complex life cycles can also allow for compounding negative responses to disturbance, accelerating population declines (Kissel et al. 2019), further underscoring the importance of stage-specific demographic analyses. In this era of increasing climate extremes (IPCC 2021), effective management and conservation relies on the nuanced insights on population resiliency that these intensive demographic analyses provide.

## Acknowledgments

We thank L. Swartz, T. Hodges, R. Wagner, M. Delamont, A. Willig, K. Barreras, R. Waters, M. Chung, M. Childs, J. Davenport, J. Hernandez, J. Jones, L. Low, J. McKenzie, T. Mitchell, L. Nagel, J. Newman, J. Rasor, M. Smith, and N. Steijn for assistance in the field. The research was

funded by the U.S. NSF (DEB-1114804, DEB-1050459, DEB-1655653). This work was conducted under Montana State IACUC #003-14WLDBS-012714. This work is a contribution of the Hubbard Brook Ecosystem Study. Hubbard Brook is part of the LTER network, which is supported by the U.S. NSF. The Hubbard Brook Experimental Forest is operated and maintained by the US Department of Agriculture, Forest Service, Northern Research Station.

## Literature cited

- Addis, B. R., and W. H. Lowe. 2020. Long-term survival probability, not current habitat quality, predicts dispersal distance in a stream salamander. *Ecology* 101:e02982. <https://doi.org/10.1002/ecy.2982>
- Amburgey, S. M., D. A. W. Miller, E. H. Campbell Grant, T. A. G. Rittenhouse, M. F. Benard, J. L. Richardson, M. C. Urban, W. Hughson, A. B. Brand, C. J. Davis, C. R. Hardin, P. W. C. Paton, C. J. Raithel, R. A. Relyea, A. F. Scott, D. K. Skelly, D. E. Skidds, C. K. Smith, and E. E. Werner. 2018. Range position and climate sensitivity: The structure of among-population demographic responses to climatic variation. *Global Change Biology* 24:439–454. <https://doi.org/10.1111/gcb.13817>
- Anderson, D. R., and K. P. Burnham. 2002. Avoiding pitfalls when using information-theoretic methods. *Journal of Wildlife Management* 66:912–918. <https://doi.org/10.2307/3803155>
- Bailey, A. S., J. W. Hornbeck, J. L. Campbell, and C. Eagar. 2003. Hydrometeorological database for Hubbard Brook Experimental Forest: 1955-2000. Newtown Square, PA, USA. <https://doi.org/10.2737/NE-GTR-305>
- Bailey, L. L., J. E. Hines, J. D. Nichols, J. Martin, S. Chamailé-Jammes, D. I. MacKenzie, H. Fritz, and C. J. Fonnesebeck. 2010. Simultaneous modeling of habitat suitability, occupancy, and relative abundance: African elephants in Zimbabwe. *Ecological Applications* 20:1173–1182. <https://doi.org/10.1890/09-0276.1>
- Barrett, K., B. S. Helms, C. Guyer, and J. E. Schoonover. 2010. Linking process to pattern: Causes of stream-breeding amphibian decline in urbanized watersheds. *Biological Conservation* 143:1998–2005. <https://doi.org/10.1016/j.biocon.2010.05.001>
- Beachy, C. K., T. J. Ryan, and R. M. Bonett. 2017. How metamorphosis is different in Plethodontids: larval life history perspective on life-cycle evolution. *Herpetologica* 176:139–148. <https://doi.org/10.1655/Herpetologica-D-16-00083.1>
- Berven, K. A. 1990. Factors affecting population fluctuations in larval and adult stages of the wood frog (*Rana sylvatica*). *Ecology* 71:1599–1608. <https://doi.org/10.2307/1938295>
- Bilby, R. E., and G. E. Likens. 1980. Importance of organic debris dams in the structure and function of stream ecosystems. *Ecology* 61:1107–1113. <https://doi.org/10.2307/1936830>
- Bonett, R. M., and P. T. Chippindale. 2006. Streambed microstructure predicts evolution of development and life history mode in the plethodontid salamander *Eurycea tynerensis*. *BMC Biology* 4:1–12. <https://doi.org/10.1186/1741-7007-4-6>
- Bonett, R. M., E. D. Hoopfer, and R. J. Denver. 2010. Molecular mechanisms of corticosteroid synergy with thyroid hormone during tadpole metamorphosis. *General and Comparative Endocrinology* 168:209–219. <https://doi.org/10.1016/j.ygcen.2010.03.014>
- Bonett, R. M., M. A. Steffen, and G. A. Robison. 2014. Heterochrony repolarized: a phylogenetic analysis of developmental timing in plethodontid salamanders. *EvoDevo* 5:27. <https://doi.org/10.1186/2041-9139-5-27>

- Bormann, F. H., and G. E. Likens. 1979. *Pattern and Process in a Forested Ecosystem*. Springer, New York, NY, USA.
- Boulton, A. J. 2003. Parallels and contrasts in the effects of drought on stream macroinvertebrate assemblages. *Freshwater Biology* 48:1173–1185. <https://doi.org/10.1046/j.1365-2427.2003.01084.x>
- Bruce, R. C. 1972. Variation in the life cycle of the salamander *Gyrinophilus porphyriticus*. *Herpetologica* 28:230–245.
- Burnham, K. P. and D. R. Anderson. 2002. *Model Selection and Inference: A Practical Information-Theoretic Approach*. Springer, New York, New York, USA.
- Campbell Grant, E. H., J. D. Nichols, W. H. Lowe, and W. F. Fagan. 2010. Use of multiple dispersal pathways facilitates amphibian persistence in stream networks. *Proceedings of the National Academy of Sciences* 107:6936–6940. <https://doi.org/10.1073/pnas.1000266107>
- Cayuella, H., D. Arsovski, S. Boitaud, E. Bonnaire, L. Boualit, C. Miaud, P. Joly, and A. Besnard. 2015. Slow life history and rapid extreme flood: Demographic mechanisms and their consequences on population viability in a threatened amphibian. *Freshwater Biology* 60:2349–2361. <https://doi.org/10.1111/fwb.12661>
- Cayuella, H., B. Monod-Broca, J.-F. Lemaître, A. Besnard, J. M. W. Gippet, and B. R. Schmidt. 2022. Compensatory recruitment allows amphibian population persistence in anthropogenic habitats. *Proceedings of the National Academy of Sciences of the United States of America* 119:e2206805119. <https://doi.org/10.1073/pnas.2206805119>
- Church, D. R., L. L. Bailey, H. M. Wilbur, W. L. Kendall, and J. E. Hines. 2007. Iteroparity in the variable environment of the salamander *Ambystoma tigrinum*. *Ecology* 88:891–903. <https://doi.org/10.1890/06-0896>
- Cover, M. R., J. A. de la Fuente, and V. H. Resh. 2010. Catastrophic disturbances in headwater streams: The long-term ecological effects of debris flows and debris floods in the Klamath Mountains, northern California. *Canadian Journal of Fisheries and Aquatic Sciences* 67:1596–1610. <https://doi.org/10.1139/F10-079>
- Datry, T., S. T. Larned, and K. Tockner. 2014. Intermittent rivers: A challenge for freshwater ecology. *BioScience* 64:229–235. <https://doi.org/10.1093/biosci/bit027>
- Death, R. G., I. C. Fuller, and M. G. Macklin. 2015. Resetting the river template: The potential for climate-related extreme floods to transform river geomorphology and ecology. *Freshwater Biology* 60:2477–2496. <https://doi.org/10.1111/fwb.12639>
- Denoël, M., and G. F. Ficetola. 2014. Heterochrony in a complex world: Disentangling environmental processes of facultative paedomorphosis in an amphibian. *Journal of Animal Ecology* 83:606–615. <https://doi.org/10.1111/1365-2656.12173>
- Denver, R. J. 1997. Proximate mechanisms of phenotypic plasticity in amphibian metamorphosis. *American Zoologist* 37:172–184. <https://doi.org/10.1093/icb/37.2.172>
- Denver, R. J. 2021. Stress hormones mediate developmental plasticity in vertebrates with complex life cycles. *Neurobiology of Stress* 14:100301. <https://doi.org/10.1016/j.ynstr.2021.100301>
- Doak, D. F., and W. F. Morris. 2010. Demographic compensation and tipping points in climate-induced range shifts. *Nature* 467:959–962. <https://doi.org/10.1038/nature09439>
- Doherty, P. F., G. C. White, and K. P. Burnham. 2012. Comparison of model building and selection strategies. *Journal of Ornithology* 152:317–323. <https://doi.org/10.1007/s10336-010-0598-5>

- Feral, D., M. A. Camann, and H. H. Welsh. 2005. *Dicamptodon tenebrosus* larvae within hyporheic zones of intermittent streams in California. *Herpetological Review* 36:26–27.
- Geffen, A. J., H. W. van der Veer, and R. D. M. Nash. 2007. The cost of metamorphosis in flatfishes. *Journal of Sea Research* 58:35–45. <https://doi.org/10.1016/j.seares.2007.02.004>
- Gibbins, C., D. Vericat, and R. J. Batalla. 2007. When is stream invertebrate drift catastrophic? The role of hydraulics and sediment transport in initiating drift during flood events. *Freshwater Biology* 52:2369–2384. <https://doi.org/10.1111/j.1365-2427.2007.01858.x>
- Greene, B. T., W. H. Lowe, and G. E. Likens. 2008. Forest succession and prey availability influence the strength and scale of terrestrial-aquatic linkages in a headwater salamander system. *Freshwater Biology* 53:2234–2243. <https://doi.org/10.1111/j.1365-2427.2008.02047.x>
- Hairston, N. A., and N. G. Hairston. 1987. *Community ecology and salamander guilds*. Cambridge University Press, New York.
- Hall, R. O., G. E. Likens, and H. M. Malcon. 2001. Trophic basis of invertebrate production in 2 streams at the Hubbard Brook Experimental Forest. *Journal of North American Benthological Society* 20:432–447. <https://doi.org/10.2307/1468040>
- Halsch, C. A., A. M. Shapiro, J. A. Fordyce, C. C. Nice, J. H. Thorne, D. P. Waetjen, and M. L. Forister. 2021. Insects and recent climate change. *Proceedings of the National Academy of Sciences of the United States of America* 118:1–9. <https://doi.org/10.1073/PNAS.2002543117>
- Hauer, F. R., H. Locke, V. J. Dreitz, M. Hebblewhite, W. H. Lowe, C. C. Muhlfeld, C. R. Nelson, M. F. Proctor, and S. B. Rood. 2016. Gravel-bed river floodplains are the ecological nexus of glaciated mountain landscapes. *Science Advances* 2:1–14. <https://doi.org/10.1126/sciadv.1600026>
- Heyer, W. R., M. A. Donnelly, R. W. McDiarmid, L. C. Hayek, and M. S. Foster. 1994. *Measuring and Monitoring Biological Diversity: Standard Methods for Amphibians*. Smithsonian Institution Press, Washington, DC, USA.
- IPCC. 2021. *Climate Change 2021: The Physical Science Basis. Contribution of Working Group I to the Sixth Assessment Report of the Intergovernmental Panel on Climate Change*. Cambridge University Press, Cambridge, United Kingdom and New York, NY, USA. <https://doi.org/10.1017/9781009157896>
- Kendall, W. L. 2006. The robust design for capture-recapture studies: analysis using program MARK. Pages 357–360. *Wildlife, Land and People: Priorities for the 21st Century*. The Wildlife Society, Bethesda, MD, USA.
- Kingsolver, J. G., H. Arthur Woods, L. B. Buckley, K. A. Potter, H. J. MacLean, and J. K. Higgins. 2011. Complex life cycles and the responses of insects to climate change. *Integrative and Comparative Biology* 51:719–732. <https://doi.org/10.1093/icb/icr015>
- Kinkead, K. E., and D. L. Otis. 2007. Estimating superpopulation size and annual probability of breeding for pond-breeding salamanders. *Herpetologica* 63:151–162. [https://doi.org/10.1655/0018-0831\(2007\)63\[151:ESSAAP\]2.0.CO;2](https://doi.org/10.1655/0018-0831(2007)63[151:ESSAAP]2.0.CO;2)
- Kissel, A. M., W. J. Palen, M. E. Ryan, and M. J. Adams. 2019. Compounding effects of climate change reduce population viability of a montane amphibian. *Ecological Applications* 29:1–12. <https://doi.org/10.1002/eap.1832>
- Kupferberg, S. J., H. Moidu, A. J. Adams, A. Catenazzi, M. Grefsrud, S. Bobzien, R. Leidy, and S. M. Carlson. 2021. Seasonal drought and its effects on frog population dynamics and

- amphibian disease in intermittent streams. *Ecohydrology*:1–15.  
<https://doi.org/10.1002/eco.2395>
- Laake, J. 2013. RMark: An R Interface for Analysis of Capture-Recapture Data with MARK. U. S. Department of Commerce, National Oceanic and Atmospheric Administration, National Marine Fisheries Service, Alaska Fisheries Science Center, Seattle, WA, USA.
- Lake, P. S. 2003. Ecological effects of perturbation by drought in flowing waters. *Freshwater Biology* 48:1161–1172. <https://doi.org/10.1046/j.1365-2427.2003.01086.x>
- Lake, S., N. Bond, and P. Reich. 2006. Floods down rivers: from damaging to replenishing forces. *Advances in Ecological Research* 39:41–62. [https://doi.org/10.1016/S0065-2504\(06\)39003-4](https://doi.org/10.1016/S0065-2504(06)39003-4)
- Larson, E. I., N. L. R. Poff, C. L. Atkinson, and A. S. Flecker. 2018. Extreme flooding decreases stream consumer autochthony by increasing detrital resource availability. *Freshwater Biology*:1483–1497. <https://doi.org/10.1111/fwb.13177>
- Laudet, V. 2011. The origins and evolution of vertebrate metamorphosis. *Current Biology* 21:R726–R737. <https://doi.org/10.1016/j.cub.2011.07.030>
- Lebreton, J.-D., J. D. Nichols, R. J. Barker, R. Pradel, and J. A. Spendelov. 2009. Modeling individual animal histories with multistate capture–recapture models. *Advances in Ecological Research* 41:87–173. [https://doi.org/10.1016/S0065-2504\(09\)00403-6](https://doi.org/10.1016/S0065-2504(09)00403-6)
- Likens, G. E., and F. H. Bormann. 1995. *Biogeochemistry of a Forested Ecosystem*. 3rd edition. Springer-Verlag, NY, USA.
- Lowe, W. H. 2012. Climate change is linked to long-term decline in a stream salamander. *Biological Conservation* 145:48–53. <https://doi.org/10.1016/j.biocon.2011.10.004>
- Lowe, W.H. 2022. Mark-recapture data of the Northern Spring Salamander (*Gyrinophilus porphyriticus*), Hubbard Brook Experimental Forest, 2012 – present ver 3. Environmental Data Initiative. <https://doi.org/10.6073/pasta/cd5f5a03df194930bf87eb12157b8182>
- Lowe, W. H., G. E. Likens, M. A. McPeck, and D. C. Buso. 2006. Linking direct and indirect data on dispersal: isolation by slope in a headwater stream salamander. *Ecology* 87:334–339. <https://doi.org/10.1890/05-0232>
- Lowe, W. H., T. E. Martin, D. K. Skelly, and H. A. Woods. 2021. Metamorphosis in an era of increasing climate variability. *Trends in Ecology and Evolution* 36:360–375. <https://doi.org/10.1016/j.tree.2020.11.012>
- Lowe, W. H., K. H. Nislow, and G. E. Likens. 2005. Forest structure and stream salamander diets: Implications for terrestrial-aquatic connectivity. *Internationale Vereinigung für theoretische und angewandte Limnologie: Verhandlungen*, 29:279–286. <https://doi.org/10.1080/03680770.2005.11902014>
- Lowe, W. H., L. K. Swartz, B. R. Addis, and G. E. Likens. 2019. Hydrologic variability contributes to reduced survival through metamorphosis in a stream salamander. *Proceedings of the National Academy of Sciences* 116:19563–19570. <https://doi.org/10.1073/pnas.190805711>
- Lytle, D. A., and N. L. R. Poff. 2004. Adaptation to natural flow regimes. *Trends in Ecology and Evolution* 19:94–100. <https://doi.org/10.1016/j.tree.2003.10.002>
- McGuire, K. J., C. E. Torgersen, G. E. Likens, D. C. Buso, W. H. Lowe, and S. W. Bailey. 2014. Network analysis reveals multiscale controls on streamwater chemistry. *Proceedings of the National Academy of Sciences* 111:7030–7035. <https://doi.org/10.1073/pnas.1404820111>



- Montgomery, D. R., and J. M. Buffington. 1997. Channel-reach morphology in mountain drainage basins. *Bulletin of the Geological Society of America* 109:596–611. [https://doi.org/10.1130/0016-7606\(1997\)109<0596:CRMIMD>2.3.CO;2](https://doi.org/10.1130/0016-7606(1997)109<0596:CRMIMD>2.3.CO;2)
- Munoz, D. J., K. Miller Hesed, E. H. C. Grant, and D. A. W. Miller. 2016. Evaluating within-population variability in behavior and demography for the adaptive potential of a dispersal-limited species to climate change. *Ecology and Evolution* 6:8740–8755. <https://doi.org/10.1002/ece3.2573>
- Muths, E., T. Chambert, B. R. Schmidt, D. A. W. Miller, B. R. Hossack, P. Joly, O. Grolet, D. M. Green, D. S. Pilliod, M. Cheylan, R. N. Fisher, R. M. McCaffery, M. J. Adams, W. J. Palen, J. W. Arntzen, J. Garwood, G. Fellers, J. M. Thirion, A. Besnard, and E. H. C. Grant. 2017. Heterogeneous responses of temperate-zone amphibian populations to climate change complicates conservation planning. *Scientific Reports* 7:1–10. <https://doi.org/10.1038/s41598-017-17105-7>
- Olden, J. D., and N. L. Poff. 2003. Redundancy and the choice of hydrologic indices for characterizing streamflow regimes. *River Research and Applications* 19:101–121. <https://doi.org/10.1002/rra.700>
- Paniw, M., T. D. James, C. Ruth Archer, G. Römer, S. Levin, A. Compagnoni, J. Che-Castaldo, J. M. Bennett, A. Mooney, D. Z. Childs, A. Ozgul, O. R. Jones, J. H. Burns, A. P. Beckerman, A. Patwary, N. Sanchez-Gassen, T. M. Knight, and R. Salguero-Gómez. 2021. The myriad of complex demographic responses of terrestrial mammals to climate change and gaps of knowledge: A global analysis. *Journal of Animal Ecology* 90:1398–1407. <https://doi.org/10.1111/1365-2656.13467>
- Perret, N., R. Pradel, C. Miaud, O. Grolet, and P. Joly. 2003. Transience, dispersal and survival rates in newt patchy populations. *Journal of Animal Ecology* 72:567–575. <https://doi.org/10.1046/j.1365-2656.2003.00726.x>
- Petranka, J. W. 1998. *Salamanders of the United States and Canada*. Smithsonian Institution Press, Washington D.C., USA.
- Powell, L. 2007. Approximating variance of demographic parameters using the delta method: A reference for avian biologists. *Condor* 109:949–954. <https://doi.org/10.1093/condor/109.4.949>
- Pradel, R. 1996. Utilization of capture-mark-recapture for the study of recruitment and population growth rate. *Biometrics* 52:703–709. <https://doi.org/10.2307/2532908>
- Price, S. J., R. A. Browne, and M. E. Dorcas. 2012. Resistance and resilience of a stream salamander to suprasedasonal drought. *Herpetologica* 68:312–323. <https://doi.org/10.1655/HERPETOLOGICA-D-11-00084.1>
- R Development Core Team. 2021. *R: A language and environment for statistical computing*. R Foundation for Statistical Computing, Vienna, Austria.
- Radchuk, V., C. Turlure, and N. Schtickzelle. 2013. Each life stage matters: The importance of assessing the response to climate change over the complete life cycle in butterflies. *Journal of Animal Ecology* 82:275–285. <https://doi.org/10.1111/j.1365-2656.2012.02029.x>
- Resetarits, W. J. 1995. Competitive asymmetry and coexistence in size-structured populations of Brook Trout and Spring Salamanders. *Oikos* 73:188–198. <https://doi.org/10.2307/3545907>
- Ries, P. R., T. J. Newton, R. J. Haro, S. J. Zigler, and M. Davis. 2016. Annual variation in recruitment of freshwater mussels and its relationship with river discharge. *Aquatic*

- Conservation: Marine and Freshwater Ecosystems 26:703–714.  
<https://doi.org/10.1002/aqc.2590>
- Rose, J. P., S. J. Kupferberg, C. A. Wheeler, P. M. Kleeman, and B. J. Halstead. 2021. Estimating the survival of unobservable life stages for a declining frog with a complex life history. *Ecosphere* 12. <https://doi.org/10.1002/ecs2.3381>
- Schneider, C. A., W. S. Rasband, and K. W. Eliceiri. 2012. NIH Image to ImageJ: 25 years of image analysis. *Nature Methods* 9:671–675. <https://doi.org/10.1038/nmeth.2089>
- Spotila, J. R. 1972. Role of temperature and water in the ecology of lungless salamanders. *Ecological Monographs* 42:95–125. <https://doi.org/10.2307/1942232>
- Székely, D., M. Denoël, P. Székely, and D. Cogălniceanu. 2017. Pond drying cues and their effects on growth and metamorphosis in a fast developing amphibian. *Journal of Zoology* 303:129–135. <https://doi.org/10.1111/jzo.12468>
- Székely, D., D. Cogălniceanu, P. Székely, D. Armijos-Ojeda, V. Espinosa-Mogrovejo, and M. Denoël. 2020. How to recover from a bad start: size at metamorphosis affects growth and survival in a tropical amphibian. *BMC Ecology* 20:1–8. <https://doi.org/10.1186/s12898-020-00291-w>
- Taylor, B. E., D. E. Scott, and J. W. Gibbons. 2006. Catastrophic reproductive failure, terrestrial survival, and persistence of the marbled salamander. *Conservation Biology* 20:792–801. <https://doi.org/10.1111/j.1523-1739.2005.00321.x>
- USDA Forest Service, Northern Research Station. 2022. Hubbard Brook Experimental Forest: Daily Streamflow by Watershed, 1956 - present ver 12. Environmental Data Initiative. <https://doi.org/10.6073/pasta/15b300e96c2d2f9785d0155b3e18b0e9>
- Vázquez, D. P., E. Gianoli, W. F. Morris, and F. Bozinovic. 2017. Ecological and evolutionary impacts of changing climatic variability. *Biological Reviews* 92:22–42. <https://doi.org/10.1111/brv.12216>
- Veith, M., M. Baubkus, S. Kugel, C. Kulpa, T. Reifenrath, M. Schafft, and N. Wagner. 2019. Drift compensation in larval European fire salamanders, *Salamandra salamandra* (Amphibia: Urodela)? *Hydrobiologia* 828:315–325. <https://doi.org/10.1007/s10750-018-3820-8>
- Villellas, J., D. F. Doak, M. B. García, and W. F. Morris. 2015. Demographic compensation among populations: What is it, how does it arise and what are its implications? *Ecology Letters* 18:1139–1152. <https://doi.org/10.1111/ele.12505>
- Wallace, J. B., S. L. Eggert, J. L. Meyer, and J. R. Webster. 1997. Multiple trophic levels of a forest stream linked to terrestrial litter inputs. *Science* 277:102–104. <https://doi.org/10.1126/science.277.5322.102>
- Walls, S., W. Barichivich, and M. Brown. 2013. Drought, deluge and declines: the impact of precipitation extremes on amphibians in a changing climate. *Biology* 2:399–418. <https://doi.org/10.3390/biology2010399>
- Warren, D. R., G. E. Likens, D. C. Buso, and C. E. Kraft. 2008. Status and distribution of fish in an acid-impacted watershed of the Northeastern United States (Hubbard Brook, NH). *Northeastern Naturalist* 15:375–390. <https://doi.org/10.1656/1092-6194-15.3.375>
- Weinbach, A., H. Cayuela, O. Grolet, A. Besnard, and P. Joly. 2018. Resilience to climate variation in a spatially structured amphibian population. *Scientific Reports* 8:1–9. <https://doi.org/10.1038/s41598-018-33111-9>
- White, G. C., and K. P. Burnham. 1999. Program mark: Survival estimation from populations of marked animals. *Bird Study* 46:S120–S139. <https://doi.org/10.1080/00063659909477239>

- Wilbur, H. M. 1980. Complex life cycles. *Annual Review of Ecology and Systematics* 11:67–93.  
<https://doi.org/10.1146/annurev.es.11.110180.000435>
- Williams, B. K., J. D. Nichols, and M. J. Conroy. 2002. *Analysis and management of animal populations*. Academic press, San Diego, CA, USA.
- Wohl, E. 2010. *Mountain rivers revisited*. American Geophysical Union, Washington, DC.
- Zylstra, E. R., R. J. Steidl, D. E. Swann, and K. Ratzlaff. 2015. Hydrologic variability governs population dynamics of a vulnerable amphibian in an arid environment. *PLoS ONE* 10:1–16. <https://doi.org/10.1371/journal.pone.0125670>

## Tables

Table 1: The top four robust design Pradel models assessing support for effects of flooding and drying intensity on annual larval recruitment ( $f$ ) and apparent survival probability ( $\phi$ ) for *Gyrinophilus porphyriticus* in the Hubbard Brook Experimental Forest, New Hampshire, USA. Estimates are from 4094 captures across three streams over eight years (2012 – 2015, 2018 – 2021). All models included effects of stream and watershed area on  $\phi$  and  $f$ , in addition to stream and reach effects on capture probability. Parameterization for  $\phi$  and  $f$  to vary by flooding or drying intensity are in parentheses; a period indicates no effect of either flooding or drying on that parameter. Number of estimated parameters ( $k$ ), second-order Akaike's information criterion values ( $AIC_c$ ),  $AIC_c$  differences ( $\Delta AIC_c$ ), and  $AIC_c$  weights ( $AIC_c$  wt) for all models are shown.

<b>Model</b>	<b>k</b>	<b>AIC<sub>c</sub></b>	<b><math>\Delta AIC_c</math></b>	<b>AIC<sub>c</sub> wt</b>
$\phi(\text{flooding}) f(\text{drying})$	22	8630.98	0.00	0.35
$\phi(\text{flooding}) f(\text{drying, flooding})$	23	8632.67	1.69	0.15
$\phi(\text{drying, flooding}) f(\text{drying})$	23	8632.95	1.97	0.13
$\phi(\text{flooding}) f(.)$	21	8633.06	2.08	0.13

Table 2: The top four robust design multi-state Cormack-Jolly-Seber models assessing support for effects of flooding and drying intensity on annual adult recruitment ( $\Psi_{LA}$ ) for *Gyrinophilus porphyriticus* in the Hubbard Brook Experimental Forest, New Hampshire, USA. Estimates are from 4094 captures across three streams over eight years (2012 – 2015, 2018 – 2021). These models also included a parameter for annual apparent survival probability ( $\phi$ ), but to get an unbiased estimate of  $\Psi_{LA}$  we needed to remove the assumption that survival is dependent on stage of an individual, and therefore we set larval survival at 1.0 and did not parameterize any models to include the effects of flooding or drying intensity on  $\phi$ . All models included effects of stream and watershed area on  $\Psi_{LA}$  and  $\phi$ , in addition to stream and reach effects on capture probability ( $p$ ). Parameterization for  $\Psi_{LA}$  to vary by flooding or drying intensity are in parentheses; a period indicates no effect of either flooding or drying on that parameter. Number of estimated parameters ( $k$ ), second-order Akaike’s information criterion values ( $AIC_c$ ),  $AIC_c$  differences ( $\Delta AIC_c$ ), and  $AIC_c$  weights ( $AIC_c$  wt) for all models are shown.

<b>Model</b>	<b>k</b>	<b>AIC<sub>c</sub></b>	<b><math>\Delta AIC_c</math></b>	<b>AIC<sub>c</sub> wt</b>
$\Psi_{LA}(\text{drying})$	22	31.11	0.00	0.71
$\Psi_{LA}(\text{drying, flooding})$	23	32.94	1.83	0.29
$\Psi_{LA}(\cdot)$	21	49.70	18.60	0.00
$\Psi_{LA}(\text{flooding})$	22	51.44	20.33	0.00

Table 3: The top four robust design multi-state Cormack-Jolly-Seber models assessing support for the effect of flooding and drying intensity on stage-specific annual apparent survival probability ( $\phi$ ) for *Gyrinophilus porphyriticus* in the Hubbard Brook Experimental Forest, New Hampshire, USA. Estimates are from 4094 captures across three streams over eight years (2012 – 2015, 2018 – 2021). This model also includes a parameter for annual adult recruitment ( $\Psi_{LA}$ ), but we did not parameterize any models to include the effects of flooding or drying intensity on  $\Psi_{LA}$ . All models included effects of stream and watershed area on  $\phi$  and  $\Psi_{LA}$ , in addition to stream and reach effects on capture probability. Parameterization for  $\phi$  to vary by flooding or drying intensity are in parentheses; a period indicates no effect of either flooding or drying on that parameter. Number of estimated parameters ( $k$ ), second-order Akaike’s information criterion values ( $AIC_c$ ),  $AIC_c$  differences ( $\Delta AIC_c$ ), and  $AIC_c$  weights ( $AIC_c$  wt) for all models are shown.

<b>Model</b>	<b>k</b>	<b>AIC<sub>c</sub></b>	<b><math>\Delta AIC_c</math></b>	<b>AIC<sub>c</sub> wt</b>
$\phi(\text{flooding*stage})$	24	-397.12	0.00	0.60
$\phi(\text{flooding*stage, drying*stage})$	26	-396.34	0.78	0.40
$\phi(\text{stage})$	22	-373.48	23.64	0.00
$\phi(\text{drying*stage})$	24	-371.63	25.49	0.00

Table 4: Summary of the negative (-), positive (+), or non-significant (NS) effects of extreme discharge conditions (i.e., flooding and drying) on larval recruitment ( $f$ ), adult recruitment ( $\Psi_{LA}$ ), larval survival ( $\phi_L$ ), adult survival ( $\phi_A$ ), combined survival ( $\phi$ ), and overall population growth rate ( $\lambda$ ) for *Gyrinophilus porphyriticus* in the Hubbard Brook Experimental Forest, New Hampshire, USA. Estimates were derived from a robust design reverse-time Pradel model (Table 1) or robust design multi-state Cormack-Jolly-Seber models (Tables 2 and 3), using *G. porphyriticus* capture-recapture and stream discharge data collected in three streams over eight years (2012 – 2015, 2018 – 2021).

<b>Parameter</b>	<b>Flooding</b>	<b>Drying</b>	<b>Model</b>
$f$	NS	-	Pradel
$\Psi_{LA}$	NS	+	CJS
$\phi_L$	-	NS	CJS
$\phi_A$	-	NS	CJS
$\phi$	-	NS	Pradel
$\lambda$	-	-	Pradel

## Figures

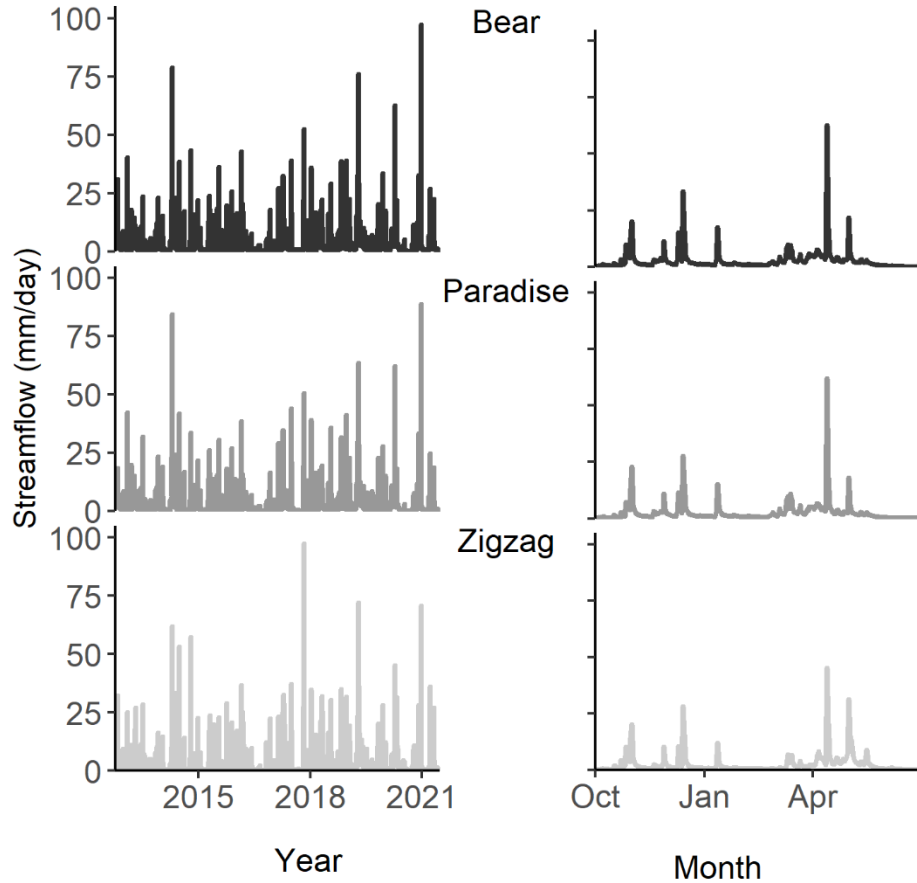


Figure 1: Hydrographs for our three study streams (Bear, Paradise, and Zigzag Brooks) in the Hubbard Brook Experimental Forest, New Hampshire, USA. The left column depicts yearly discharge variation from 2012 – 2021 (the entire study period). The right column depicts monthly variation in discharge from October 2020 – September 2021. Q99, the discharge exceeded only 1% of the year and our index of flooding intensity, occurred in late April of that year. Minimum 7-day lowest discharge, our index of stream drying intensity, occurred in August of that year.



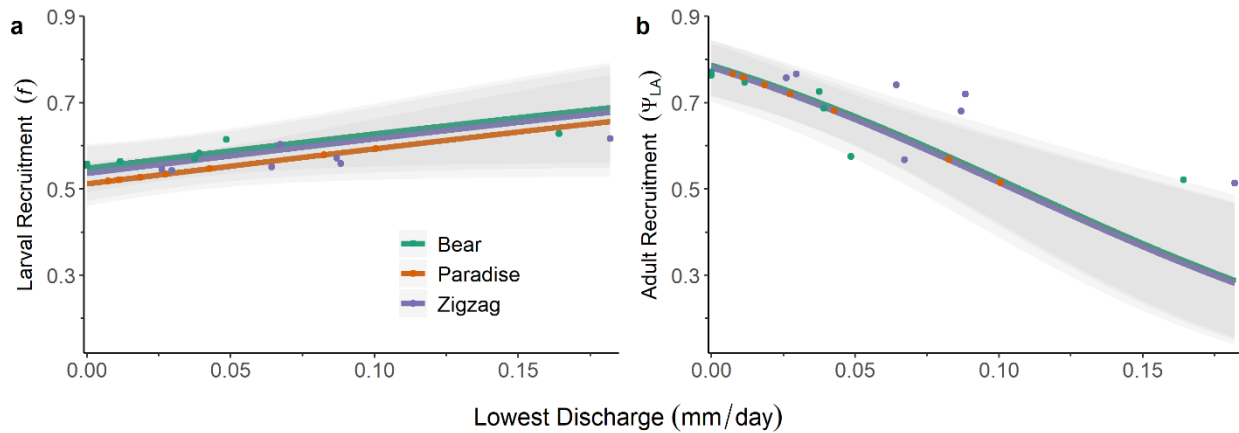


Figure 2. Relationships (bold lines) between the minimum 7-day lowest discharge (i.e., stream drying intensity) and annual larval recruitment (a) and annual adult recruitment (b) for *Gyrinophilus porphyriticus* across three streams (Bear, Paradise, and Zigzag) in the Hubbard Brook Experimental Forest, New Hampshire, USA. Points are year- and stream-specific recruitment estimates. The gray ribbon represents the 95% confidence interval in mean responses. Larval recruitment was estimated with a robust-design Pradel model (Table 1). Adult recruitment was estimated with a robust-design multi-state Cormack-Jolly-Seber model (Table 2).

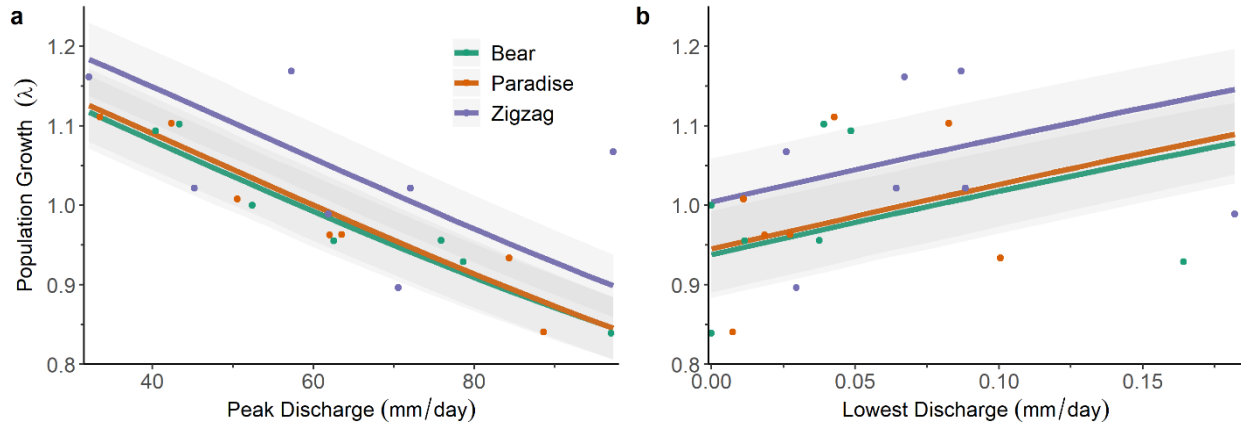


Figure 3. Relationships (bold lines) between peak annual discharge (a) and minimum 7-day lowest discharge (b) and population growth ( $\lambda$ ) for *Gyrinophilus porphyriticus* across three streams (Bear, Paradise, and Zigzag) in the Hubbard Brook Experimental Forest, New Hampshire, USA. Colored points represent year- and stream-specific population growth estimates. The gray ribbon represents the 95% confidence interval in mean responses. Population growth rates were derived from the top robust-design Pradel model estimating the effects of discharge extremes on larval recruitment and apparent survival rates of all individuals (i.e., pooling larvae and adults; Table 1)

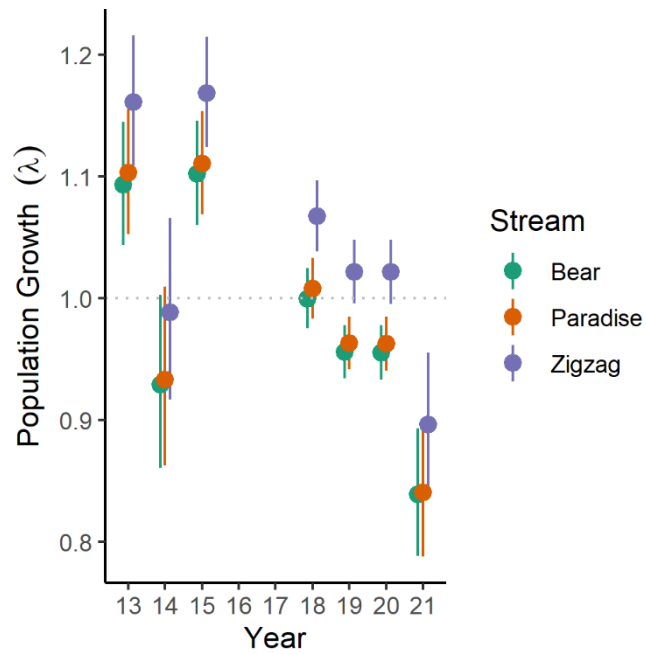


Figure 4. Estimated annual population growth ( $\lambda$ ) for *Gyrinophilus porphyriticus* across three streams (Bear, Paradise, and Zigzag) from 2012 – 2021 in the Hubbard Brook Experimental Forest, New Hampshire, USA. Colored points represent year- and stream-specific  $\lambda$  estimates derived from a robust-design Pradel model (Table 1). Bars represent the 95% confidence interval in mean responses.

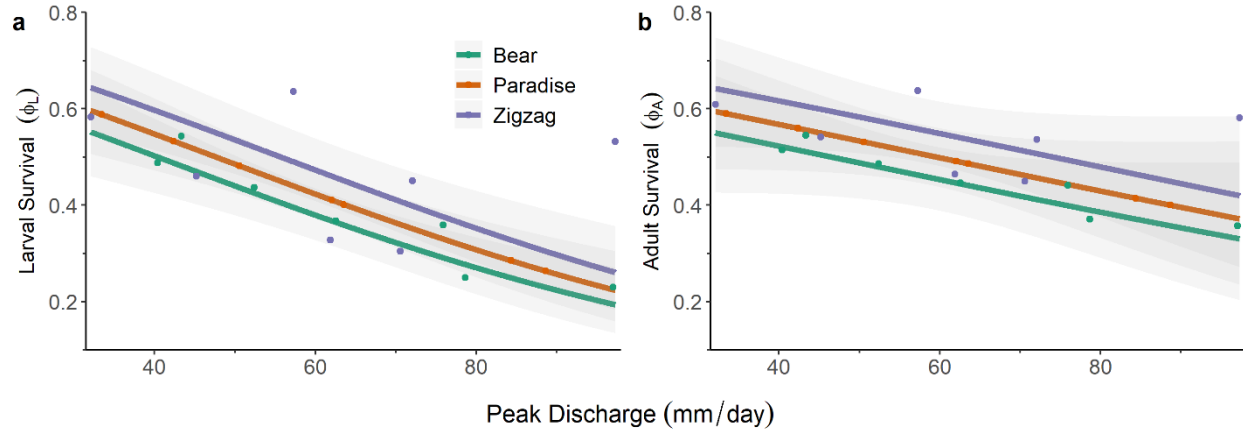


Figure 5: Relationships (bold lines) between peak annual discharge and annual larval apparent survival (a) and annual adult apparent survival (b) for *Gyrinophilus porphyriticus* across three streams (Bear, Paradise, and Zigzag) in the Hubbard Brook Experimental Forest, New Hampshire, USA. Colored points represent year- and stream-specific survival estimates. Gray ribbons represent the 95% confidence interval in mean responses. Survival estimates are from a robust-design multi-state Cormack-Jolly-Seber model (Table 3).

## Supplementary Materials

Table S1. List of candidate models tested to describe the effect of flooding intensity, drying intensity, or neither on larval recruitment ( $f$ ; Pradel model set), adult recruitment ( $\Psi_{LA}$ ; CJS model set), and stage-specific survival ( $\phi$ ; CJS model set). Stream and watershed area were also included to describe all survival and recruitment parameters. Recapture rates varied by stream and reach for both model types, and by stage in CJS models.

Model Type	Parameter of Interest	Model Number	Survival Parameter	Recruitment Parameter
Pradel	larval recruitment ( $f$ )	1	$\phi(\cdot)$	$f(\cdot)$
		2	$\phi(\cdot)$	$f(\text{flooding})$
		3	$\phi(\cdot)$	$f(\text{drying})$
		4	$\phi(\cdot)$	$f(\text{flooding, drying})$
		5	$\phi(\text{flooding})$	$f(\cdot)$
		6	$\phi(\text{flooding})$	$f(\text{flooding})$
		7	$\phi(\text{flooding})$	$f(\text{drying})$
		8	$\phi(\text{flooding})$	$f(\text{flooding, drying})$
		9	$\phi(\text{drying})$	$f(\cdot)$
		10	$\phi(\text{drying})$	$f(\text{flooding})$
		11	$\phi(\text{drying})$	$f(\text{drying})$
		12	$\phi(\text{drying})$	$f(\text{flooding, drying})$
		13	$\phi(\text{flooding, drying})$	$f(\cdot)$
		14	$\phi(\text{flooding, drying})$	$f(\text{flooding})$
		15	$\phi(\text{flooding, drying})$	$f(\text{drying})$
		16	$\phi(\text{flooding, drying})$	$f(\text{flooding, drying})$
CJS	adult recruitment ( $\Psi_{LA}$ )	1	$\phi(\cdot)$	$\Psi_{LA}(\cdot)$
		2	$\phi(\cdot)$	$\Psi_{LA}(\text{flooding})$
		3	$\phi(\cdot)$	$\Psi_{LA}(\text{drying})$
		4	$\phi(\cdot)$	$\Psi_{LA}(\text{drying, flooding})$
CJS	stage-specific survival ( $\phi$ )	1	$\phi(\cdot)$	$\Psi_{LA}(\cdot)$
		2	$\phi(\text{stage})$	$\Psi_{LA}(\cdot)$
		3	$\phi(\text{flooding*stage})$	$\Psi_{LA}(\cdot)$
		4	$\phi(\text{drying*stage})$	$\Psi_{LA}(\cdot)$
		5	$\phi(\text{drying*stage, flooding*stage})$	$\Psi_{LA}(\cdot)$

Table S2. The top four robust design Pradel models to describe the best covariate structure for capture probability ( $p$ ) for *Gyrinophilus porphyriticus* in the Hubbard Brook Experimental Forest, New Hampshire, USA. Parameterization for  $p$  to vary by reach, stream, or time are in parentheses. Apparent survival ( $\phi$ ) and larval recruitment ( $f$ ) varied by time in all models. Number of estimated parameters ( $k$ ), second-order Akaike's information criterion values ( $AIC_c$ ),  $AIC_c$  differences ( $\Delta AIC_c$ ), and  $AIC_c$  weights ( $AIC_c$  wt) for all models are shown.

<b>Model</b>	<b>k</b>	<b>AICc</b>	<b><math>\Delta AIC</math></b>	<b>AICc wt</b>
$p$ (reach + stream)	26	8594.11	0.00	0.87
$p$ (reach + stream + time)	33	8597.84	3.73	0.13
$p$ (reach + time)	31	8657.64	63.53	0.00
$p$ (reach)	24	8658.72	64.61	0.00

Table S3. Parameter estimates from the top robust design Pradel model assessing support for effects of flooding and drying intensity on annual larval recruitment ( $f$ ) and apparent survival probability ( $\phi$ ) for *Gyrinophilus porphyriticus* in the Hubbard Brook Experimental Forest, New Hampshire, USA. Standard error (SE), lower confidence limit (LCL), and upper confidence limit (UCL) provided for all parameter estimates. Models were forced to include the effects of stream (Bear, Paradise, and Zigzag) and watershed area on  $\phi$  and  $f$ , and stream and reach effects on capture probability.

Parameter	Estimate	SE	LCL	UCL
$\phi$				
Intercept	-0.44	0.10	-0.64	-0.24
Paradise	0.18	0.13	-0.07	0.43
Zigzag	0.32	0.15	0.03	0.61
Watershed area	-0.11	0.07	-0.24	0.03
Flooding	-0.36	0.07	-0.49	-0.22
$f$				
Intercept	0.37	0.11	0.15	0.59
Paradise	-0.15	0.13	-0.40	0.11
Zigzag	-0.05	0.15	-0.35	0.25
Watershed area	0.14	0.07	0.00	0.28
Drying	0.16	0.08	0.00	0.33
$p$				
Intercept	-2.82	0.05	-2.91	-2.72
Paradise	-0.01	0.04	-0.08	0.06
Zigzag	-0.30	0.04	-0.38	-0.22
Downstream reach	-0.53	0.03	-0.59	-0.46

Table S4. Parameter estimates from the top robust design multi-state Cormack-Jolly-Seber model assessing support for effects of flooding and drying intensity on annual adult recruitment ( $\Psi_{LA}$ ) for *Gyrinophilus porphyriticus* in the Hubbard Brook Experimental Forest, New Hampshire, USA when larval survival was fixed at 1.0. This model also includes a parameter for apparent annual survival ( $\phi$ ). Standard error (SE), lower confidence limit (LCL), and upper confidence limit (UCL) provided for all parameter estimates. Models were forced to include the effects of stream (Bear, Paradise, and Zigzag) and watershed area on  $\phi$  and  $\Psi_{LA}$ , and stream and reach effects on capture probability.

<b>Parameter</b>	<b>Estimate</b>	<b>SE</b>	<b>LCL</b>	<b>UCL</b>
$\phi$				
Intercept	-0.91	0.22	-1.35	-0.48
Paradise	0.51	0.28	-0.03	1.05
Zigzag	1.00	0.29	0.42	1.57
Watershed area	0.07	0.12	-0.16	0.30
$\Psi_{LA}$				
Intercept	0.64	0.15	0.36	0.93
Paradise	-0.03	0.18	-0.38	0.32
Zigzag	-0.03	0.24	-0.51	0.45
Watershed area	0.14	0.11	-0.08	0.36
Drying	-0.61	0.14	-0.88	-0.34
$p$				
Intercept	-3.77	0.05	-3.87	-3.67
Paradise	-0.02	0.04	-0.09	0.06
Zigzag	-0.29	0.04	-0.37	-0.21
Downstream reach	-0.52	0.03	-0.59	-0.46
Larvae	0.77	0.03	0.71	0.84



Table S5. Parameter estimates from the top robust design multi-state Cormack-Jolly-Seber model assessing support for the effect of flooding and drying intensity on stage-specific annual apparent survival probability ( $\phi$ ) for *Gyrinophilus porphyriticus* in the Hubbard Brook Experimental Forest, New Hampshire, USA. This model also includes a parameter for annual adult recruitment ( $\Psi_{LA}$ ). Standard error (SE), lower confidence limit (LCL), and upper confidence limit (UCL) provided for all parameter estimates. Models were forced to include the effects of stream (Bear, Paradise, and Zigzag) and watershed area on  $\phi$  and  $\Psi_{LA}$ , and stream and reach effects on capture probability.

Parameter	Estimate	SE	LCL	UCL
$\phi$				
Intercept	-0.22	0.14	-0.49	0.05
Paradise	0.18	0.13	-0.07	0.43
Zigzag	0.38	0.15	0.08	0.69
Watershed area	-0.11	0.07	-0.25	0.02
Flood	-0.27	0.16	-0.58	0.04
Larvae	-0.33	0.14	-0.61	-0.05
Flooding*larvae	-0.22	0.19	-0.59	0.15
$\Psi_{LA}$				
Intercept	-1.22	0.29	-1.78	-0.66
Paradise	0.31	0.35	-0.37	0.99
Zigzag	0.71	0.41	-0.10	1.52
Watershed area	0.04	0.19	-0.34	0.41
$p$				
Intercept	-3.15	0.06	-3.26	-3.04
Paradise	-0.01	0.04	-0.08	0.06
Zigzag	-0.28	0.04	-0.36	-0.20
Downstream reach	-0.50	0.03	-0.57	-0.44
Larvae	0.58	0.03	0.51	0.65

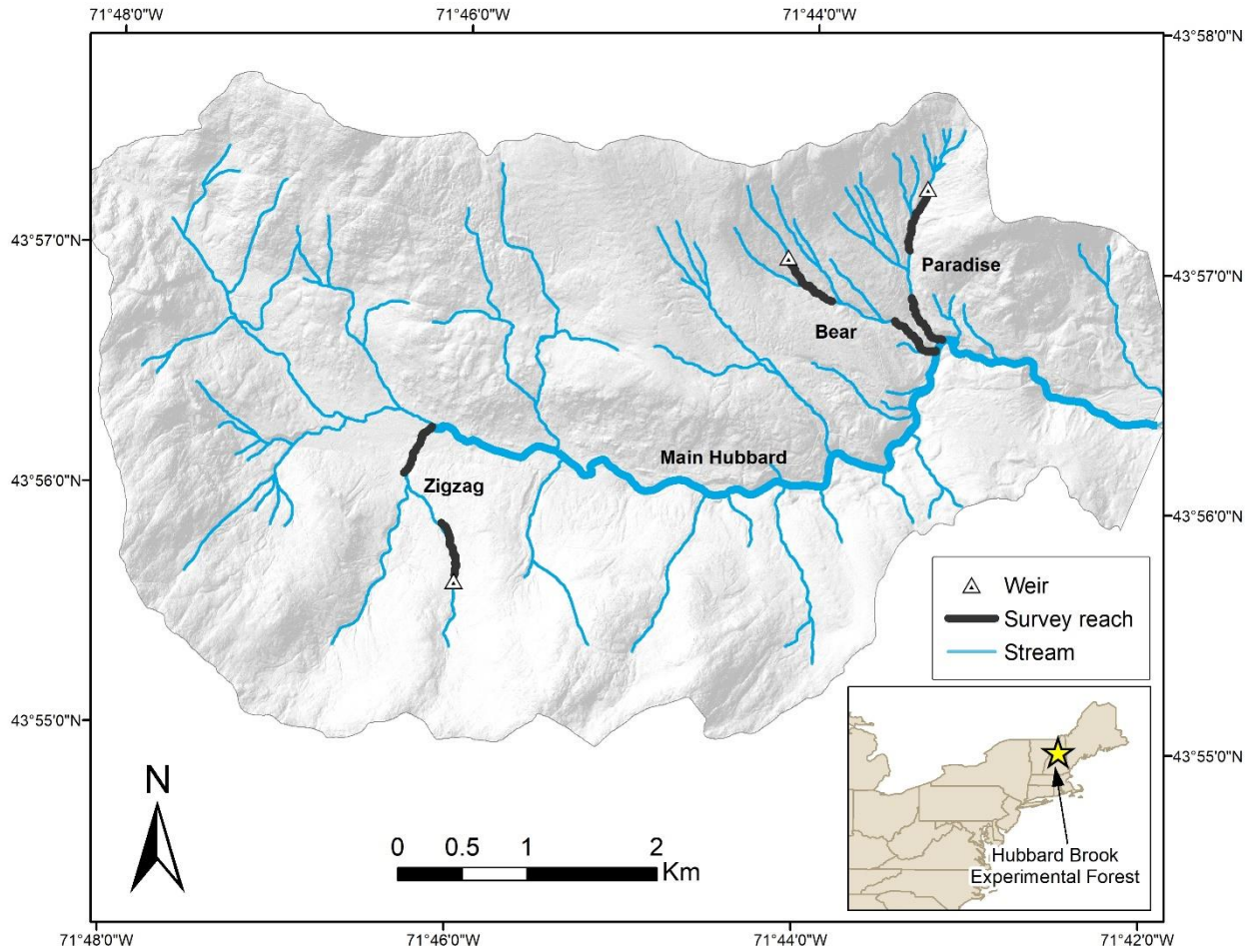


Figure S1. Map of the six study reaches (black lines) across three streams (Bear, Paradise, and Zigzag Brooks) in the Hubbard Brook Experimental Forest in New Hampshire, USA where capture-recapture data was collected for *Gyrinophilus porphyriticus* from 2012 – 2015, 2018 – 2021. Map also includes locations of gauged weirs (triangles) that recorded discharge data for each stream.